

**Characterization of the
mono-ADP-ribosylation by ARTD10:
substrates, consequences and reversibility**

Von der Fakultät für Mathematik, Informatik und Naturwissenschaften der RWTH
Aachen University zur Erlangung des akademischen Grades einer Doktorin der
Naturwissenschaften genehmigte Dissertation

vorgelegt von

Master of Science
Karla Feijs

aus Heerlen, Niederlande

Berichter: Universitätsprofessor Dr.rer.nat. Bernhard Lüscher
 Universitätsprofessor Dr.rer.nat. Werner Baumgartner

Tag der mündlichen Prüfung: 20. Dezember 2012

Diese Dissertation ist auf den Internetseiten der Hochschulbibliothek online verfügbar.

“Choose a job you love and you’ll never
have to work a day in your life.”

Confucius

Table of contents

Summary	1
Zusammenfassung.....	2
Introduction.....	3
Posttranslational modifications: in control of <i>everything</i>	4
ADP-ribosylation	9
ARTD10: a mono-ADP-ribosyltransferase	15
Mechanistic insights into ADP-ribosylation	18
Removing and reading ADP-ribosylation	23
Measuring ADP-ribosylation	26
Research aims	29
Experimental procedures	30
Materials.....	31
Cloning	34
Human, bacterial and insect cell cultivation	36
Protein purification and detection	38
Cell-based assays.....	41
<i>In vitro</i> assays	44
Mass spectrometry methods.....	46
Peptide- and ProtoArrays®.....	48
Bioinformatical analysis.....	50
Results and discussion	51
Identification of novel substrates of ARTD10 and ARTD8	52
mono-ADP-ribosylation of GSK3β regulates kinase activity	60
de-ADP-ribosylation by MDO2 restores GSK3β activity	70
Phosphorylation of ARTD10 by GSK3β	77
Bioinformatical models of ARTD10 with NAD⁺ and GSK3β	81
Mapping modification sites using mass spectrometry and peptide arrays	88
Conclusions	93
References	97
Attachments.....	110

Summary

Posttranslational modifications are involved in basically all cellular processes. Some of them have been studied quite extensively, such as phosphorylation and ubiquitination. Others, mono-ADP-ribosylation for example, have currently barely been investigated. Mono-ADP-ribosylating enzymes transfer an ADP-ribose moiety from the cofactor NAD⁺ onto a target substrate. ARTD10 has been demonstrated to be an enzyme catalyzing the transfer of mono-ADP-ribose, but has not been investigated in more detail.

Here a protein microarray-based substrate-screen is presented, not only for ARTD10 substrates but also for ARTD8 substrates. The results are validated and analyzed. To characterize the functional consequences of mono-ADP-ribosylation, GSK3 β is used as prototype substrate. We could show that mono-ADP-ribosylation of GSK3 β inhibits kinase activity *in vitro* as well as in cells. Moreover, we identified MDO2 as ADP-ribosylhydrolase capable of removing ADP-ribose from both ARTD10 itself and GSK3 β , which suffices to restore kinase activity. The interaction between ARTD10 and GSK3 β was addressed by bioinformatical modeling studies and GSK3 β was identified as kinase of ARTD10 *in vitro*. Lastly, we investigated methods to identify ADP-ribosylation sites by mass spectrometry and by peptide arrays, for which the currently employed methods are summarized in the introduction.

This study implies that mono-ADP-ribosylating enzymes are highly specific, as only a small percentage of the 8000 proteins tested on the protein microarrays were modified. Moreover, the functional consequence of mono-ADP-ribosylation for a substrate protein described here has not been shown before for any eukaryotic intracellular mono-ADP-ribosylating enzyme and adds a new dimension to the known regulatory mechanisms of GSK3 β . The hydrolyzing activities of MDO2 are also a novelty unlike any published before for the removal of mono-ADP-ribosylation and indicate that mono-ADP-ribosylation is a dynamic posttranslational modification. Together, these findings provide a basis for future research addressing the physiological relevance of mono-ADP-ribosylation in eukaryotic cells.

Zusammenfassung

Posttranslationale Modifikationen spielen in fast allen zellulären Prozessen eine zentrale Rolle. Im Gegensatz zu Phosphorylierung und Ubiquitinierung, die bereits exzessiv untersucht wurden, ist über Mono-ADP-Ribosylierung nicht viel bekannt. Mono-ADP-ribosylierende Enzyme übertragen einen ADP-Ribose-Rest des Cofaktors NAD^+ auf ein Zielprotein. Ein solches Enzym ist ARTD10. Doch genau wie über Mono-ADP-Ribosylierung selbst, ist das Wissen über dieses katalysierende Enzym begrenzt.

In dieser Arbeit werden zwei *Microarray*-basierte Substrat-*Screens* präsentiert, sowohl für ARTD10 als auch für ARTD8. Die Ergebnisse dieser Untersuchungen wurden validiert und analysiert, wobei GSK3 β als Prototyp-Substrat für die Charakterisierung der funktionalen Konsequenzen von Mono-ADP-Ribosylierung diente. Wir konnten zeigen, dass Mono-ADP-Ribosylierung von GSK3 β dessen Kinase-Aktivität sowohl *in vitro* als auch in Zellen inhibiert. Weiterhin konnte demonstriert werden, dass die Entfernung der ADP-Ribose von GSK3 β durch MDO2 ausreichend ist, um die Kinase-Aktivität wieder herzustellen. Mittels *in silico* Modell-Simulationen wurde die Interaktion zwischen ARTD10 und GSK3 β analysiert und ein Motiv in ARTD10 identifiziert, welches durch GSK3 β *in vitro* phosphoryliert werden kann. Zuletzt haben wir auf Massenspektrometrie und *Peptidarrays* basierte Methoden untersucht, mittels derer ADP-Ribosylierungsstellen identifiziert werden sollen. Derzeit hierfür angewandte Methoden werden in der Einleitung zusammengefasst.

Die Ergebnisse dieser Arbeit implizieren, dass Mono-ADP-Ribosylierung hoch spezifisch ist, da nur ein kleiner Prozentsatz der getesteten 8000 Proteine des *Microarrays* durch ARTD10 oder ARTD8 modifiziert wurden. Weiterhin wurden die hier beobachteten Auswirkungen der intrazellulären Mono-ADP-Ribosylierung eines Proteins, nämlich GSK3 β , erstmalig für ein eukaryotisches ADP-ribosylierendes Enzym beschrieben. Dadurch können die bereits bekannten Regulationsmechanismen für GSK3 β um eine weitere Dimension ergänzt werden. Erstmals konnte außerdem mit MDO2 ein Enzym identifiziert werden, das in der Lage ist mono-ADP-Ribosylierung wieder zu entfernen, was eine Dynamik dieser posttranslationalen Modifikation impliziert. Zusammenfassend stellen die hier präsentierten Ergebnisse eine Basis für zukünftige Forschung dar, welche die physiologische Relevanz von Mono-ADP-Ribosylierung in eukaryotischen Zellen zum Thema hat.

Introduction

“Imagination is more important than knowledge. For knowledge is limited, whereas imagination embraces the entire world, stimulating progress, giving birth to evolution.”

A. Einstein

Posttranslational modifications: in control of *everything*

To get a first impression of the relevance of posttranslational modifications (PTMs), one can search PubMed for “posttranslational modification” and come up with approximately 40,000 articles. Over the past decades, it has become apparent that PTMs regulate basically everything that occurs in cells. Whether it is degradation of unwanted proteins, directing of proteins to different organelles or regulation of DNA accessibility, PTMs take care of it all. PTMs occur in different variants, ranging from the smaller ones like phosphorylation to the modification of proteins with small proteins like ubiquitin. Complexity is added to this system by enzymes that can selectively remove modifications or by proteins that contain binding modules for specific modifications. Some of the best characterized PTMs are described below by highlighting some exemplary enzymes for each class of PTM, although a lot more PTMs exist than can be discussed within the scope of this thesis.

Phosphorylation performed by GSK3 β

Phosphorylation is a well-studied PTM, in which the γ -phosphate is transferred by a protein kinase from ATP onto a serine, threonine or tyrosine of a substrate. Glycogen synthase kinase 3 β (GSK3 β) was initially identified as the kinase phosphorylating glycogen synthase (Embi et al., 1980) and was shown to be serine/threonine specific. Later on it became clear that it phosphorylates multiple other proteins, thereby influencing a diversity of signaling networks (Cohen and Frame, 2001). A prominent role of GSK3 β is for instance phosphorylation of β -catenin, an event that will lead to ubiquitination of β -catenin and its subsequent proteasomal degradation (Wu and Pan, 2010). GSK3 β has been reported to influence processes as diverse as immunity (Beurel et al., 2010), cancer (Mills et al., 2011) and neuronal processes (Grimes and Jope, 2001). A closer look at the catalytic mechanism of GSK3 β reveals a complex substrate binding pattern, in which a so-called priming phosphorylation docks into the priming phosphate site, upon which GSK3 β is able to phosphorylate a second site (Dajani et al., 2001; Frame et al., 2001). An example of a primed GSK3 β substrate is the transcription factor MYC. After phosphorylation of serine 62 by ERK or CDKs, GSK3 β modifies threonine 58. This will lead to MYC activation but also K48-linked ubiquitination and subsequent proteasomal degradation (Adhikary and Eilers, 2005; Vervoorts et al., 2006). There are known exceptions to the substrate recognition mechanism through priming phosphorylations however, as there are also descriptions of proteins being modified by GSK3 β although not carrying a priming phosphate, such as presenilin-1 (Twomey and McCarthy, 2006). It is not clear for some of the identified substrates whether they are also being modified in cells or are only *in vitro* substrates as reviewed in (Sutherland, 2011).

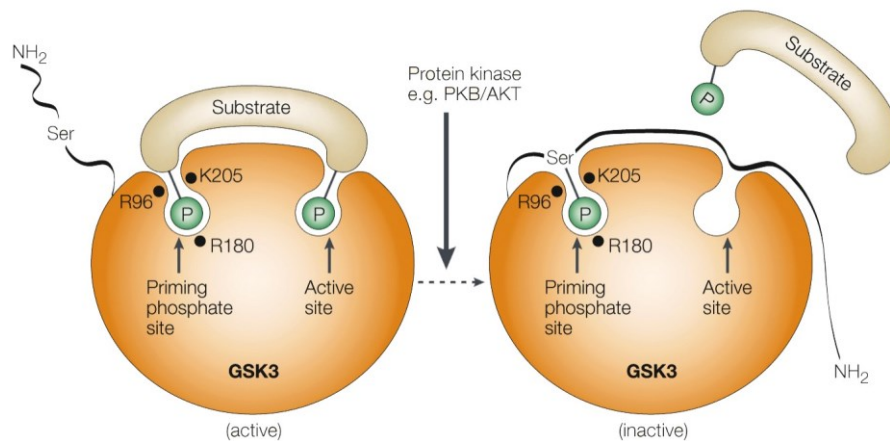


Figure 1 Schematic representation of the catalytic mechanism of GSK3 β . Upon binding of the priming phosphate into the priming phosphate site, GSK3 β phosphorylates a second site. Phosphorylation of serine 9 by e.g. AKT, will lead to folding of the N-terminus onto the catalytic site and occupation of the priming phosphorylation site, thereby inactivating GSK3 β . Modified from (Frame and Cohen, 2001).

The best-characterized GSK3 β inhibitory mechanism makes use of this priming phosphorylation substrate recognition, as phosphorylation of serine 9 can serve as pseudo-substrate, which is schematically depicted in Figure 1 (Frame et al., 2001). The flexible N-terminus will fold back onto the kinase domain, with the phosphorylated serine 9 extending into the priming phosphate site, thereby preventing other substrates from being phosphorylated. Upon mitogenic stimuli, PI3K is activated, which in turn activates Akt/PKB, leading to serine 9 phosphorylation of GSK3 β (Cross et al., 1995). Other GSK3 β inhibitory mechanisms are indirect, as is for example the case in Wnt signaling. GSK3 β is normally present in the β -catenin destruction complex, containing amongst others Axin, GSK3 β and β -catenin, where GSK3 β phosphorylates β -catenin upon priming phosphorylation by CKI (Amit et al., 2002), leading to its subsequent ubiquitination and degradation by the 26S proteasome. Upon binding of Wnt to its receptors, Axin and GSK3 β are recruited there to phosphorylate several other proteins and thus β -catenin is free to translocate into the nucleus, as reviewed in (Wu and Pan, 2010).

Moreover, diverse phosphatases have been discovered that are able to remove the phosphate groups again, making phosphorylation a highly dynamic PTM. An example thereof is the necessity of dephosphorylation of the C-terminal domain of RNA Pol II at transcription termination to allow RNA Pol II recruitment to a new pre-initiation complex as summarized in (Moorhead et al., 2007). Research of phosphorylation has evolved quite far, with first papers mapping single modification sites being hot topics but nowadays complete phosphoproteome analysis using mass spectrometric methods such as SILAC is becoming more common (Mann, 2006). Several other tools exist that facilitate the study of phosphorylation, such as [32 P]- γ -ATP or phospho-specific antibodies.

The importance of phosphorylation for normal cellular physiology is underlined by a number of diseases that have been linked to disturbed phosphorylation in one way or another. In chronic myeloid leukemia for instance, the tyrosine kinase ABL is often reported hyperactive, caused by fusion of the *Abl1* gene to the *breakpoint cluster region* on the so-called Philadelphia chromosome, leading to the production of a BCR-ABL fusion protein (Melo, 1996) The pharmaceutical industry has implemented this knowledge and has developed a specific inhibitor for BCR-ABL, Gleevec and follow-up substances such as dasatinib, which is successfully being employed in the clinic (Cook et al., 2002; Sawyers et al., 2002). Adaptation of cancer cells, often by acquiring a point mutation in the ATP binding site in ABL and consequentially resistance against the therapies, are occurring frequently (Radich et al., 2006).

Ubiquitination by SCF^{FBW7}

The ubiquitination system seems to be even more complex than phosphorylation, considering the fact that at least 3 enzymes are involved in the attachment of ubiquitin to target proteins. The E1 enzyme, also known as ubiquitin-activating enzyme (UBA), activates ubiquitin by binding it to its active site cysteine, a process that uses ATP. The activated ubiquitin is subsequently transferred to the cysteine of an E2 enzyme, alternatively called ubiquitin-conjugating enzyme (UBC). Finally, the E2 will bind an E3 ligase to transfer the ubiquitin onto a substrate (Figure 2)(Hershko and Ciechanover, 1998). 4 major classes of E3s exist, the HECT, RING-finger, U-box and Phd-finger types, with a further subdivision of the RING-finger type ligases as reviewed in (Nakayama and Nakayama, 2006).

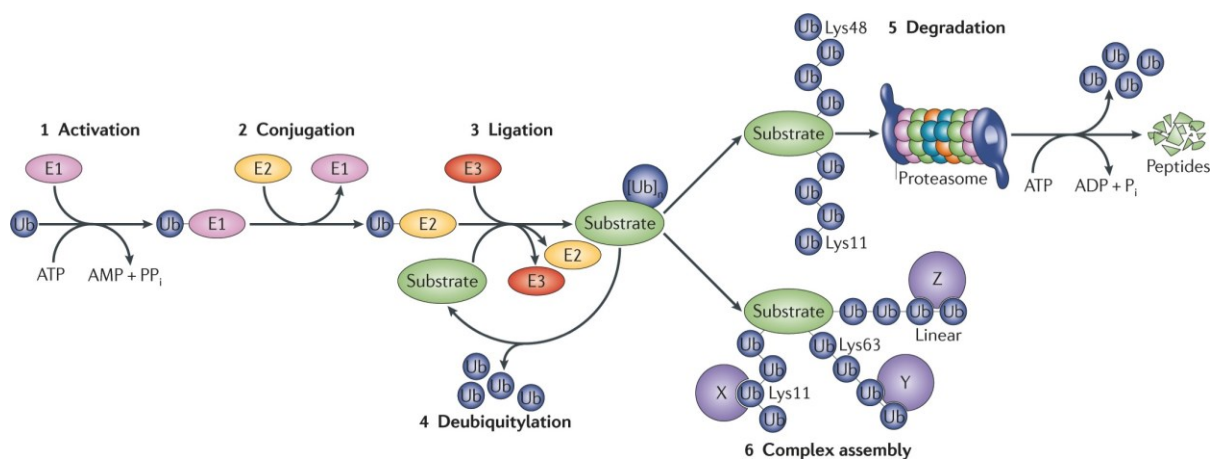


Figure 2 Representation of the ubiquitin conjugation system. An E1-enzyme activates ubiquitin and transfers it to an E2-enzyme. The E2 ubiquitin-conjugating enzyme will then transfer ubiquitin to a target protein assisted by the E3 ligase. This leads to diverse functional consequences such as degradation or recruitment of other proteins. Modified from (Vucic et al., 2011).

Ubiquitin is a small protein of 76 amino acids and was discovered in 1975 by later Chemistry Nobel Prize winners Hershko, Ciechanover and Rose, reviewed in (Hershko and Ciechanover, 1998). It has long been thought that ubiquitin can only be linked through lysine 48 of ubiquitin, with the typical consequence of substrate protein degradation (Figure 2). Later on it became clear that ubiquitin chains linked via lysine 63 do not lead to protein degradation, but have been reported to regulate protein-protein interactions and protein trafficking (Chen and Sun, 2009). Nowadays it is believed that all 7 lysine residues present in ubiquitin can be used to build chains, as for example demonstrated by mass spectrometry (Xu et al., 2009). It is however not clear yet which roles the diverse ubiquitin linkages may have. Ubiquitin is a dynamic PTM, because deubiquitinating enzymes exist that can remove the ubiquitin chains (Figure 2). Ubiquitination is thought to be highly regulated, both spatially and temporally (Grabbe et al., 2011), partially also by ubiquitination of essential components (Weissman et al., 2011).

It has previously been suggested that the E3 ligases are responsible for substrate specificity on their own, but it has become clear that they often work together with their E2 enzymes or even larger complexes, sometimes needing a specific “priming” phosphorylation or other PTMs to recognize a substrate, such as the WWE-domain containing E3 ligase Iduna/RNF146 that was reported to bind to poly-ADP-ribosylated Axin only, upon which Axin gets ubiquitinated with K48-linked ubiquitin and degraded (Zhang et al., 2011). Another example of E3 ligases with peculiar substrate specificity is formed by the SCF complex ligases. As depicted in Figure 3A, multiple components are responsible for substrate modification (Welcker and Clurman, 2008).

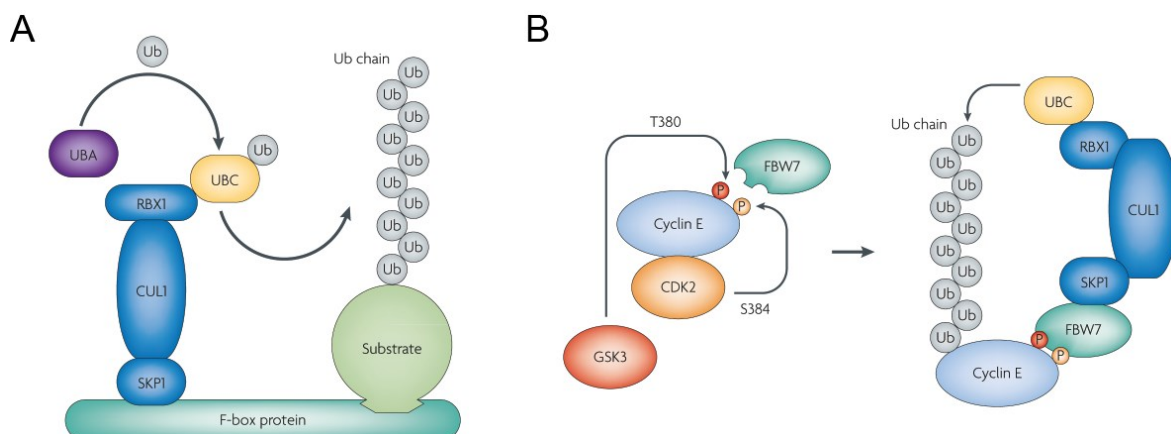


Figure 3 Modification of proteins by the SCF ubiquitin ligases. (A) Multiple complex-components work together for substrate modification by SCF E3-ligase complexes. (B) Representation of the modification of Cyclin E by SCF^{FBW7}, where SCF^{FBW7} recognizes a specific phospho-epitope. Modified from (Welcker and Clurman, 2008).

The F-box protein is the substrate-recognition part of the SKP1-Cul1-RBX1 (SCF) complex. RBX1 binds to the UBC, previously loaded with ubiquitin, and modifies the substrate protein. FBW7 however also binds to the substrate, bringing it into the right spatial conformation for modification to take place. The K48-linked ubiquitination performed by this complex leads to subsequent proteasomal degradation of the target proteins. Especially interesting about FBW7 is the so-called Cdc4-phosphodegron (CDP) that it recognizes, which contains two phosphorylated residues 4 spaces apart (Orlicky et al., 2003). Cdc4 is the budding yeast homolog of FBW7 and was reported to recognize a conserved phospho-epitope on its substrates. This recognition preference links FBW7 activity to GSK3 β activity (Figure 3B). Because GSK3 β usually needs a priming phosphate, the primed sites modified by GSK3 β will form a FBW7 recognition epitope (Welcker et al., 2004). In a way this makes sense, because GSK3 β activity is high in absence of mitogenic signaling. Cells thus downregulate proteins important for proliferation such as MYC (Welcker et al., 2004), which is an obvious response to an environment with low mitogenic stimuli. This mechanism provides an interesting crosstalk between phosphorylation and ubiquitination. Because of its ability to control several proto-oncogenes, FBW7 has become known as a tumor suppressor that is indeed deregulated in certain tumors (Minella and Clurman, 2005). Other diseases, such as Alzheimer's (Riederer et al., 2011), have also been linked to disruptions in the ubiquitin conjugation system, indicating that a correct functioning ubiquitin system is essential for normal cellular homeostasis.

ADP-ribosylation

ADP-ribosylation is a posttranslational modification where, as the name already implies, ADP-ribose is attached to substrate proteins. In this process, β -NAD⁺ is used as co-factor by ADP-ribosyltransferases that attach ADP-ribose onto an amino acid side chain of a substrate, thereby releasing nicotinamid (NAM) (Hassa et al., 2006). Alternatively, ADP-ribose can be transferred onto an acetyl group to generate free O-acetyl-ADP-ribose. This takes place during the deacetylation of lysines by enzymes of the SIRT family of β -NAD⁺-dependent deacetylases (Denu, 2005; Tong and Denu, 2010; Zhao et al., 2004). β -NAD⁺ is however probably best known for its role as cofactor in several other processes such as redox reactions and as cyclic ADP-ribose precursor as reviewed in (Magni et al., 2004; Massudi et al., 2012; Ziegler, 2000). One should thus keep in mind that through ADP-ribosylation not only the modified proteins are influenced, but that a link exists to a multitude of other processes that might also be influenced upon activation of ADP-ribosyltransferases. The intracellular β -NAD⁺ concentration is estimated to be around 500 μ M (Dolle et al., 2010), extracellular β -NAD⁺ levels in human plasma are estimated to be in the 50-60 nM range (Zocchi et al., 1999). Extracellular NAD⁺ has long been thought to originate from dying cells, but it has been shown that there are also channels that can transport NAD⁺ across the membrane of viable cells (Bruzzone et al., 2001). The role of extracellular NAD⁺ is not entirely clear yet although it has been reported to have an immune modulating role as reviewed in (Haag et al., 2007).

The ARTC family of proteins, where the abbreviation ARTC is derived from ADP-ribosyltransferase cholera toxin-like, encompasses membrane-bound extracellular mono-ADP-ribosyltransferases that mono-ADP-ribosylate other membrane-bound proteins or secreted factors (Hottiger et al., 2010). It was for example reported that ARTC2 mono-ADP-ribosylates an arginine of P2X7 (Seman et al., 2003), which is the initiation of a series of signaling events culminating in apoptosis. This was described as the cause for NAD⁺-induced cell death (NICD) (Koch-Nolte et al., 2006). Interestingly, ARTC2 can be released from activated T-cells mediated by metallo-proteases, a process during which ARTC2 retains activity (Kahl et al., 2000). It is currently unknown whether the secreted enzyme could also be taken up again by neighboring cells, akin to the mechanism used by some bacterial toxins. Intracellular ADP-ribosylation is performed by ADP-ribosyltransferases of the ARTD protein family.

The ARTD family

Eukaryotic intracellular ADP-ribosylation is carried out by enzymes of the ARTD family, identified based on the characteristic ADP-ribosyltransferase (ART) domain they all contain (Schreiber et al., 2006). Formerly known as the PARP family, the nomenclature has recently been changed to better fit their mechanism of catalysis (Hottiger et al., 2010) as explained in more detail below. This protein

superfamily can be further subdivided based on diverse criteria. One of the major differences between the enzymes is the type of ADP-ribosylation performed. Class I enzymes are capable of forming poly-ADP-ribose (PAR)-chains on their substrates, whereas class II enzymes can transfer mono-ADP-ribose only and members of class III have no reported transferase activity at all (Kleine et al., 2008).

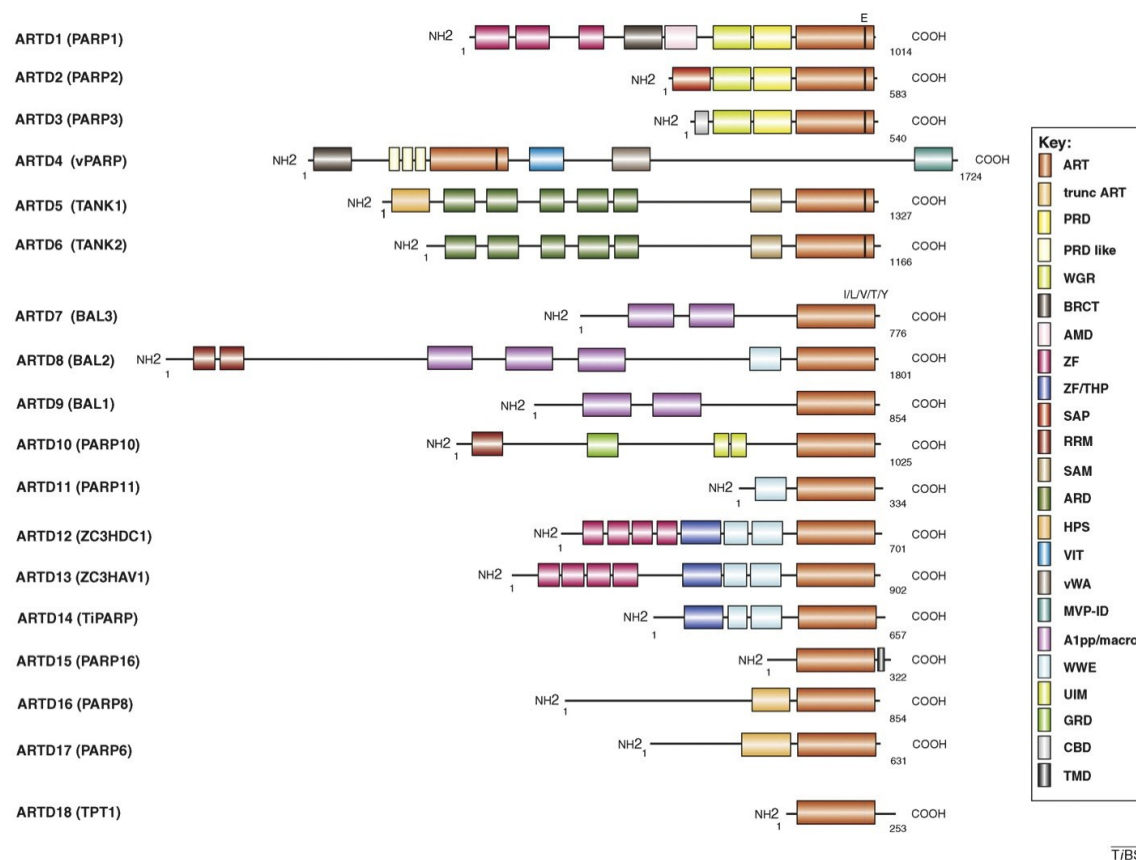


Figure 4 Summary of the ARTD family of enzymes. Schematic representation of the ARTD superfamily with previous protein names given in brackets. Depicted domains are: ART: ADP-ribosyltransferase; PRD: PARP regulatory domain; WGR domain: conserved central motif W-G-R; BRCT: BRCA1 carboxy-terminal domain; AMD: automodification domain; ZF: zinc finger; ZF/THP: zinc finger/TiPARP homologous domain; SAP: SAF/Acinus/PIAS DNA-binding domain; RRM: RNA recognition motif; SAM: sterile alpha motif; ARD: ankyrin repeat domain; HPS: histidine-proline-serine region; VIT: vault protein inter-alpha-trypsin domain; vWA: von Willebrand type A domain; MVP-ID: Major-vault particle interaction domain; A1pp/macro: A1pp or macrodomain; WWE: conserved residues W-W-E; UIM: ubiquitin interaction motif; GRD: glycine-rich domain; CBD: central binding domain; TMD: trans-membrane domain. Depicted in black within the ART-domains are the catalytic glutamates of ARTD1-6. Modified from (Hottiger et al., 2010).

The schematic representation in Figure 4 of the proteins within the ARTD family shows that a multitude of different domains are present. Ranging from ADP-ribose interaction modules like the WWE-domains to DNA interaction motifs like the zinc fingers to ubiquitin interaction motifs in ARTD10. Thus outside of the catalytic domain these enzymes are highly dissimilar. This is also reflected in the different pathways that are influenced by the different ARTD enzymes as exemplified in the following.

ARTD1, formerly known as PARP1, is the founding member of this protein superfamily and has thus been studied most extensively. It is renowned for its role in DNA damage repair, but also in controlling chromatin and transcription (Hassa et al., 2006; Krishnakumar and Kraus, 2010). In addition to ARTD1, ARTD2 also participates in DNA repair and *Artd1/Artd2* double knockout animals do not survive (Menissier de Murcia et al., 2003; Schreiber et al., 2002). In *BRCA1*-negative breast cancer, tumor cells rely on ARTD1 for DNA damage repair (Ashworth, 2008). This is being utilized in the clinic, where ARTD1 is inhibited with for example olaparib, leading to death of the cancer cells specifically, an effect that is enhanced when used in combination with DNA-damaging agents such as cisplatin (Jagtap and Szabo, 2005). These therapies are currently being extended to other cancers as well, hinting at the possible future possibilities of ARTD inhibitors (Javle and Curtin, 2011; Sandhu et al., 2011). Moreover, additional compounds inhibiting not only ARTD1, but targeting for example also ARTD5 are currently being developed (Wahlberg et al., 2012). ARTD1 has also been suggested to function in other signaling networks such as NF- κ B signaling and apoptosis, although the molecular mechanisms remain largely unclear (Hassa and Hottiger, 2002; Schreiber et al., 2006). Not only ARTD1 has been implicated in immunity, but for example ARTD13 as well (Welsby et al., 2012).

The role of ARTD5 in Wnt-signaling was identified quite recently. It was shown that ARTD5 synthesizes PAR chains on Axin, leading to its degradation and subsequent increased β -catenin signaling (Huang et al., 2009) as usually happens upon activation of Wnt signaling through spatial regulation of GSK3 β and Axin (McNeill and Woodgett, 2010). By employing a synthetic compound, XAV939, ARTD5 was inhibited in this study, leading to Axin-stabilization and subsequent reduced Wnt-signaling. Later on, Iduna was identified as E3 ubiquitin ligase binding to the PAR chains on Axin. Ubiquitination of Axin by Iduna then targets Axin for degradation (Zhang et al., 2011). Previously, ARTD5 and ARTD6 were identified as interaction partner of TRF1, a negative regulator of telomerase, which inhibits telomerase function (Cook et al., 2002; Smith et al., 1998). Phosphorylation of ARTD5 by polo-like kinase 1 (PLK1) stabilizes ARTD5, thereby increasing telomeric ART activity (Ha et al., 2012). Additionally, ARTD5 and ARTD6 control the stability of the adaptor 3BP2, mutations of which are mechanistically linked to Cherubism, a syndrome characterized by progressive loss of bone in the jaws and accumulation of inflammatory tissue (Guettler et al., 2011; Levaot et al., 2011). ARTD6 binds to 3BP2 through its ankyrin repeat and a targeting sequence in 3BP2 and poly-ADP-ribosylates it (Figure 5). This leads to subsequent poly-ubiquitination by Iduna and proteasomal degradation. In Cherubism, the targeting sequence within 3BP2 is mutated and thus not recognized by ARTD6. The known functions of poly-ADP-ribosylation have recently been summarized, however the final conclusion drawn states that a lot of essential information is still lacking, such as a better knowledge of the intracellular targets and how they vary under different physiological conditions (Gibson and Kraus, 2012).

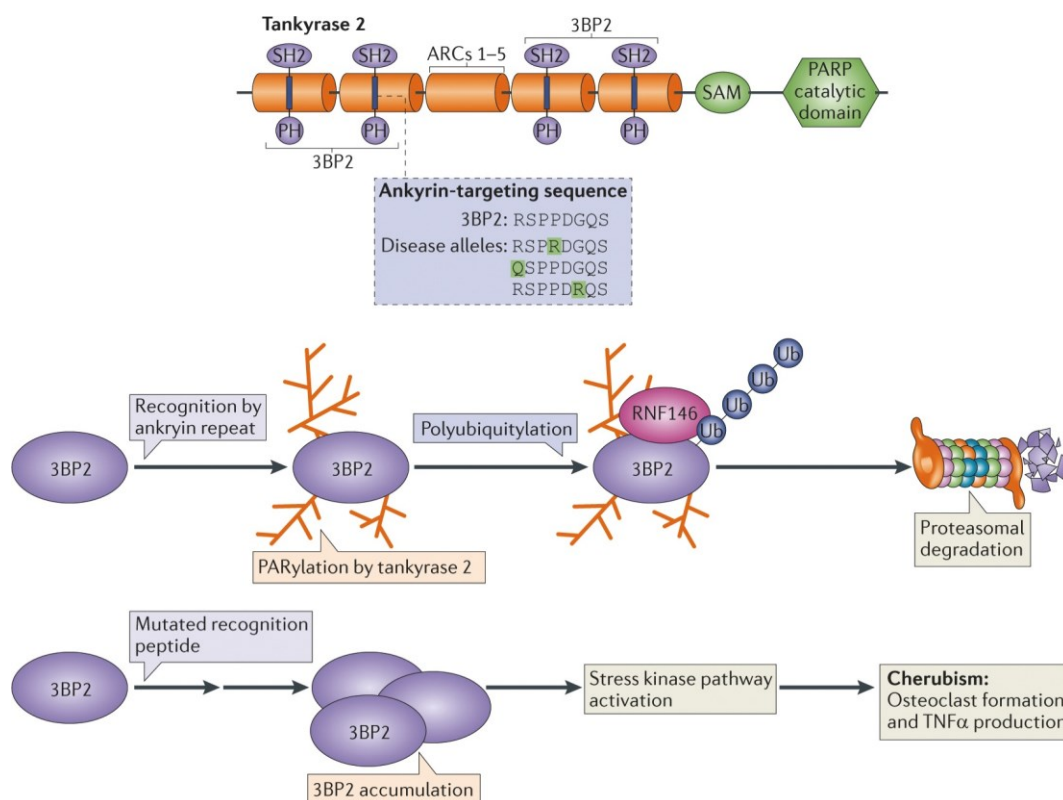


Figure 5 Consequences of modification of 3BP2 by ARTD6. ARTD6 (formerly Tankyrase 2) recognizes the recognition peptide present in 3BP2 and poly-ADP-ribosylates 3BP2, leading to its poly-ubiquitination by Iduna and subsequent proteasomal degradation. In Cherubism, the recognition sequence of 3BP2 is mutated and thus the protein is not ADP-ribosylated and becomes stabilized. Modified from (Gibson and Kraus, 2012).

ARTD7, -8 and -9, formerly BAL1, -2 and -3, or PARP9, PARP14 and PARP15, have been identified as risk factors in diffuse large B-cell lymphoma (Aguiar et al., 2005; Aguiar et al., 2000). They are unique within the ARTD family because of the macrodomains they share. ARTD9 lacks catalytic activity due to a change in the catalytic triad from H-Y-E in ARTD1 to Q-Y-T (Kleine et al., 2008), as described in more detail below, but has been shown to repress transcription in reporter gene assays, dependent on its macrodomains (Aguiar et al., 2005). ARTD9 shares a promoter with the E3-ligase B-cell aggressive lymphoma and BAL1 binding partner (BBAP) that is inducible by IFN γ , moreover it could be shown that the synthesized proteins shuttle into the cytoplasm together, most likely driven by an NES in BBAP (Juszczynski et al., 2006). Lymphoma cells transfected with ARTD7 upregulate several interferon-stimulated genes (ISGs) (Juszczynski et al., 2006). In support of a role for ARTD7-9 in lymphomagenesis is the proposed role of ARTD8 in IL-4 induced survival signaling, although it is not clear yet whether catalytic activity is necessary for ARTD8s capacity to regulate cellular metabolic rates and enhance glycolysis (Cho et al., 2011; Cho et al., 2009). ARTD8 actually has originally been identified as factor potentiating STAT6 mediated transcription and has accordingly been named co-activator of Stat6 (CoaSt6) in earlier studies (Goenka and Boothby, 2006). This seems to contradict the function of ARTD9 although the activation of STAT6-mediated transcription by

ARTD8 is no general effect since ARTD8 does not stimulate IFN γ -induced transcription (Goenka et al., 2007). ARTD8 has also been linked to gastric and colorectal cancers, because frame-shift mutations were found in the *ARTD8* gene in tumors with high microsatellite instability, that lead to a protein with intact macrodomains but lacking catalytic activity (Kim et al., 2011).

IFNs have also been linked to ARTD12, formerly known as PARP12 or ZC3HDC1. In a study of *alphavirae*, a noncytopathic *Venezuelan equine encephalitis virus* (VEEV) mutant was employed that is able to replicate in cells lacking IFN production (Atasheva et al., 2012). One of the genes that are upregulated during VEEV infection is the long isoform of ARTD12. ARTD12 exhibits an inhibitory effect on the replication of VEEV as well as on other alpha- and RNA viruses in this study (Atasheva et al., 2012). These findings are in accordance with an earlier publication wherein the role of ISGs was investigated and ARTD12 was found to counteract HCV infectivity (Schoggins et al., 2011), although only mentioned in the supplementary tables and not investigated mechanistically. These findings hint at a function for ARTD12 in viral immunity, although both papers are mainly descriptive and do not address whether for example catalytic activity is needed.

ARTD13, formerly known as ZAP or ZC3HAV1, is one of the ARTDs that lack catalytic activity (Kleine et al., 2008). Nevertheless, also for ARTD13 a role has been proposed in virus immunity, hence the name zinc-finger antiviral protein (ZAP). It was identified in a study wherein cells were transduced with retrovirus, followed by selection of virus-resistant clones. An antiviral cDNA was recovered, coding for ARTD13. Overexpression of ARTD13 leads to a loss of viral RNAs from the cytoplasm, indicating that ARTD13 is involved in antiviral immunity (Gao et al., 2002). ARTD13 gene expression is induced upon viral infection in an IRF3-dependent manner (Wang et al., 2010). The long isoform of ARTD13 contains not only the ART domain, but also a WWE-domain and a CCCH zinc finger-containing domain, which it shares with ARTD14 (formerly PARP7 or TipARP) and ARTD8 (Schreiber et al., 2006). The function of ARTD14 is also not clear yet, although it has been implicated in T-cell functions and contributes to tumor promotion upon its induction by 2, 3, 7, 8-tetrachlorodibenzo-*p*-dioxin (Ma et al., 2001). Mechanistically, the function of ARTD13 in virus immunity has been better investigated than the roles of the other mono-ARTDs described above. Through its zinc-fingers, ARTD13 binds to a broad range of different viruses as first described for the 3'LTR of the *Moloney murine leukaemia virus* (MMLV) and for a sequence in the genome of the *alphavirus* Sindbis (SINV) (Guo et al., 2004). Here it could also be shown that binding of RNAs is mainly mediated by zinc finger 2 and 4. The different viruses that ARTD13 can bind to are reviewed in (Welsby et al., 2012). ARTD13 interacts with the p72 DEAD box RNA helicase (DDX17), which is required for ARTD13-mediated RNA degradation (Chen et al., 2008) and although ARTD13 is inactive (Kleine et al., 2008), the longer isoform containing the ARTD domain displays an enhanced suppression of viruses (Kerns et al., 2008). ARTD13 binds to the RNA helicase RIG-I through its zinc

finger domain upon stimulation with 5'-triphosphate modified RNA (Hayakawa et al., 2011). This triggers RIG-I ATPase activity and oligomerization, which are both necessary for induction of NF- κ B activity. Accordingly, downregulation of ARTD13 reduced the response to influenza and Newcastle Disease virus infection (Hayakawa et al., 2011). Multiple reports indicate that ARTD13 synergizes with diverse ISGs to inhibit *alphavirae*, which could be a starting point for future studies to further define the underlying mechanism (Karki et al., 2012; MacDonald et al., 2007). Phosphorylation of ARTD13 by GSK3 β is suggested to enhance antiviral activity (Sun et al., 2012). Together, these reports indeed support a role of the mono-ARTDs in viral immunity, perhaps even independently of ART activity as in the case of ARTD13.

The only report on the function of ARTD15 states that it interacts with and modifies karyopherin- β 1, although it remains open what the consequence of mono-ADP-ribosylation is for the function of karyopherin- β (Di Paola et al., 2012). Additionally, the modification site within karyopherin- β is not investigated. The crystal structure of ARTD15 reveals that there is an α -helical domain next to the ART domain that does not resemble the regulatory domain of ARTD1, which was proposed to be important for ARTD15 regulation (Karlberg et al., 2012).

An interesting observation is that most of the functions unraveled so far for PAR chains depend on the recruitment of other proteins to those PAR chains, such as the E3 ubiquitin ligase Iduna, but have mostly not been reported to directly influence the proteins these chains are synthesized on. These reports show that the ARTDs are not only involved in DNA damage repair, but have diverse functions to fulfill as already suggested by the multitude of domains present in the different members. Unfortunately, most of the ARTD family members are currently poorly understood, especially the mono-ADP-ribosyltransferases such as ARTD10. The data on roles of the mono-ARTDs in intracellular pathways are very limited and mainly descriptive; the underlying mechanisms remain to be uncovered in future investigations.

ARTD10: a mono-ADP-ribosyltransferase

The mono-ADP-ribosylating enzyme that is currently characterized best, is the enzyme that is nowadays called ARTD10 (Hottiger et al., 2010). ARTD10 was known under a different name in the early days, namely p150. The reason for this name was an experiment, in which “p150” was identified as an interaction partner of the proto-oncoprotein MYC (Yu et al., 2005). It was reported that ARTD10 undergoes automodification and is able to modify core histones, but it could not be shown to modify MYC or its binding partner Max in this study. Independent of enzymatic activity, ARTD10 is capable of inhibiting MYC and E1A mediated co-transformation of rat fibroblasts, indicating a role for ARTD10 in proliferation. In support of a role of ARTD10 in proliferation is the finding that knockdown of ARTD10 using siRNA also leads to a disturbed cell cycle and disturbed proliferation rates (Chou et al., 2006). ARTD10 can be distinguished from the other ARTDs based on protein architecture (Schreiber et al., 2006).

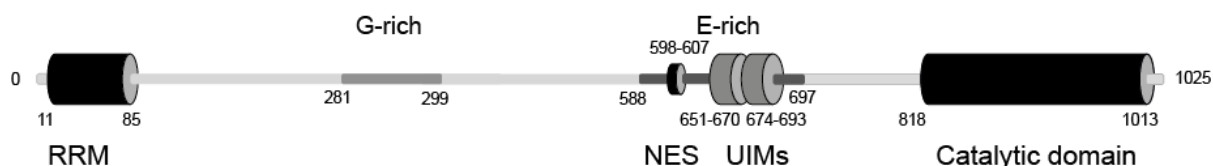


Figure 6 ARTD10 domain architecture. The domains that have been identified so far in ARTD10 are displayed, numbers indicate amino acids of human ARTD10. RRM: RNA recognition motif; G-rich: glycine rich region; E-rich: glutamate rich region; NES: nuclear export signal; UIM: ubiquitin interaction motif.

Apart from the characteristic catalytic domain, ARTD10 contains an RNA recognition motif, two ubiquitin interacting motifs, a nuclear export sequence, a glycine-rich region and a glutamate-rich region (Figure 6). None of these domains have been investigated in more detail as yet, apart from the nuclear export sequence and the catalytic domain, so it is not clear currently which functions they mediate. Detailed investigations of the catalytic mechanism of ARTD10 revealed that, in contrast to its name at the time, poly-ADP-ribose polymerase 10, ARTD10 is capable of transferring only one ADP-ribose moiety (Kleine et al., 2008). The loop connecting β -strands 4 and 5 is shorter in ARTD10 than in the poly-ARTDs, which is proposed to account for a higher substrate specificity of ARTD10 than for example ARTD1. ARTD10 shares this short loop with the other mono-ARTDs (Kleine et al., 2008).

Investigation of different cell lines has shown that ARTD10 is highest expressed in hematopoietic tissues, although RNA transcripts were found in a broad range of cell types (Yu et al., 2005). ARTD10 is a cytoplasmic protein and shuttles out of the nucleus in a Crml1-dependent manner (Yu et al., 2005). These findings were further validated and expanded by studying overexpressed protein, that localizes to cytoplasmic bodies of unknown nature that are highly dynamic and wherein ARTD10 colocalizes

with p62 and poly-ubiquitin (Kleine et al., 2012). p62 is an ubiquitin-binding adaptor protein targeting ubiquitinated proteins for degradation by autophagy (Johansen and Lamark, 2011), but it remains unclear whether ARTD10 has an active role to play in autophagy or whether it is being degraded itself through autophagy. ARTD10 could for example be ubiquitinated itself and targeted to the autophagosomes, it could however also bind to ubiquitinated proteins through its UIMs and deliver those to the autophagosomes. Moreover, it is currently unknown whether certain stimuli such as stress or mitogens can induce localization of ARTD10 to different structures.

Another study identified ARTD10 as protein interacting with an avian influenza virus non-structural protein, NS1 (Yu et al., 2011). The region of interaction was mapped to both the glutamate-rich region and the catalytic domain of ARTD10. Overexpression of NS1 not only led to accumulation of ARTD10 in the nucleus, but also to a downregulation of endogenous ARTD10. Lastly, it was shown that apparently combined NS1 overexpression and knockdown of ARTD10 lead to an increase of cells in the G2-M phase of the cell cycle from 10% in controls cells to 45% in NS1 overexpressing/ARTD10 knockdown cells. NS1 overexpression or ARTD10 knockdown alone could not produce this effect (Yu et al., 2011). In a study where the antiviral properties of ARTD12 were analyzed, ARTD10 could also be identified as ARTD that inhibits VEEV replication, although not as efficiently as ARTD12 or ARTD7. The authors postulate that this might be due to RNA binding through the zinc fingers in ARTD7 and ARTD12 and the RRM in ARTD10 (Atasheva et al., 2012), although they do not follow up on this hypothesis in the current publication.

The posttranslational regulation of ARTD10 has been investigated in only one publication so far. Chou and colleagues identified a phosphorylation site in ARTD10, threonine 101, which is phosphorylated by cyclin E/CDK2. The phosphorylated form of ARTD10 could only be detected in the nucleus in late G₁ to S-phase of the cell cycle (Chou et al., 2006). In *in vitro* assays, phosphorylated ARTD10 possesses higher catalytic activity (Chou et al., 2006). The influence of phosphorylation on threonine 101 on catalytic activity could not be reproduced however (H. Kleine, unpublished data). Moreover, a colocalization with RNA Pol II during mitosis could be noted. This phosphorylation disappears in growth-arrested cells (Chou et al., 2006). The same authors also knocked down ARTD10 mRNA using shRNA, which led to a decrease in cell number. This indicates that tightly regulated ARTD10 levels are vital for normal cell physiology, as it was shown before that overexpression of ARTD10 also leads to decreased cell numbers in colony formation assays (Kleine et al., 2008).

Several other studies however have found the *ARTD10* mRNA level up- or downregulated under certain experimental conditions. Upon treatment of peripheral blood mononuclear cells with live *Borrelia burgdorferi*, but not borrelial lysates, *ARTD10* mRNA was found to be upregulated, as well

as *ARTD8* mRNA (Salazar et al., 2009). In sooty mangabeys *ARTD10* mRNA was reported upregulated 7 days after infection with *simian immunodeficiency virus* (SIV), together with an upregulation of *ARTD8*, *ARTD9* and *ARTD11* mRNA (Bosinger et al., 2009). By using whole-genome microarrays and subsequent promoter reporter gene constructs, *ARTD10* was identified as gene upregulated by interferon- α (IFN α) treatment. *ARTD10* was one of the genes upregulated after 16 hours of treatment but not after 6 hours, which makes it part of a late response. This late response hints at an as yet unidentified indirect regulatory mechanism. The same study also identified the *Newcastle disease virus* (NDV) as potent *ARTD10* mRNA inducing agent, in contrast to several other tested DNA and RNA viruses that could not induce *ARTD10* mRNA upregulation (Mahmoud et al., 2011). *ARTD10* and *ARTD12* were both reported to belong to the proteins present in red blood cells (D'Alessandro et al., 2010). On the contrary, *ARTD10* mRNA was downregulated in THP-1 macrophages treated with oxidized low-density lipoprotein (Kang et al., 2009). Additionally, knockdown of *ARTD10* in primary hepatocytes leads to decreased apolipoprotein B levels (Shen et al., 2012), both articles thus linking *ARTD10* to lipid metabolism. Transcriptome analysis in bovine endometrium revealed *ARTD10* as gene differentially regulated during the estrous cycle (Bauersachs et al., 2008; Mitko et al., 2008). Finally, *ARTD10* is one of the genes upregulated in invasive functional pituitary adenomas but not in non-invasive pituitary adenomas (Galland et al., 2010). Since these studies were not aimed at investigating *ARTD10* specifically, it remains open how up- or downregulation of *ARTD10* mRNA was achieved under the circumstances tested, moreover most of these data need to be validated. These findings suggest that ARTD10 might not only have a role to fulfill in the immune response, as has been suggested previously for several other mono-ARTDs, but also in lipid metabolism and possibly fertility and cancer.

The transcriptional regulation of *ARTD10* expression has not been studied so far, apart from the above-mentioned study that identified IFN α as cytokine indirectly inducing ARTD10 expression. The *ARTD10* gene has been mapped to the same chromosome as the *MYC* gene, at the tip of the long arm of chromosome 24 (8q24) (Yu et al., 2005). The murine *Artd10* gene was analyzed in more detail and was described to share its most 3'- exons, exon 10 and 11 with the neighboring gene, *Plectin1*. Moreover it was proposed that intron 9 of *Artd10* contains a promoter of the *Plectin1* gene. Although the murine gene was studied, the described overlap with *Plectin1* is also present in rat and human genomes. Lastly, conservation throughout the species was studied. The *ARTD10* gene was found in multiple vertebrates, but not in any invertebrates, indicating that ARTD10 has evolved in the vertebrate lineage (Lesniewicz et al., 2005). It has not been studied yet how the *ARTD10* promoter is regulated or whether the overlap with the *PLECTINI* gene has further consequences. The ARTD10 protein however has been utilized as proto-type mono-ADP-ribosyltransferase to investigate the catalytic mechanism employed by these enzymes in more detail.

Mechanistic insights into ADP-ribosylation

The functional consequence and molecular mechanism of ADP-ribosylation, is currently best understood not for eukaryotic ADP-ribosylation, but for prokaryotic ADP-ribosylation. Pertussis toxin, produced by *Bordetella pertussis*, exists of 5 subunits and can be taken up by target cells through receptor-mediated endocytosis. The enzymatically active S1 subunit modifies the α -subunit of trimeric G proteins in cells, leading to a disturbance of cellular processes as reviewed in (Locht et al., 2011). The first toxin that was identified as ADP-ribosyltransferase is diphtheria toxin, a secreted protein produced by the bacterium *Corynebacterium diphtheriae*. The protein can be divided in three domains, a catalytic, a translocation and a receptor-binding domain. Through the receptor-binding domain, it can bind to and enter most human cell types. Required for activity is cleavage of the toxin in an endosomal compartment, releasing the N-terminal catalytic domain into the cytosol aided by its translocation domain (Collier, 2001). Inside the cells, diphtheria toxin mono-ADP-ribosylates eukaryotic elongation factor 2 (eEF2) (Webb et al., 2008). ADP-ribosylation disturbs its association with other proteins and thus blocks protein synthesis.

The bacterial endotoxins can be subdivided into two different subclasses based on the amino acids in their catalytic center that are involved in catalysis (Hottiger et al., 2010). The first group contains a histidine, tyrosine and glutamate (H-Y-E) residue that interact with the NAD^+ -moiety, the second group contains an arginine, serine and glutamate (R-S-E) that are necessary for NAD^+ -binding (Figure 7). Amongst others, diphtheria toxin belongs to the first class while pertussis toxin belongs to the second class. Toxins of the H-Y-E class have been demonstrated to modify glutamate residues whereas toxins of the R-S-E class modify arginine residues. Based on this, the eukaryotic ADP-ribosylating enzymes were also subdivided: the ARTC class for ADP-ribosyltransferase cholera toxin-like and the ARTD enzymes, the ADP-ribosyltransferases diphtheria toxin-like, with corresponding catalytic triad (Hottiger et al., 2010).

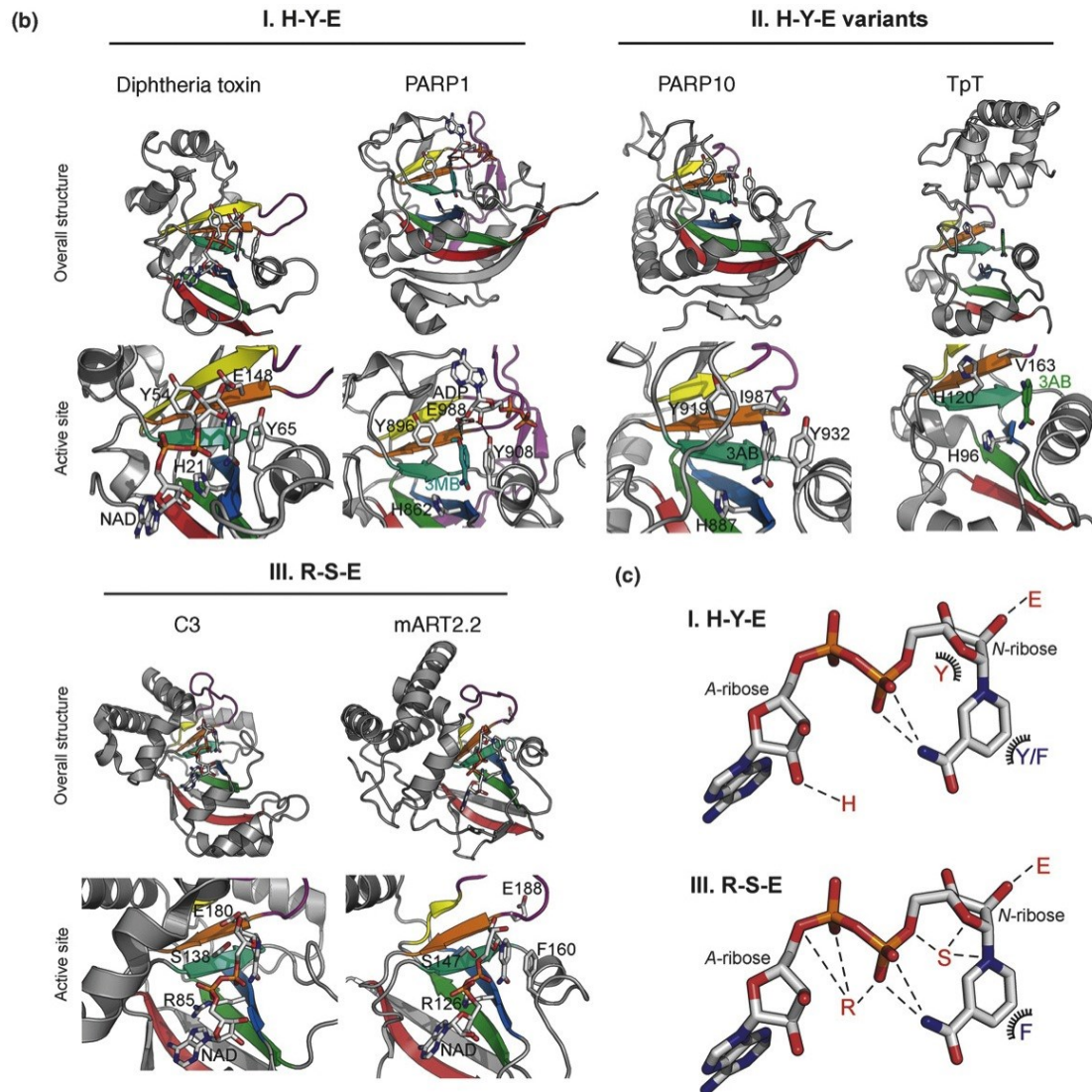


Figure 7 Structural alignments of the conserved elements of ADP-ribosyl transferring catalytic domains. Category I contains the poly-ADP-ribosylating enzymes, exemplified by a comparison of ARTD1 with diphtheria toxin. Category II are the mono-ADP-ribosylating enzymes, where ARTD10 is compared with tRNA phosphotransferase. Category III enzymes are the ecto-ADP-ribosylating enzymes, where ARTD2 compared with C3 exotoxin. In III, the interaction of NAD^+ with the residues of the H-Y-E and R-S-E motifs are displayed schematically, with interacting residues labeled in red. Modified from (Hottiger et al., 2010).

Eukaryotic intracellular poly-ADP-ribosylation was first described in 1963 (Chambon et al., 1963), subsequently its crystal structure was solved and finally, more than 20 years after the initial discovery of PAR, the gene for ARTD1 was identified as reviewed in (D'Amours et al., 1999). Nowadays, several enzymes with ADP-ribosyltransferase activity have been identified as described above and a distinction has been made between enzymes that can transfer multiple ADP-ribose moieties onto a substrate and the ones that can transfer only one ADP-ribose (Kleine et al., 2008). The poly-ADP-ribosylation process has been researched relatively well and can be divided into three parts, initiation, elongation and branching as reviewed elsewhere (Diefenbach and Burkle, 2005). As described above

for the bacterial toxins, the catalytic residues H-Y-E of the eukaryotic intracellular transferases are responsible for NAD^+ -binding and subsequent transfer of ADP-ribose onto substrates.

The mono-ADP-ribosyltransferases all lack the glutamate of the H-Y-E triad that is necessary to support the oxacarbenium ion transition state arising during catalysis (Kleine et al., 2008). It has been proposed that these enzymes use a glutamate of their substrates instead to stabilize the reaction in a process called substrate-assisted catalysis. During this process, these glutamates not only stabilize the reaction, but also get modified (Figure 8).

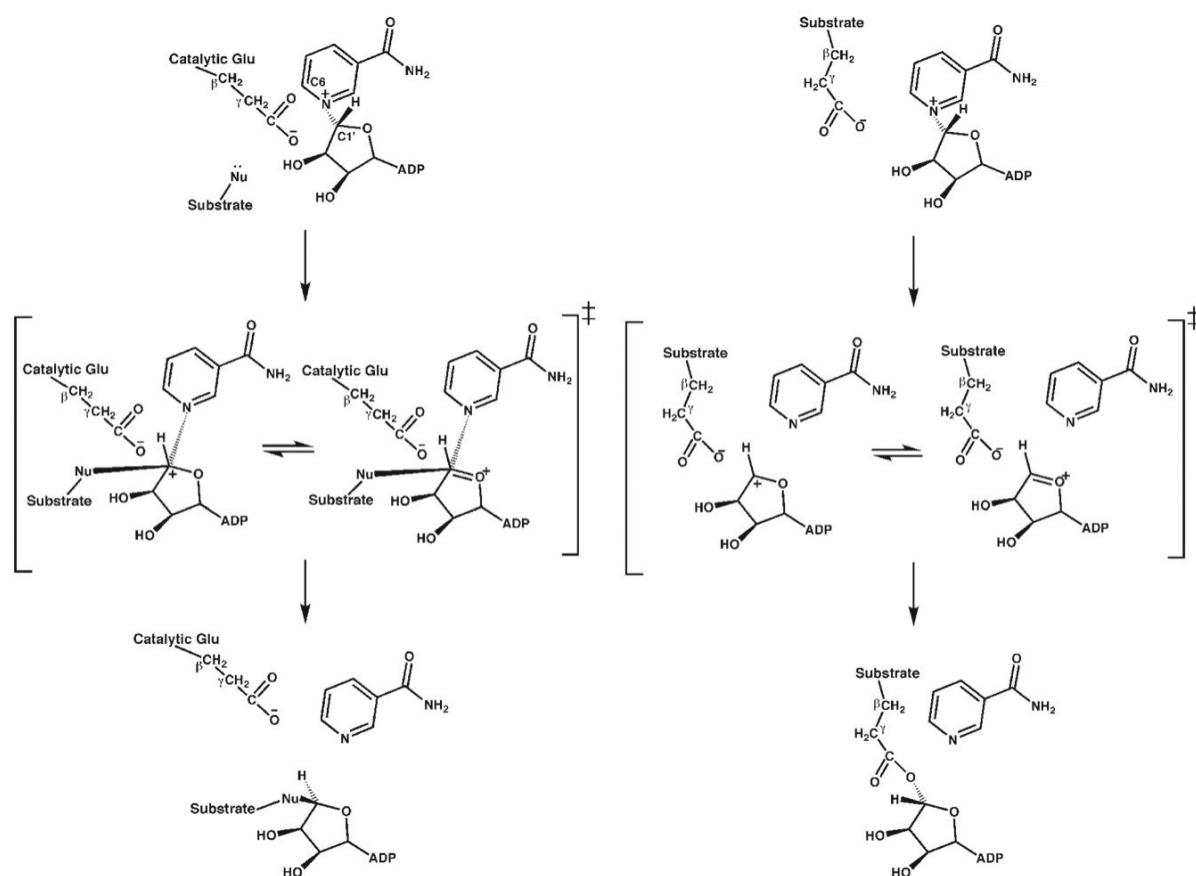


Figure 8 Representation of the catalytic mechanism of the poly-ARTDs and the mono-ARTDs. The poly-ARTDs contain a catalytic glutamate as represented on the left. The mono-ARTDs lack this glutamate as depicted on the right and were proposed to employ their substrates glutamate to stabilize the oxacarbenium ion transition state that arises during catalysis. This glutamate not only stabilizes the reaction in this model, but is also the ADP-ribose acceptor amino acid. Modified from (Kleine et al., 2008).

This explains why these enzymes transfer only one ADP-ribose moiety onto substrates, because once the substrates glutamate has been modified, it cannot assist in catalysis anymore (Kleine et al., 2008). In agreement with this, *in vitro* assays with ARTD10 and its substrate H2B revealed glutamate 2 of the histone tail as modification site using mutagenesis (Moyle and Muir, 2010), although it is suggested in

this study that this is not the only modification site in H2B. This process has not been accepted as a general mechanism for all mono-ADP-ribosyltransferases of the ARTD family yet, as it was reported recently that ARTD15 might actually modify serines or threonines, although no direct evidence was provided (Di Paola et al., 2012). Furthermore it is unclear how the catalytic mechanism would function in a reaction wherein serine or threonine function as acceptor sites. Taking a closer look at the attempts to distinguish which enzyme modifies what residue by what mechanism, it becomes clear that this is a very complicated issue with no satisfying explanation available yet.

To distinguish between the different amino acids as acceptor residues, neutral hydroxylamine treatment has been the most prominent tool so far. Neutral hydroxylamine has been described to disrupt not only the ester bond between acidic residues and ADP-ribose but also the ketamine bond between arginine or lysine and ADP-ribose, although with different kinetics (Moss et al., 1983). ADP-ribosylated proteins with a high susceptibility to neutral hydroxylamine treatment, with a half-life of about 3 minutes, are generally believed to be ester linkages between acidic residues and ADP-ribose whereas the half-life of arginine-ADP-ribose bonds is approximately one hour (Hsia et al., 1985). More stable is the bond between cysteine and ADP-ribose (Hsia et al., 1985). No eukaryotic intracellular enzymes have been identified so far that can ADP-ribosylate cysteines however.

Early papers have hinted at the presence of both modified arginines and glutamates in histone extracts as determined by diverse chemical approaches, where it was also noted that mono-ADP-ribosylation is the major modification taking place on histones rather than poly-ADP-ribosylation (Bredehorst et al., 1978; Burzio et al., 1979). Interestingly, a connection has been made between acetylation and ADP-ribosylation, as it could be shown that acetylated histone H4 subspecies have increased ADP-ribosylation compared to non-acetylated histones (Golderer and Grobner, 1991). In this report a distinction was also made between arginine and glutamate-linked ADP-ribosylation, which apparently were both present on histones in isolated nuclei from macroparasitidia (Golderer and Grobner, 1991).

Contradictory reports exist concerning the amino acids that are being modified by the intracellular ARTD enzymes. In ARTD1, mutation of the glutamates within an ARTD1 Δ BRCT construct, did not lead to abolished automodification, indicating that glutamic acid residues within ARTD1 at least are not the only acceptor sites. Moreover, since 30 minutes incubation with 1 M neutral hydroxylamine did not lead to release of the modification, the authors conclude that lysines or arginines are the acceptor sites instead of acidic residues. Upon mutation of K498, K521 and K524, automodification was significantly decreased, implying that these lysines are the sites automodified by ARTD1 (Altmeyer et al., 2009). The same group also identified lysines on ARTD2 as automodification and acetylation sites (Haenni et al., 2008). Contradicting these findings is a report on glutamates within ARTD1 as automodification site (Tao et al., 2009). Concerning substrates other than automodification,

reports exists on the modification of histones by ARTD1, in which certain lysines could be mapped as modification site by using electron transfer dissociation (ETD) mass spectrometry (Messner et al., 2010). For ARTD10, so far only glutamates have been identified as acceptor sites (Kleine et al., 2008; Moyle and Muir, 2010). Finally, ARTD15 supposedly modifies neither acidic nor basic residues, but threonine or serine instead (Di Paola et al., 2012). This was concluded since the automodification could not be removed by hydroxylamine treatment, nor by mercuric chloride, which would have disturbed an ADP-ribose-cysteine bond. Instead, the linkage seems destabilized by HCl treatment, which was reported before to disturb serine- or threonine-ADP ribose bonds (Cervantes-Laurean et al., 1995).

Matters are complicated by possible *in vitro* artifacts, in which for instance mutation of a certain site leads to a conformational change, in such a way that a modification site becomes covered or a binding surface is disturbed. This could lead to the false assumption that the mutated site is the modification site. Glycation, the process in which lysines can get modified non-enzymatically (Caldes et al., 2011; Cervantes-Laurean et al., 1996; Fedorova et al., 2010) complicates matters even further as it can lead to false positives. Finally, the lack of tools such as antibodies against mono-ADP-ribosylation on specific residues and the lack of reliable mass spectrometry methods make the identification of modification sites a real challenge.

Removing and reading ADP-ribosylation

Current understanding of the enzymes capable of removing ADP-ribose is not as extensive as current knowledge on e.g. the deubiquitinating enzymes and moreover, most research is directed at poly-ADP-ribose chains. It is for example known that poly-ADP-ribosylglycohydrolase (PARG) is capable of cleaving the glycosidic bond between ADP-ribose units, summarized in (Bonicalzi et al., 2005) and is thus unable to remove the last ADP-ribose moiety attached to substrates. PARG seems to be vital for development, as knock-out mice display embryonic lethality (Koh et al., 2005). However, the study of PARG has been complicated by the existence of multiple isoforms that display a different intracellular localization pattern (Haince et al., 2006; Meyer-Ficca et al., 2004).

ADP-ribosylhydrolase 1-3 (ARH1-3) have different substrate preferences, ARH1 cleaves only linkages between arginine and ADP-ribose (Takada et al., 1993). ARH1 seems to be vital for normal cell proliferation, as cells from *ARH1*^{-/-} mice have higher proliferation rates and *ARH1*^{+/-} mice spontaneously develop different cancers (Kato et al., 2011). No studies have been made of ARH2 yet. ARH3 was reported to have glycohydrolase activity towards PAR-chains but does not display activity against bonds between ADP-ribose and arginine, cysteine, diphthamide or asparagine, similar to PARG (Oka et al., 2006). ARH3 however has a structure differing from PARG and could also be shown to hydrolyze the reaction product of the sirtuins, *O*-acetyl-ADP-ribose (Ono et al., 2006). Additionally, *ARH3*^{-/-} mice show reduced PAR-degradation at mitochondria, indicating that ARH3 and not PARG is the responsible enzyme for PAR degradation at mitochondria (Niere et al., 2012). An additional class of proteins with ADP-ribose hydrolase activity at least *in vitro* for some of the superfamily members, are the NUDIX proteins (McLennan, 2006). It is not clear however whether they degrade PAR or *O*-acetyl-ADP-ribose in cells.

The little information available on the ADP-ribose hydrolases leaves room for speculations. It is not known whether there really are only so few ADP-ribosylhydrolases or whether there are other classes of hydrolases that remain to be discovered yet, for example enzymes that can remove ADP-ribose from lysine or glutamate. The very presence of intracellular arginine-ADP-ribosylhydrolases is actually paradoxical, since the eukaryotic arginine-modifying ARTCs modify extracellular proteins. Either this is some kind of protection against arginine-ADP-ribosylation by toxins or there are also intracellular arginine-specific ADP-ribosyltransferases that have not been discovered yet. Mice lacking ARH1 display a higher sensitivity towards the toxic effects of cholera toxin (Kato et al., 2007), arguing for a role in protection against the products of bacterial toxins. It remains unknown how the last ADP-ribose unit attached to glutamates is removed, as has been reported to occur in ARTD1 and ARTD10 automodification (Kleine et al., 2008; Tao et al., 2009). The recently solved crystal structure of PARG (Slade et al., 2011) may provide more insight in this issue. PARG quite

surprisingly folds like a macrodomain, which was not expected since the protein sequence had not revealed the presence of a macrodomain (Hassler et al., 2011). In these structures, only the PAR terminus fits in the catalytic center, leading the authors to postulate that PARG has only exoglycohydrolase activity (Slade et al., 2011). Since the macrodomain-fold of PARG could not be deduced from amino acid sequence alone, it can be hypothesized that there are more proteins unrecognized yet that have a macrodomain fold and corresponding PARG activity.

The macrodomain is an ADP-ribose binding module (Karras et al., 2005), with reported deacetylase activity of *O*-acetyl-ADP-ribose for some of macrodomain containing proteins (Chen et al., 2011; Peterson et al., 2011). The macrodomain containing archaeobacterial protein Af1521 from *Archaeoglobus fulgidus* was used to pull-down the ADP-ribosylated proteins from Chinese hamster ovary cells (Dani et al., 2009), indicating that macrodomains might become an important tool in the investigation of mono-ADP-ribosylation. Several of the macrodomain-containing proteins have been shown to bind to ADP-ribose not only *in vitro* but also in cells (Ahel et al., 2009; Gottschalk et al., 2009), reviewed in (Han et al., 2011; Kleine and Luscher, 2009). It could be shown that upon DNA damage induced with laser-microirradiation, ARTD1 becomes poly-ADP-ribosylated and as a consequence diverse macrodomains are attracted to the site of damage (Timinszky et al., 2009).

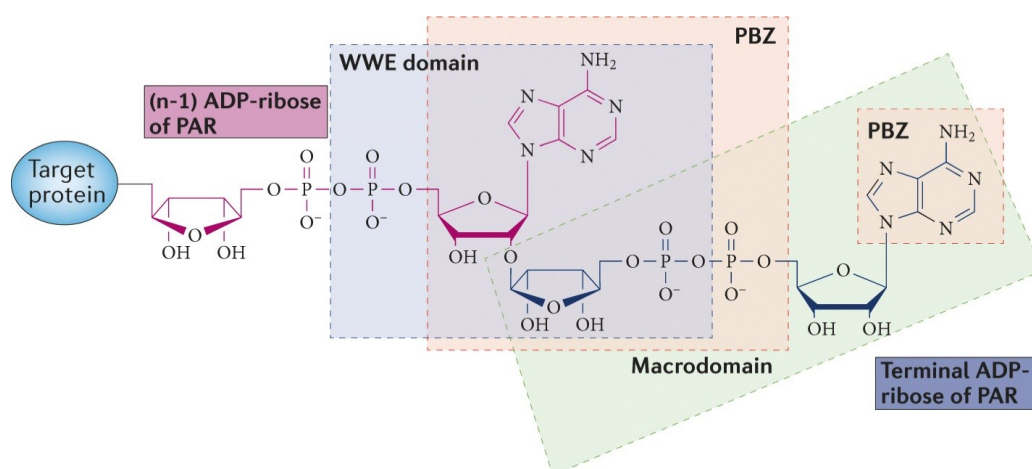


Figure 9 Representation of the binding properties of different ADP-ribose binding modules. Depicted are a substrate protein with in pink the (n-1) ADP-ribose and in blue the terminal ADP-ribose. The WWE domain recognizes the iso-ADP-ribose residue, unique to PAR chains, highlighted with a blue box. The PBZ recognizes mainly the same, but can occasionally also bind to the distal phosphate and ADP-ribose residue, depicted with an orange box. The macrodomain binds to the terminal ADP-ribose residue as depicted with a green box. Modified from (Gibson and Kraus, 2012).

Two more domains have been identified that interact with poly-ADP-ribose, the WWE domain, named after its most conserved residues (Aravind, 2001) and the poly-ADP-ribose-binding zinc finger (PBZ) found in DNA-repair/checkpoint proteins (Ahel et al., 2008). Proteome-wide analysis of PAR-interacting proteins has identified another motif binding to ADP-ribose, existing of 8 amino acid residues (PAR-binding motif, PBM) (Gagne et al., 2008). A schematic representation of the different

recognition patterns of these modules is given in Figure 9. The binding specificity of PBM is not clear yet and therefore not depicted in this overview. What becomes clear in this figure is that the WWE domain and PBZ probably only recognize poly-ADP-ribose, since mono-ADP-ribosylation forms no ribose-ribose glycosidic bond. However, a recent NMR investigation of the WWE domains from Iduna and ARTD11 contradict this representation, as the WWE domain from Iduna indeed binds to iso-ADP-ribose according to these models but the WWE domain from ARTD11 in contrast seems to recognize the terminal ribose of PAR chains (He et al., 2012). The ARTD8 WWE domain seems unable to bind any form of ADP-ribose because the binding pocket appears to be covered by its $\beta 3$ strand. These findings led the authors to speculate that in ARTD8 the macrodomains have taken over this function (He et al., 2012). These findings will have to be further evaluated in future studies.

An example of a protein binding to PAR chains through a WWE-domain is Iduna, which is recruited to ADP-ribosylated proteins or proteins that are bound to PAR and becomes active only after binding to ADP-ribosylation. It then ubiquitinates for example ARTD1, thereby targeting it for proteasomal degradation, additional Iduna substrates are amongst others XRCC-1 and KU70 (Kang et al., 2011) and the above described Axin (Callow et al., 2011; Zhang et al., 2011). A general mechanism of crosstalk between ubiquitination and ADP-ribosylation through the WWE-domain has already been suggested (Wang et al., 2012).

Obviously, a lot of open questions remain regarding the removal of mono-ADP-ribose as well as the intracellular recognition of mono-ADP-ribose, as above mentioned studies mainly focus on poly-ADP-ribosylation. The reports on proteins recognizing PAR in cells are also not numerous, implying that there is much to be learned on recognition of and binding to ADP-ribosylation in cells, for both mono-ADP-ribose and poly-ADP-ribose chains. One major hindrance that has to be overcome first is the lack of suitable tools to study mono-ADP-ribosylation in cells.

Measuring ADP-ribosylation

Poly-ADP-ribosylation can be detected in cells, as an antibody recognizing PAR chains has been developed. This can be employed to detect PAR chains in Western Blots as well as in cells in immunofluorescence approaches, as demonstrated in several publications investigating poly-ADP-ribosylation (Davis et al., 2012; Kang et al., 2011; Murawska et al., 2011). As described above, there is no consensus yet which amino acids serve as acceptor residue for which ARTD enzyme. There have been several attempts to create methods to solve the difficulties in the detection of ADP-ribosylation in cells and in the determination of acceptor sites within substrate molecules, as summarized below.

Antibodies have been raised against mono-ADP-ribose linked to arginine (Eide et al., 1986; Meyer and Hilz, 1986; Osago et al., 2008; Schwab et al., 2000), these antibodies are however reported to have low specificity, as they apparently cross-react with other ADP-ribose species (Laing et al., 2011). Additionally, these antibodies are not commercially available and moreover, antibodies against other possibly modified amino acids other than arginine have never been generated. Making the generation of specific antibodies by traditional methods difficult is the need for large amounts of antigen for immunization, for which the enzymatic reaction might be limiting, although recently a method was published to synthetically generate mono-ADP-ribose-conjugated peptides (Moyle and Muir, 2010). Finally, generated ADP-ribose carrying peptides are highly susceptible to phosphodiesterases (PDE) that would cleave the ADP ribose and leave only a phospho-ribosylated protein (Figure 10).

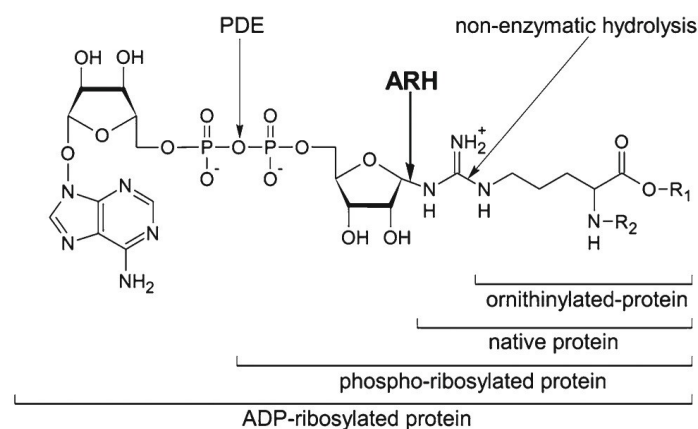


Figure 10 Cleavage of arginine-ADP-ribose. Depicted are the different sites where ADP-ribose on arginine might be cleaved with different mechanisms leading to this cleavage indicated. ARH: ADP-ribosylhydrolase; PDE: phosphodiesterase. Modified from (Laing et al., 2011).

Non-enzymatic cleavage gives rise to ornithinylated-proteins in the case of arginine-ADP-ribosylation (Stevens et al., 2009), which would be unsuited as antigen for mono-ADP-ribose antibodies as well (Figure 10). No published attempts have been made so far at generating antibodies against mono-ADP-ribose on other amino acids.

In addition to detection by specific antibodies, mass spectrometry is a method commonly used to map smaller modifications such as phosphorylation and acetylation sites in proteins. HPLC analysis of domain D of ARTD1, mono-ADP-ribosylated by the mono-ADP-ribosylating ARTD1 mutant E988Q, shows that there are only peptides with one ADP-ribose moiety attached as there is only one extra elution peak (Tao et al., 2009). After a trypsin digest of this peak and LC-MS/MS the authors note that the modification is lost to a large extent, but are still able to measure two distinct peptides carrying one ADP-ribose moiety, E488 and E491. Additionally, they identified a third peptide without measurable ADP-ribose, which contains D387 as putative modification site. Upon modification of these residues, automodification becomes weaker but is not completely abolished, indicating that there might still be other automodification sites. The authors argue that “secondary” modification sites become available when the “primary” sites are unavailable (Tao et al., 2009). Contradicting these findings, others mutated all glutamic acid residues in this domain and found that this does not influence modification, leading to the conclusion that glutamates are not the main acceptor sites (Altmeyer et al., 2009). However, aspartic acid residues were not tested. Automodified ARTD1 was stable in 1 M neutral hydroxylamine, excluding acidic residues as acceptor site. Upon mutation of several lysine residues, automodification is greatly decreased, leading to the conclusion that not glutamic acids but lysines are the acceptor sites (Altmeyer et al., 2009). This does not explain why a weak automodification signal is still present. Moreover, this suboptimal modification could be an artifact due to structural changes after mutation wherein the modification site is much less accessible.

Other attempts at MALDI analysis of ADP-ribosylated samples revealed that it is not possible to search databases in the traditional manner by adding 541 Da for the modification (Margarit et al., 2006) to identify the modified peptides. As e.g. described for arginine-ADP-ribose (Osago et al., 2009) and as reviewed in (Hengel and Goodlett, 2012), ADP-ribose can be fragmented during different mass spec approaches in different manners as schematically depicted (Figure 11). Unspecific cleavage during ionization thus complicates the analysis of spectra of ADP-ribosylated peptides. In a recent reanalysis of a phosphoproteome dataset, 88 mono-ADP-ribosylation sites were identified (Matic et al., 2012). 8 of those represented ribose-phosphate, indicating that the ADP-ribose moieties are indeed unstable. Interestingly, 87 mono-ADP-ribosylation sites were present on arginine and only 1 modified glutamate was identified (Matic et al., 2012). Most of these sites were mapped in liver tissue; none were present in 5 out of 9 tissue types studied. Most abundant amongst the identified modified proteins are tubulins and translation initiation factors (Matic et al., 2012). This is a hint that also this study does not approach the full extent of intracellular ADP-ribosylation, since there should be some ARTD automodification or histone modification signals (Burzio et al., 1979). One possible explanation is that the more stable arginine-linked mono-ADP-ribose moiety can be measured, but that the labile glutamate-linked ADP-ribose moiety is harder to detect. These findings however raise the question again which enzymes are responsible for intracellular ADP-ribosylation of arginine.

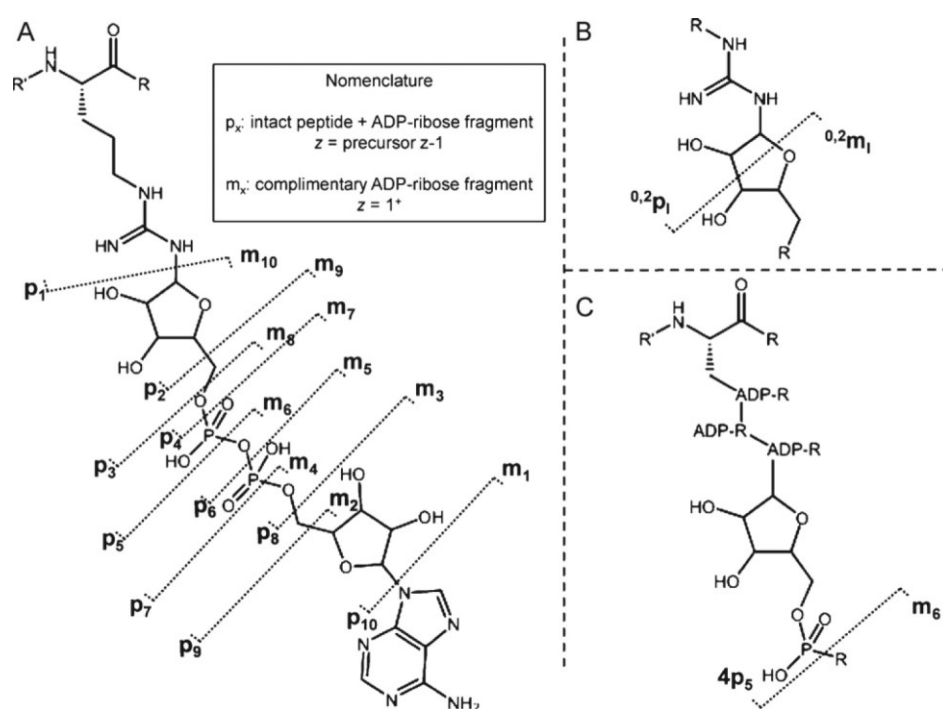


Figure 11 Representation of fragmentation behavior of ADP-ribose in mass spectrometry. Proposed nomenclature for (A) mono-ADP-ribose fragmentation (B) cross-ring fragmentation (C) PAR fragmentation. Modified from (Hengel and Goodlett, 2012).

The solution for the difficulties presented by the fragmentation of ADP-ribose in MALDI-based approaches, might be to employ different methods such as electron transfer dissociation (ETD), as glycosylated lysines proved more stable in measurements with ETD (Fedorova et al., 2010). Since ADP-ribosylated arginines can also be measured using ETD (Zee and Garcia, 2010), one would assume that enzymatically modified lysines should behave similarly. Indeed, a method has been developed to enrich ADP-ribosylated peptides and to measure them using ETD (Rosenthal et al., 2011). ARTD1 was used to optimize this method, but the PAR-chains were degraded by PDE treatment before enrichment of the ADP-ribosylated peptides, indicating that mono-ADP-ribosylated peptides can be enriched using this method and measured correspondingly. Thus this method might be applicable for substrates of the mono-ARTDs as well. A major drawback however is the currently limited availability of machines capable of ETD and the complicated nature of the results due to peptide backbone fragmentation.

Considering the scarcity of reports on the measurement of ADP-ribosylation and the contradictory results, it is obvious that more reliable methods are necessary to be able to study this modification in-depth.

Research aims

The catalytic mechanism of ARTD10 has been analyzed (Kleine et al., 2008), but not further validated so far. This study aims to provide an increased understanding of the mono-ADP-ribosylation reaction as performed by ARTD10, by expanding the current knowledge of automodification of ARTD10 onto novel substrates.

Since no substrates are known besides ARTD10 itself and core histones, it is necessary to identify ARTD10s physiological substrates to be able to understand the role ARTD10 plays in cellular processes. The results of an ARTD10 and ARTD8 substrate screen are analyzed and validated. The consequences of mono-ADP-ribosylation for target proteins are illustrated by investigating the novel ARTD10 substrate GSK3 β as an exemplary substrate *in vitro* as well as in cells. Kinase assays are employed to assess the effect of mono-ADP-ribosylation on GSK3 β activity.

Reversibility of mono-ADP-ribosylation is investigated by testing different ADP-ribosylhydrolases and *O*-acetyl-ADP-ribose-deacetylases. The identified hydrolase with activity towards ARTD10 and its substrates, MDO2, is subsequently utilized to test whether the mono-ADP-ribose induced functional consequence on GSK3 β activity can be reversed by removal of the ADP-ribose moiety.

To increase our understanding of the interaction between ARTD10 and GSK3 β bioinformatical models were generated to investigate the most likely ADP-ribosylation sites in GSK3 β . Phosphorylation of ARTD10 by GSK3 β is investigated as well as a putative regulatory feedback mechanism.

Finally, since no good tools are available to study mono-ADP-ribosylation in cells or to reliably map modification sites, mass spectrometry and peptide array based methods are investigated to enable future studies of mono-ADP-ribosylation sites in substrates of the mono-ARTDs.

Experimental procedures

Materials and Methods are described according to standard protocols used in the Institute of Biochemistry and Molecular Biology, RWTH Aachen University, and modified regarding individual differences in experimental procedures.

“If you try and take a cat apart to see how it works,
the first thing you have on your hands is a non-working cat.”

Douglas Adams

Materials

Oligonucleotides

Construct name	Forward (5' → 3')	Reverse (5' → 3')
GSK3S9A	GCCCAGAACCACCGCCTTTGCGGAGAG	CTCTCCGCAAAGGCGGTGGTTCTGGG
GSK3K85R	AGAACTGGTCGCCATCAGGAAAGTATT GCAGGACA	TGTCCTGCAATACTTTCCTGATGGCGACCA GTTCT
GSK3E53A_E12 1A_E279A	CCAGACAGGCCACAAGCAGTCAGCTAT ACAGAC CTTCTACTCCAGTGGTGCGAAGAAAGA TGAGGTCT GGGAACTCCAACAAGGGCGCAAATCAG AGAAATGA	GTCTGTATAGCTGACTGCTTGTGGCCTGTC TGG AGACCTCATCTTCTTCGCACCACTGGAGT AGAAG TCATTTCTCTGATTTGCGCCCTTGTTGGAG TTCCC
GSK3E211A_D2 64A_E290A	CAGCTGGTCCGAGGAGCACCCAATGTT TCGTAT CAGGGGATAGTGGTGTGGCTCAGTTGG TAGAAATAAT AGAAATGAACCCAAACTACACAGCATT TAAATTCCTCAAATTAAGG	ATACGAAACATTGGGTGCTCCTCGGACCAG CTG ATTATTTCTACCAACTGAGCCACACCACTA TCCCCTG CCTTAATTTGAGGGAATTTAAATGCTGTGT AGTTTGGGTTCATTTCT
pDONR/zeo- CDK9	GGGGACAAGTTTGTACAAAAAGCAGG CTTCATGGCAAAGCAGTACGACTC	GGGGACCACTTTGTACAAGAAAGCTGGGTC TTATCAGAAGACGCGCTCAAAC
pDONR/zeo- KCNAB1	GGGGACAAGTTTGTACAAAAAGCAGG CTCCATGCAAGTCTCCATAGCCTG	GGGGACCACTTTGTACAAGAAAGCTGGGTC TTATGATCTATAGTCCTTCTTGCTGTA

Plasmids

GSK3 β plasmids:

Name	Reference
pDONR/zeo-GSK3β	(Feijs, 2009)
pcDNA3.1-HA-GSK3β	Addgene plasmid 14753 (He et al., 1995)
pBAC-GST-GSK3β	Created by GW- <i>lr</i> -recombination between pDONR/zeo-GSK3 β and GW-pBAC-GST (K. Feijs)
pcDNA3.1-HA-GSK3β mutants	Created by site-directed mutagenesis with appropriate primers on pcDNA3.1-HA-GSK3 β (K. Feijs)

ARH1 plasmids:

Name	Reference
pcDNA4.1-V5-His-mARH1	Gift from J. Moss
pcDNA4.1-V5-His-mARH1D60, 61A	Gift from J. Moss
pGEX-2T-hARH1	Gift from J. Moss
pGEX-2T-hARH1D60, 61A	Gift from J. Moss

ARTD10 plasmids:

Name	Reference
pEVRF0-HA-ARTD10	(Yu et al., 2005)
pEVRF0-HA-ARTD10-G888W	(Yu et al., 2005)
pEVRF0-HA-ARTD10-dNES	(Yu et al., 2005)
pEVRF0-HA-ARTD10-dUIM	(Milke, 2007)
pEVRF0-HA-ARTD10-dK	(Chauvistré, 2008)
pEVRF0-HA-ARTD10-G888W-dUIM	(Verheugd et al., manuscript in revision)
dsRed-ARTD10	(Schuchlantz, 2008)
dsRed-ARTD10-G888W	(Schuchlantz, 2008)
pEGFP-ARTD10	(Kleine et al., 2012)
GST-ARTD10(1-255)	(Montzka, 2006)
GST-ARTD10(206-459)	(Montzka, 2006)
GST-ARTD10(408-649)	(Montzka, 2006)
GST-ARTD10(600-868)	(Montzka, 2006)
GST-ARTD10(818-1025)	(Montzka, 2006)
pSUPER_ARTD10_1	(Schuchlantz, 2008)
pSUPER_ARTD10_6	(Schuchlantz, 2008)

MDO2 plasmids:

Name	Reference
pcDNA3-HA-MDO2fl/wt	(Rosenthal, Feijs et al)
pcDNA3-HA-MDO2fl/G100E	(Rosenthal, Feijs et al)
pcDNA3-HA-MDO2sh/wt	(Rosenthal, Feijs et al)
pcDNA3-HA-MDO2sh/G100E	(Rosenthal, Feijs et al)
pcDNA3-HA-MDO2sh/4mut	(Rosenthal, Feijs et al)
pETM-33-His-GST-MDO2fl/wt	(Rosenthal, Feijs et al)
pETM-33-His-GST-MDO2fl/G100E	(Rosenthal, Feijs et al)
pETM-33-His-GST-MDO2sh/wt	(Rosenthal, Feijs et al)
pETM-33-His-GST-MDO2sh/G100E	(Rosenthal, Feijs et al)
pETM-33-His-GST-MDO2sh/4mut	(Rosenthal, Feijs et al)

Other plasmids:

Name	Reference
pEVRF0-HA	(Matthias et al., 1989)
pEGFP-C1	Clontech, #6084-1
pEQ176P2	Derived from pEQ176, where most of the β -galactosidase was cut out by a <i>PvuII</i> restriction digest. (J. Lüscher-Firzlaff)
pEQ176	(Firzlaff et al., 1991)
pCMV-His6-Ubiquitin	Vector encoding for His ₆ -tagged-ubiquitin under control of a CMV-promotor. (M. Treier)
pSUPER_ash_#5_falsh	Scrambled oligo ligated into the <i>BglII</i> and <i>HindIII</i> sites of pSUPER. (J. Lüscher-Firzlaff)
pCMV-HA-HectH9	(Adhikary et al., 2005)
pBabe-Puro	(Morgenstern and Land, 1990)

pcDNA3-Flag-MYC	Human c-MYC was cloned into pcDNA3-Flag by <i>Bam</i> HI/ <i>Bgl</i> II restriction digests (S. Schreek).
pM4-mintkluc	4 MYC binding sites cloned in front of the minimal TK promotor in front of the luciferase cDNA.
pDONR/zeo-CDK9	Entry vector created by <i>bp</i> -recombination of a CDK9 PCR fragment and pDONR/zeo. (K. Feijs)
pDONR/zeo-CDK9-D167N	Entry vector created by <i>bp</i> -recombination of a CDK9D167N PCR fragment and pDONR/zeo. (K. Feijs)
pDONR/zeo-AFF4	Entry vector created by <i>bp</i> -recombination of a AFF4 PCR fragment and pDONR/zeo. (K. Feijs)
pDONR/zeo-KCNAB1	Entry vector created by <i>bp</i> -recombination of a KCNAB1 PCR fragment and pDONR/zeo. (K. Feijs)
GW-pHA-KCNAB1	Destination vector created by <i>lr</i> -recombination of pDONR/zeo-KCNAB1 and GW-pHA (K. Feijs)
pDONR/zeo	Invitrogen, #1253-035
GW-pHA	pEVRF0-HA, made compatible with the GW-system by insertion of the Gateway cassette reading frame into the <i>Sma</i> I site. (R. Lilischkis)
GW-pBAC-GST	GW-compatible baculoviral expression vector for GST-tagged proteins (R. Lilischkis)

Antibodies

Antigen	Clone/information
α-actin	C4, mouse monoclonal, #69100 MP Biomedicals
α-ARTD10	5H11, rat monoclonal, E. Kremmer, raised against GST-ARTD10(1-907)
α-GFP	mouse monoclonal, 600-301-215 Rockland
α-GSK3β	H-76 rabbit polyclonal, sc-9166 Santa Cruz
α-GSK3β-pS9	rabbit monoclonal, Cell Signaling
α-GST	6G9, rat monoclonal, E. Kremmer
α-HA	3F10, rat monoclonal, Roche
α-His	H15, rabbit monoclonal, sc-803 Santa Cruz
α-MCM2	N-19, goat monoclonal, sc-9839 Santa Cruz
α-MYC	N-262, rabbit monoclonal, sc-764 Santa Cruz
α-p65	E948, rabbit monoclonal, #3987, Cell Signaling
α-p65-pS468	rabbit monoclonal, #3039, Cell Signaling
α-γ-tubulin	GTU88, mouse monoclonal, #T-6557 Sigma
α-goat IgG + IgM, HRP-conjugated	Jackson Immuno Research
α-mouse IgG + IgM, HRP-conjugated	Jackson Immuno Research
α-rabbit IgG + IgM, HRP-conjugated	Jackson Immuno Research
α-rat IgG + IgM, HRP-conjugated	Jackson Immuno Research

Cloning

DNA preparation

Small amounts of DNA were purified from bacterial cultures grown overnight at 37°C using the Zyppy™ Miniprep Kit (Zymo Research) or using a PureLink™ Quick Plasmid Miniprep Kit (Invitrogen) according to manufacturer's instructions. DNA prepared for subsequent sequencing was eluted with ddH₂O instead of the elution buffer delivered with the kits. Larger quantities were purified using the Qiagen MaxiPrep Kit according to manufacturer's instructions. Quantity and quality of the prepared DNA was measured on a NanoDrop (PiqLab).

Conventional cloning

Optimal conditions for double digests were determined by using the online DoubleDigest™ tool from Fermentas, reactions were carried out at 37°C for one hour unless recommended differently by the DoubleDigest™ program. Digested vectors and inserts were purified from 0.8 – 1.5% agarose gels using the Zyppy™ Gel DNA Recovery Kit (Zymo Research) according to manufacturer's manual. When necessary, 5'-phosphates were removed by incubation with thermosensitive alkaline phosphatase FastAP™ (Fermentas). Ligation was performed with T4 Ligase (Fermentas) at RT overnight, ligated products were transformed into bacteria by heat shock transformation.

Gateway cloning

Primers to create PCR products with flanking attB sites suitable for the Gateway® System (Invitrogen) were designed according to manufacturer's instructions and ordered from MWG or Sigma. 1-2 U Phusion® Polymerase (New England Biolabs) were used in the PCR according to manufacturer's instructions. PCR products were purified from agarose gels using the Zyppy™ Gel DNA Recovery Kit (Zymo Research) and used in the *bp*-recombination reaction overnight according to manufacturer's instructions, with half the reaction volume recommended. Entry vectors created thus were sequenced (SeqLab, Göttingen) before continuing with the *lr*-recombination reactions.

Site-directed mutagenesis

Primers were designed using Agilent Technologies' QuickChange Primer Design tool. Phusion® Polymerase was used for the PCR according to manufacturer's instructions with exception of the elongation time, which was increased to 1 minute per kb. 2 U *DpnI* (Fermentas) were added to the PCR reaction mixture afterwards and incubated for at least one hour at 37°C to digest all methylated, i.e. non-mutated DNA, before heat shock transformation. All constructs created thus were sequenced

to ensure successful mutagenesis without acquisition of any other mutations. For multiple mutations in one plasmid, sequential rounds of mutagenesis and sequencing were performed.

Human, bacterial and insect cell cultivation

Human cells

U2OS (ATCC HTB-96™), HeLa (ATCC CCL-2™) and HEK293 (ATCC CRL-1573™) cells were kept at a humidified atmosphere at 37°C with 5% CO₂ at all times and were cultivated in DMEM (Gibco) supplemented with 10% heat-inactivated fetal calf serum (Gibco) and 1% penicillin/streptomycin (Gibco, 10,000 U/ml/10,000 µg/ml). Cells were passaged on Ø10cm dishes (Sarstedt) by using 1 ml trypsin (Gibco) to detach the PBS-washed cells from the dish. Passages were counted, cells reaching passage 25 were discarded to be replaced by a freshly thawed aliquot.

Stably transfected Flp-In™-T-REx™-293 (Invitrogen R780-07) cell lines, such as the C-TAP-ARTD10-Flp-In™-T-REx™-293 cells (Schuchlantz, 2005), were cultured in DMEM supplemented with 15 µg/ml blasticidin S (InvivoGen) and 50 µg/ml hygromycin B (InvivoGen).

Cryoconservation

To thaw cells, frozen cells were warmed in a water bath at 37°C and transferred to a 15 ml tube immediately after melting of the ice crystals. 9 ml pre-warmed DMEM was added. After pelleting of the cells by centrifugation, medium was removed, followed by resuspension of the pellet in 10ml fresh fully supplemented DMEM and cells were plated out on a Ø10 cm dish.

To freeze cells, 80% confluent cells were removed from the dishes by trypsinization. The cells were pelleted and washed with PBS, followed by a resuspension in a solution of 10% DMSO and 90% FCS. Cells were transferred to a cryotube (Nunc) and kept on ice for 20 minutes, after which the tubes were transferred to -80°C in an insulated box for slow cooling for 24-72 hours. For long-term storage, cells were transferred to -150°C.

Bacterial cells

Several different bacterial strains were used, *E.coli* XL10 Gold® were generally used for plasmid preparation and conventional cloning, *E.coli* DH5α™ were employed for GateWay® cloning, *E.coli* BL21 were used for regular protein purification and *E.coli* Rosetta-Gami were used for proteins rendering multiple breakdown products when purified from *E.coli* BL21.

XL10-Gold® (Stragene)	Tetr <i>D(mcrA)183 D(mcrCB-hsdSMR-mrr)173 endA1 supE44 thi-1 recA1 gyrA96 relA1 lac Hte</i> [F' <i>proAB lacIqZDM15 Tn10</i> (Tetr) Amy Camr]
--------------------------	---

DH5 α TM (Invitrogen)	F- 80 <i>dlacZ</i> M15 (<i>lacZYA-argF</i>) U169 <i>recA1 endA1 hsdR17</i> (rk- mk+) <i>phoA supE44</i> - <i>thi-1 gyrA96 relA1</i>
BL21(DE3)pLysS (Stratagene)	B F- <i>dcm ompT hsdS</i> (r _B - m _B -) <i>gal</i> (DE3) [pLysS Camr]
Rosetta-Gami TM B(DE3)Lys (Novagen)	F- <i>ompT hsdS_B</i> (r _B - m _B -) <i>gal dcm lacY1 ahpC</i> (DE3) <i>gor522::Tn10 trxB</i> pLysSRARE (Cam ^R , Kan ^R , Tet ^R)

Bacterial transformation was achieved by first thawing the bacteria on ice, followed by mixing with 5 ng-1 μ g DNA in 14 ml round-bottom tubes (Falcon). After an incubation of 10 minutes, bacteria were heat-shocked for 45 seconds at 42°C immediately followed by a one-minute incubation on ice. Pre-warmed LB medium (1% tryptone, 0.5% yeast extract, 1% NaCl, pH 7.0) was added and the bacteria were allowed to recover at 37°C for 30-60 minutes. Finally, bacteria were pelleted by centrifugation and plated out on LB-plates. LB-Amp plates contained 100 μ g/ml ampicillin (Binotal), LB-kan plates contained 30 μ g/ml kanamycin (Applichem) and low-salt-LB plates contained 50 μ g/ml zeocin (Invivogen). Low salt LB medium contained only 0.5% NaCl.

Insect cells

SF9 cells (ATCC CRL-1711TM) were kept in Grace's medium (Gibco) supplemented with 10% FCS (Gibco) and 20 μ g/ml gentamycin (Merck) at 27°C.

For virus production, 1×10^6 cells were seeded in 10 ml complete medium and allowed to settle on the bottom of the flask. 200 μ l complete medium were mixed with 10 μ l LT1 (Mirus) and 2 μ g pBAC-GST-GSK3 β was mixed with 0.1 μ g BaculoGold DNA (BD Biosciences). Both mixtures were incubated for 10 minutes, mixed together and incubated another 5 minutes. The medium was replaced by FCS-free medium and the transfection mixture was added drop-wise to the cells. Cells were incubated for 4 hours, washed once in FCS-free medium and finally 5 ml medium was added. After 7 to 10 days, the supernatant was filtered through a 0.22 μ m filter and added to newly seeded cells. Protein expression was tested in the left over cells after the first amplification round. For final protein purification, 2×10^7 cells were seeded in 30 ml medium per 175 cm² flask (Greiner). One ml virus-containing sterile-filtered supernatant was added to each flask, with one ml containing approximately 1×10^8 plaque forming units.

Protein purification and detection

Human tandem affinity protein purification

Stable C-TAP-ARTD10-Flp-InTM-T-RExTM-293 cells were grown under selection until a minimum amount of 6 Ø10 cm plates with a confluency of 80% were available, upon which the cells were transferred to spinner flasks in regular DMEM. Protein expression was induced by adding 1 µg/ml doxycycline for 16 hours. Cells were pelleted by centrifugation at 500 xg, washed with ice-cold PBS and lysed using 15 ml TAP lysis buffer (50 mM Tris pH 7.5, 150 mM NaCl, 1 mM EDTA, 10% Glycerol, 1% NP-40, 1 mM DTT, 100 µM NaVO₄, 0.14 mg/ml aprotinin, 4 µM leupeptin, 0.5 mM PMSF) per 500 ml suspension and incubated 30 minutes under rotation, followed by centrifugation at 10,000 xg for 20-30 minutes. Samples were kept on ice throughout the entire following procedure. The supernatant was transferred to 200 µl equilibrated IgG Sepharose beads (Amersham Biosciences) and incubated for 1 hour under rotation. Beads were pelleted at 200 xg in 2 minutes and washed 1x in lysis buffer, 2 times in TEV buffer (50 mM Tris pH 7.5, 150 mM NaCl, 0.5 mM EDTA, 1 mM DTT) and subsequently resuspended in 200 µl TEV buffer. 2 µl TEV protease (Invitrogen) was added and samples were incubated for 2 hours under vigorous shaking or alternatively incubated overnight. After centrifugation at 200 xg, the supernatant was transferred to 200 µl equilibrated CaM beads (Amersham Biosciences) in 1.5 ml CaM binding buffer (10 mM Tris pH 7.5, 150 mM NaCl, 0.2% NP-40, 1 mM MgOAc, 2 mM CaCl₂, 1 mM Imidazol, 10 mM β-mercaptoethanol). CaCl₂ was added in a 1:200 ratio and the samples were incubated for 90 minutes under rotation. Beads were washed 3 times in CaM wash buffer (50 mM NH₄HCO₃, 75 mM NaCl, 1 mM MgOAc, 1 mM Imidazol, 2 mM CaCl₂) and resuspended in two volumes elution buffer. After an incubation period of 30 minutes, beads were spun down and supernatants collected. Samples were stored at -80°C, with addition of MgCl₂ in a ratio of MgCl₂:eluate 1:200. Concentrations were determined using SDS-PAGE and a BSA standard, enzymatic activity was tested in ADP-ribosylation assays. Tested protein was stored in aliquots to avoid repeated freezing and thawing.

E.coli GST-protein purification

The construct of interest was transformed by heat-shock transformation as described above. A single colony was picked to inoculate a starter culture in 49 mL LB medium, supplemented with 0.5% glucose and the appropriate antibiotic. This culture was allowed to grow overnight at 37°C. 25 mL of the starter culture was transferred to 500 ml LB also supplemented with glucose and antibiotic. At an OD₆₀₀ in the range of 0.5-0.7, protein expression was induced by addition of 0.5 mM IPTG and incubated for another 2 to 3 hours at 37°C, followed by an overnight incubation at RT. Bacteria were pelleted by centrifugation at 5,000 xg and either frozen at -80°C to continue the next day or

immediately resuspended in 30 ml ice-cold TNE (20 mM Tris pH 8.0, 150 mM NaCl, 1 mM EDTA pH 8.0, 5 mM DTT, 1 mM Pefa-Bloc, 1% Trasylol). After lysis on ice for 30 minutes with 100 µg/ml lysozyme, cells were solubilized by sonication. The samples were centrifuged at 10,000 xg and 4°C, followed by a 1-2 hour incubation of the supernatant with 0.5 ml Glutathion Sepharose 4B Beads (Amersham Biosciences). Beads were subsequently washed with PBS three times and transferred to a 0.8x4 cm chromatography column (Biorad). After washing with GST wash buffer (100 mM Tris pH 8.0, 120 mM NaCl), bound proteins were eluted in 3 fractions of 300 µl GST-elution buffer (20 mM glutathione in GST wash buffer). Samples of each fraction were subjected to SDS-PAGE and coomassie staining and quantified using a BSA standard.

E.coli His-protein purification

E.coli His-protein purifications were performed similar to the *E.coli* GST-protein purifications, with the following differences. Pellets were resuspended in IMAC lysis/wash buffer (20 mM HEPES pH 7.5, 10% glycerol, 300 mM NaCl, 0.1% NP-40, 5 mM imidazole and 14 µg/ml aprotinin) instead of TNE buffer. Instead of Glutathion Sepharose 4B Beads, 0.5 ml TALON™ Metal Affinity Resin (BD Biosciences) was used per 500 ml bacterial culture. Beads were washed in IMAC lysis/wash buffer, the protein was eluted by incubation of the beads in IMAC elutionbuffer (20 mM HEPES pH 7.5, 10% glycerol, 200 mM NaCl, 0.1% NP-40, 10 mM EDTA, 10 mM DTT and 14 µg/ml aprotinin) for 10 minutes, which was repeated, resulting in two elution fractions per purification.

Insect GST-protein purification

SF9 cells were infected as described above. 5-7 days after infection cells were pelleted by centrifugation at 500 xg, medium removed and the pellet resuspended in kinase lysis buffer (50 mM HEPES pH 7.5, 0.5% Tween-20, 10% glycerol, 300 mM NaCl, 5 mM NaF, 1 mM EDTA, 1 mM EGTA, 10 µg/ml aprotinin, 10 µg/ml leupeptin, 0.1 mM orthovanadate, 1 mM pefabloc and 1 mM DTT). The lysate was sonicated with 2 x 15 pulses at 70% output. Debris was pelleted by 10 minutes centrifugation at 15,000 xg and the supernatant was incubated with equilibrated Glutathion Sepharose 4B Beads (Amersham Biosciences). Beads were washed with wash buffer I (50 mM HEPES pH 7.5, 0.5% Tween-20, 10% glycerol, 300 mM NaCl, 5 mM NaF, 1 mM EDTA, 1 mM EGTA, 0.1 mM orthovanadate, 1 mM pefabloc and 1 mM DTT), transferred to eppendorf tubes in wash buffer II (50 mM HEPES pH 8.0, 0.01% Tween-20, 10% glycerol, 100 mM NaCl, 1 mM pefabloc and 1 mM DTT). Protein was eluted in 500 µl elution buffer (20 mM glutathione in wash buffer II) by overnight incubation at 4°C.

SDS-PAGE

Sodium dodecyl sulfate polyacrylamide running gels were prepared with acrylamide concentrations ranging from 10% to 20%, depending on the size of the proteins analyzed. Stacking gels contained 5% acrylamide. Samples were boiled briefly in sample buffer (2x: 160 mM Tris pH 6.8, 20% glycerol, 10% SDS, 0.25% bromophenol blue, 100 mM β -mercapthoethanol) before loading. Gels were placed in a tank with Laemmli buffer (25 mM Tris base, 250 mM glycine, 0.1% SDS) and 25 mA was applied until the samples formed one line in the stacking gel, after which the current was increased to 35 mA. A Protein Ladder (PageRuler™ Prestained Protein Ladder, Fermentas) was loaded onto each gel to be able to estimate protein sizes.

Rapid coomassie staining

Coomassie stains proteins nonspecifically through interaction with hydrophobic and cationic amino acids. After SDS-PAGE, gels were fixed and stained in staining solution (10% acetic acid, 0.006% coomassie brilliant blue G250 (Bio-Rad)) under slight agitation until bands became visible. Gels were destained overnight in ddH₂O to reduce background staining.

Western Blot

Using a semi-dry blotting system, the proteins were transferred from the gel onto a nitrocellulose membrane (Millipore) in semi-dry blotting buffer (25 mM Tris-base, 192 mM glycine, 20% methanol), applying 2 V per cm² for one hour. The membrane was dyed with Ponceau (0.2% Ponceau S in 3% TCA) to visualize the proteins and check transfer efficiency. Subsequently the membranes were blocked in 5% non-fat milk in PBS-T (140 mM NaCl, 2.6 mM KCl, 2 mM Na₂HPO₄, 1.45 mM KH₂PO₄, 0.05% Tween-20) or 5% non-fat milk in TBS-T (50 mM Tris-HCl, 140 mM NaCl, 0.05% Tween-20) for phospho-specific antibodies. The first antibody was applied either overnight at 4°C or for 2 hours at RT, diluted in a range of 1:200 to 1:2000 in PBS-T or in 5% BSA in TBS-T for phospho-specific antibodies. 0.02% sodium azide was added for storage of diluted antibodies at 4 °C. After several PBS-T or TBS-T washes, the secondary, species-specific horseradish peroxidase (HRP)-coupled antibody was applied for 30-60 minutes at RT in 5% non-fat milk in PBS-T or in 5% non-fat milk in TBS-T for phospho-specific antibodies. After further PBS-T or TBS-T washes, the substrate for HRP, ECL Pico or Femto (Pierce), was applied and the resulting chemiluminescence signals read-out immediately using a LAS-3000 (Fuji).

Cell-based assays

Transfection methods

Calcium-phosphate precipitation-based transfection

Transfections of U2OS, HeLa and HEK293 cells were performed using the calcium phosphate precipitation technique unless stated otherwise. U2OS were seeded at a density of 8×10^5 cells per Ø10 cm dish the day before transfection, HeLa cells at a density of 8.5×10^5 cells per Ø10 cm dish. HEK293 cells were seeded two days before transfection at a density of 1×10^6 cells per Ø10 cm dish. 20 µg DNA was diluted in 950 µl HBS buffer (138 mM NaCl, 17 mM Hepes, 5 mM KCl and 0.71 mM $\text{Na}_2\text{HPO}_4 \cdot 2\text{H}_2\text{O}$, pH 6.95). 50 µl 2.5 M CaCl_2 was added and the mixture was mixed thoroughly. After an incubation of 20 to 40 minutes, the mixture was added drop-wise to the medium. Cells were washed with warm PBS 12-24 hours after transfection and were collected for subsequent assays 24-48 hours after transfection.

Lipid-based transfection

Dharmacon siRNA pools were transfected using Lipofectamin™ (Invitrogen) according to manufacturer's instructions. U2OS cells were seeded in Ø6 cm dishes at a higher density than recommended, approximately 80% confluent and were divided equally onto 2 Ø6 cm dishes the day after transfection.

Protein preparation

Cells were washed with cold PBS, subsequently 300-350 µl TAP (see above) or RIPA lysis buffer (10 mM TrisCl, pH 7.4, 0.15 M NaCl, 1% NP-40, 0.1% SDS, 1% deoxycholate) was added to the plates. ProteoBlock™ Protease Inhibitor Cocktail (Fermentas) was added freshly. Additional phosphatase inhibitors (0.1 mM vanadate, 20 mM β-glycerophosphate and 50 mM oicadaic acid) were added freshly only when preparing lysates for phospho-analysis. Cells were collected by scraping and transferred to eppendorf tubes. RIPA lysates were sonicated in a water-bath sonicator (Bioraptor, Diagenode) for 15 minutes with 30 second cycles at maximum intensity and were subsequently cleared by centrifugation. TAP lysates were cleared directly by centrifugation at 16,000 xg for 15-20 minutes at 4°C. The supernatants were transferred to a new tube and stored at -20 °C or analyzed directly with SDS-PAGE.

Colony Formation Assays

HeLa or U2OS cells were seeded in Ø6 cm dishes at a density of 3.0×10^5 respectively 2.5×10^5 cells per dish, as determined using a Casy@Counter (Innovatis). One day after seeding, cells were

transfected with indicated amounts of genes of interest and 0.8 µg pBabePuro on a total of 8 µg for selection, rendering transfected cells puromycin resistant. 6-16 hours after transfection the culture medium was refreshed and puromycin (Sigma) was applied with a final concentration of 2 µg/ml. Selection took place for 24 hours, after which the medium was refreshed again. Colonies were allowed to grow for 4-10 days, with refreshment of the medium as necessary. Cells were washed with PBS once time and stained with 0.2% methylene blue in methanol. After an incubation of approximately 30 minutes the dye was removed, the plates were washed with ddH₂O, air-dried and documented.

Reporter gene assays

Cells were seeded at a density of 4-5 x10⁴ cells per well in a 12-well plate and transfected the next day using the calcium-phosphate method. A total amount of 2 µg DNA was transfected per well, with 0.2 µg β-galactosidase control plasmid, 0.2 µg pEGFP, 0.5 µg reporter-gene construct, 0.2 µg transcription factor of interest, e.g. MYC, and varying amounts of other constructs of interest. Cells were washed 24 hours after transfection and lysed 48 hours after transfection in extraction buffer (5 mM Tris pH 7.8, 0.4 mM EDTA, 2% glycerol, 0.2% Triton-X100 and 10 mM DTT). Cell debris was removed by 20 minutes centrifugation at 4°C and 16,000 xg. 20 µl cleared lysate was pipetted into one white and one clear 96-well plate. 100 µl β-galactosidase buffer (60 mM Na₂HPO₄, 40 mM NaH₂PO₄.H₂O, 10 mM KCl, 1 mM MgSO₄ and 20 mM β-mercaptoethanol) was added to the lysates in the clear plates, 100 µl luciferase buffer (25 mM glycylglycine, 15 mM MgSO₄ 7H₂O and 5 mM ATP) was added to the lysates in the white plates. 25 µl ortho-nitrophenyl-β-galactoside (ONPG) (Applichem) was added in regular time intervals to the lysate-β-galactosidase buffer mixture in the clear plates. The reaction product, o-nitrophenol (ONP), has a visible yellow color and can be measured. The enzymatic reaction was stopped by adding 60 µl Na₂CO₃ in the same time intervals and subsequently measured at 405 nm using a spectrometer (Victor, PerkinElmer). After automated addition of 35 µl luciferin (0.25 mM in 25 mM NaOH) (Applichem) luciferase activity was measured at 405 nm. Relative luciferase units (RLU) were calculated by dividing the measured luciferase values through the β-galactosidase extinction values.

In vivo ubiquitination

Cells were seeded and transfected with the calcium-precipitate methods as described above. 8 µg pCMV-His6-Ubiquitin, 2 µg pEGFP and 4-10 µg of constructs of interest were transfected. Optionally, cells were treated with the proteasome inhibitor MG132 (Sigma) at a final concentration of 25 µM for 2-4 hours. Cells were lysed in 8 M urea buffer (8 M Urea, 0.1 M NaPO₄, 10 mM imidazole) and sonicated. Lysates were cleared from cell debris by full-speed centrifugation at RT. Supernatants were incubated with 20 µl equilibrated TALON™ Metal Affinity Resin (BD Biosciences) for 2-3

hours at RT. After extensive washing in urea buffer, beads were boiled in sample buffer supplemented with 200 mM imidazole. Samples were analyzed by SDS-PAGE and Western Blot.

(co-)Immunoprecipitation

Cells were lysed in 350 μ l co-IP buffer (20 mM HEPES pH 7.4, 50 mM NaCl, 30 mM $\text{Na}_4\text{P}_2\text{O}_7$, 50 mM NaF, 0.2% TritonX-100, 10% glycerol, 5 μ M ZnCl_2), freshly supplemented with ProteoBlock™ Protease Inhibitor Cocktail (Fermentas), 100 μ M NaVO_4 and 10 mM natrium- β -glycerophosphate or in 350 μ l TAP-lysis buffer (see above) per 10 cm plate or per 7×10^5 suspension cells and kept on ice for 10-30 minutes. Lysates were cleared from cellular debris by high-speed centrifugation for 20 minutes. Supernatants were incubated two hours or overnight at 4 °C with an antibody recognizing the protein of interest and beads (protein G or A-Sepharose 4 Fast Flow, GE Healthcare) appropriate for the antibodies. Beads were washed in co-IP buffer or TAP-lysis buffer before boiling in sample buffer and loading on SDS-PAGE.

***In vitro* assays**

ADP-ribosylation assays

ADP-ribosylation assays were carried out at 30°C for 30 minutes unless indicated otherwise. The reaction mixture (50 mM Tris-HCl, pH 8.0, 0.2 mM DTT, 5 mM MgCl₂, 50 μM β-NAD⁺ (Sigma) and 1 μCi [³²P]-β-NAD⁺ (Perkin Elmer)) was added to 1 μg purified substrate protein or to IgG-beads with immunoprecipitated material and 0.5 μg enzyme in a total reaction volume of 30 μl. Reactions were stopped by adding SDS sample buffer, boiled and run on SDS-PAGs. Incorporated radioactivity was analyzed by exposure of the dried gel to X-ray film (Fujifilm, 100NIF). Samples used in subsequent kinase assays were incubated with 50 μM β-NAD⁺ only and cooled on ice before washing of the beads with kinase assay buffer.

Kinase assays

Kinase buffer: 5 mM MOPS pH 7.2, 2.5 mM β-glycerophosphate, 1 mM EGTA, 0.4 mM EDTA, 4 mM MgCl₂, 50 μM DTT and 40 ng/μl BSA. [³²P]-γ-ATP (Hartmann) was diluted to 0.16 μCi/μl in 250 μM ATP in 3x kinase assay buffer. 25 ng GST-GSK3β or precipitated material was incubated in a reaction volume of 25 μl containing 5 μl 0.16 μCi/μl [³²P]-ATP-solution and 5 μg substrate peptide RRRPASVPPSPSLSRHS(pS)HQRR (Millipore), unless titrated in indicated concentrations. After incubating at 30°C for 15 minutes the reaction was stopped by placing on ice. Routinely 10 μl aliquots were spotted on P81 paper in duplicate, washed with 0.5% phosphoric acid and air-dried before scintillation counting. SDS-sample buffer was added to the samples analyzed by SDS-PAGE and autoradiography. Statistical significance was determined by employing two-sided Student's t-tests.

de-ADP-ribosylation assays

ADP-ribosylation assays were performed as described above with 1 μCi [³²P]-β-NAD⁺, but were terminated by washing the beads with coupled proteins in high-salt ADP-ribosylation assay buffer (50 mM Tris-HCl, pH 8.0, 0.2 mM DTT, 5 mM MgCl₂, 200 mM NaCl). Subsequently, 500 ng MDO2, ARH1 or Macro1-3 were added to the beads in 30 μl high-salt ADP-ribosylation assay buffer. After incubation at 30°C for 20-30 minutes, the reaction was stopped by addition of SDS sample buffer and boiling for analysis by SDS-PAGE and autoradiography. For subsequent kinase assays, beads with coupled GST-GSK3β were cooled and washed after incubation with MDO2 to allow kinase assays as described above. Statistical significance was determined by employing two-sided Student's t-tests.

GST-pull down assays

GST-pull down assays were used to examine direct interactions between proteins. Two different methods were used, one utilizing *in vitro* translated protein and one using purified proteins only. For *in vitro* translation, ARTD10 or MYC were *in vitro* translated exactly as recommended by the manufacturer of the kit (Promega), using [³⁵S]-methionine, T3 polymerase and a pBlueScript ARTD10 or MYC plasmid. Glutathion Sepharose 4B Beads were equilibrated using GST pull-down buffer (20 mM HEPES pH 7.4, 50 mM NaCl, 1.5 mM EDTA, 0.1% NP40, 0.1% aprotinin, 1 mg/ml pefablock, 1 g/ml pepstatin A, 0.5 µg/ml leupeptin) and subsequently incubated for at least 90 minutes at 4°C with the GST-tagged protein of interest. After several washes with GST-pull-down buffer, *in vitro* translated protein was added to the beads and incubated for 2 hours at 4°C under constant rotation. After further washes, the beads were boiled in sample buffer and analyzed using SDS-PAGE. 10% of the *in vitro* translated protein was loaded as a control for the *in vitro* translation. Gels were stained with coomassie blue and destained overnight. Amplify (GE Healthcare) was applied for 30 minutes, followed by vacuum-drying of the gel and exposure to film at -80°C using an amplifier screen.

For non-labeled pull-downs, a GST-tagged protein was coupled to Glutathion Sepharose 4B Beads as described above, upon which a second, differentially tagged protein was added. This mixture was incubated at 4°C under constant rotation for 1-2 hours, washed in GST-pull down buffer and analyzed by SDS-PAGE and Western Blot. Both proteins were detected in the Western Blot, in the pull-down as well as in input samples.

Mass spectrometry methods

Identification of phosphorylation sites

For the identification of unknown phosphorylation sites in proteins, *in vitro* kinase assays were performed as described above. All solutions were filtered through a 0.22 μm filter (Millipore) to avoid possible contaminations and work was carried out under a clean bench as far as possible. 4x sample buffer was added to the kinase assay mixture, boiled for 5 min at 95 °C and subsequently cooled on ice. Freshly prepared iodoacetamid was added to a final concentration of 100 mM and incubated in the dark at 55 °C for 10 minutes. Subsequently, the samples were subjected to SDS-PAGE as described above. After electrophoresis, the gel was fixed with sterile-filtered fixing solution (25% isopropanol, 10% acetic acid) and stained with Gel-Code Blue (Pierce). Gels for analysis by the laboratory of David W. Litchfield (University of Ontario, London, Canada) were documented, shrink-wrapped and shipped.

Identification of mono-ADP-ribosylation-sites

In-solution trypsin digests of mono-ADP-ribosylated samples

ADP-ribosylation assays were performed as described above but without radiolabeled NAD^+ . 30 μl 8 M urea (in 50 mM ammonium bicarbonate) was added to each assay, which was then incubated for 15 minutes. 10 mM freshly prepared DTT was added, followed by an incubation of one hour at 56°C. Finally, iodoacetamide was added to a final concentration of 55 mM and the mixture was incubated in the dark for 45 minutes at RT. This mixture was diluted with 50 mM ammonium bicarbonate to 2 M urea. Trypsin (Trypsin Gold, Promega) was added in a ratio trypsin:protein 1:50. Digestion took place overnight at 37°C and was stopped by freezing at -20°C. Samples were desalted by using C-18 (3M) home-packed tips or purchased C-18 tips (Pierce ThermoScientific). Tips were wetted with acetonitrile and washed with 0.1% trifluoroacetic acid (TFA) before loading of the samples. After washing again with 0.1% TFA, samples were eluted in 80% acetonitrile containing 0.1% TFA. Samples were dried after desalting.

Purification of mono-ADP-ribosylated peptides

Tryptic peptides from ADP-ribosylation reactions were produced as described above and subsequently incubated with equilibrated ProSep® PB Resin (Millipore), essentially as described in (Rosenthal et al., 2011). 10% of the tryptic peptides were saved to analyze by MALDI directly. Eluates in 0.1% acetic acid were completely dried in a SpeedVac Concentrator (Eppendorf) before redissolving and MALDI analysis. Alternatively, 50 μM biotin-labeled NAD^+ was used in the ADP-ribosylation reaction and the subsequent pull-down performed with Dynabeads® MyOne Streptavidin C1

(Invitrogen). These samples were washed in RIPA buffer and ddH₂O before elution in 6M guanidine-HCl. Samples were desalted and dried before MALDI analysis.

Chromatographic separation of mono-ADP-ribosylated peptides

ADP-ribosylation assays were performed with approximately 2 µg GST-ARTD10(818-1025) and 10 µCi [³²P]-NAD⁺. After the 30-minute incubation, samples were boiled in sample buffer and loaded on 12%-SDS-PAGs. After coomassie staining as described above, gels were vacuum-wrapped and exposed to an X-ray film overnight to assess incorporated radioactivity. In-gel tryptic digests were performed basically as described before (Kelm et al., 2002). In brief, gel pieces were cut out and macerated, subsequently incubated with 40% isopropanol, then with 50% methanol/50 mM NH₄HCO₃. Gel pieces were dried completely in the SpeedVac Concentrator before resuspension in 50 µl 50 mM NH₄HCO₃, containing 1.5 µg trypsin (Trypsin Gold, Promega). After overnight incubation with shaking at 37 °C, another 1.5 µg trypsin was added and incubated for 6-16 hours. The supernatant was taken off and 100 µl acetonitrile was added to the gel pieces. After 30 minutes shaking at 37°C, supernatants were collected and pooled with the previous supernatants and dried in the SpeedVac Concentrator. Peptides were redissolved in 30 µl pH 1.9 buffer (van der Geer and Hunter, 1994) and spotted onto cellulose thin layer plates (Merck) with 0.75 µl aliquots at a time. Two different buffers were used for chromatography, phospho chromatography buffer and isobutyric acid buffer as described by Hunter (van der Geer and Hunter, 1994), with the runs taking 10-12 hours. After completion, plates were air-dried, wrapped in plastic wraps, marked fluorescently and exposed to films in the presence of intensifier screens at -80°C.

Peptide- and ProtoArrays®

ProtoArrays®

All solutions used were filtered through 0.22 µm filter devices prior to use to eliminate background-causing dust particles. ProtoArrays® (Invitrogen) were removed from -20°C and allowed to thaw at RT for 20 minutes before transferring to a 10 cm tissue culture plate. Roti®-Block (Roth) was used to block the arrays by incubating for 1 hour at 4°C, shaking with 50 rpm. Arrays were washed once in plain reaction buffer (50 mM Tris-HCl, pH 8.0) and dried at the back and sides with Kimwipes®. The reaction mixture (50 mM Tris-HCl, pH 8.0, 0.2 mM DTT, 4 mM MgCl₂, 25 µM biotin-NAD⁺ (Trevigen) and approximately 1.5 µg enzyme) was applied to the slides upon which LifterSlips™ (Nunc) were placed on the arrays to prevent evaporation of the reaction mixture. This was incubated for 1 hour at 30°C and subsequently washed at least 3x with 1% fatty-acid-free BSA in TBS/T, 3x with 0.5% SDS in TBS/T and again at least 3x with 1% fatty-acid-free BSA, each wash step taking 10 minutes. To detect the biotinylated proteins, streptavidin-AlexaFluor® 647 (Invitrogen) was applied in the dark for 90 minutes at 4°C at a concentration of 2 µg/ml in 1% fatty-acid-free BSA in TBS/T, after which 5 10-minute wash steps with 1% fatty-acid-free BSA in TBS/T and 5 wash steps with ddH₂O were performed. Arrays were centrifuged at 200xg for 2 minutes to remove residual ddH₂O and subsequently analyzed using an Axon GenePix® 4100A microarray reader with the GenePix®Pro 6.0 program. Results were analyzed with the Prospector software provided by Invitrogen.

Z-scores were calculated to assess statistical significance, according to the following formula: $z = (x - \mu) / \sigma$ where x is the raw value, μ the population mean and σ the standard deviation of the population. All proteins having a Z-score ≥ 2.5 were considered as a positive hit and were displayed in the supplementary tables. Gene ontology analysis was performed with the online available BioCompendium data analysis platform (<http://biocompendium.embl.de/>).

PepStar™ Histone Tail Peptide Arrays

All solutions used were filtered through 0.22 µm filter devices prior to use to eliminate background-causing dust particles. Arrays (JPT, Berlin) were placed in a cell culture dish with the label facing up. This dish was placed in a larger dish stuffed with wet Kimwipes®. Roti®-Block (Roth) was applied to block the arrays by incubating 1 hour at RT. Subsequently arrays were washed twice in TBS and once in Tris pH 8.0. Spacers were placed on the ends of the arrays, a dummy slide was placed on top, leaving a small strip of array uncovered to pipette the reaction mixture onto, as depicted in Figure 12.

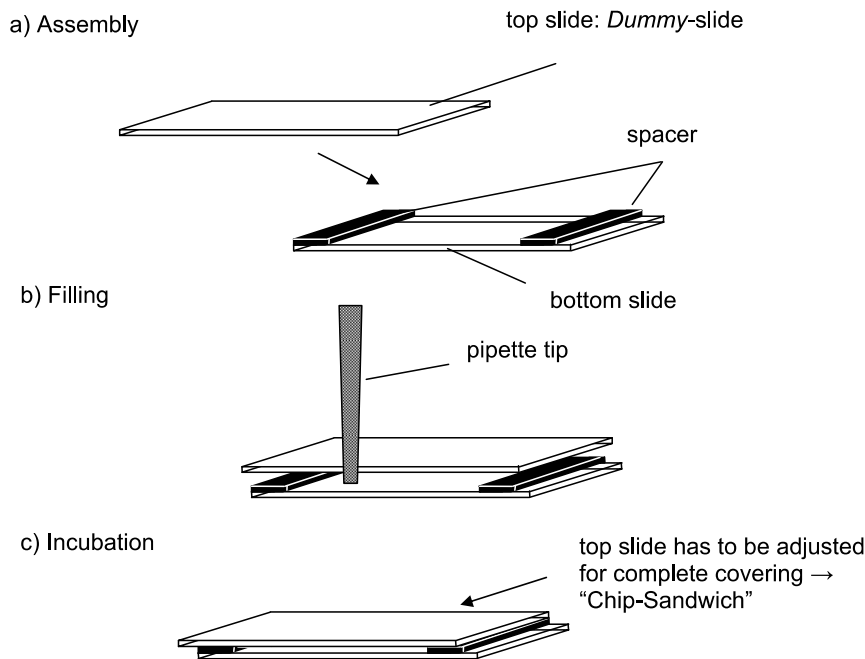


Figure 12 Schematic overview of PepStar™ Histone Tail Peptide Array setup. From Protocol PepStar™ Histone Tail Peptide Array, JPT. The subsequent steps in the preparation of the enzymatic reaction are displayed.

300 μ l reaction mixture (25 μ M biotin-NAD, 2 μ g TAP-ARTD10 or BSA, 50 mM Tris pH8.0, 0.2 mM DTT, 4 mM $MgCl_2$) was pipetted between array and dummy slide, upon which the dummy slide could be slid into place. The ADP-ribosylation reaction took place for one hour at 30°C, followed by two washes in TBS, one in 0.5 % SDS and two in TBS/T. AlexaFluor® 647 was applied in a 1:5000 dilution in TBS/T for 90 minutes in the dark. 3 More wash steps with TBS/T followed to remove antibody traces, 5 water wash steps were applied to completely clean the arrays. Arrays were air-dried and subsequently analyzed using an Axon GenePix® 4100A microarray reader with GenePixPro® 6.0. The resulting gpr-files were then analyzed by JPT.

Bioinformatical analysis

Docking of NAD into the catalytic center of ARTD10

The structure of ARTD10 in complex with NAD⁺ was predicted by protein-ligand docking, based on the published crystal structure of ARTD10 (Protein Data Bank (PDB) ID 3HKV) in complex with the inhibitor 3-aminobenzamide (3AB). In order to guide the docking procedure, we introduced two sets of information: 1) interactions (hydrogen bonds and hydrophobic interactions) formed by 3AB at its ARTD10 pocket; 2) common structural features shared by other ARTs and ADP-ribosylating toxins (Lee et al., 2010). The protein-ligand docking was performed using the software HADDOCK (Dominguez et al., 2003). Hydrogen bonds and hydrophobic interactions formed between 3AB and ARTD10 were derived from the “Ligand explorer” feature at the PDB website. They were introduced as unambiguous distance restraints, i.e. restraints unambiguously derived from experimental data. However, in HADDOCK it is also possible to introduce ambiguous interaction restraints (AIRs), generally defining interface interactions. AIRs involve two sets of residues, named active and passive residues. Active residues are those known to make contacts within the complex and solvent accessible. Passive residues are their closest solvent accessible neighbors. In this case, the ARTD10 catalytic residues H887 and Y919 and NAD⁺ were defined as active residues. Thus, we docked the 8 NAD⁺ conformations described in (Lee et al., 2010) against the ARTD10 structure, which underwent a preliminary short (2000 steps) energy minimization. The ligand parameters were obtained using the PRODRG server (<http://davapc1.bioch.dundee.ac.uk/prodrg/>). For each docking run, that generated 1000 rigid and 200 water-refined docking complexes, the best structure was retained. Among the 8 results, the ARTD10-NAD⁺-complex obtained by using the NAD⁺ conformation from ART2.2 was selected, as it showed the lowest scoring function value and satisfied all of the imposed restraints.

Modeling of the interaction between ARTD10 and GSK3β

The protein-protein docking calculations performed using HADDOCK (Dominguez et al., 2003) require the definition of ambiguous distance restraints, usually derived from experimental data, in order to guide the docking procedure. In this study, the restraints were defined as follows: 1) In ARTD10, the catalytic residues H887, Y919, and I987 were defined as active residues. The ARTD10 structure used includes the cofactor NAD⁺ docked in the catalytic site as described above. 2) In GSK3β, every glutamate (E), aspartate (D), lysine (K) and arginine (R) was alternatively defined as active residue. After each docking run, the best structure belonging to the best cluster was retained. Results were evaluated on the basis of: a) the HADDOCK scoring function; b) the interacting surface; c) the free-energy solvation, d) salt bridges and hydrogen bonds formation. c) and d) were evaluated with the PISA method (Krissinel and Henrick, 2007).

Results and discussion

“The most exciting phrase to hear in science, the one that heralds new discoveries, is not ‘Eureka!’ (I found it!) but ‘That’s funny...’.”

Isaac Asimov

Identification of novel substrates of ARTD10 and ARTD8

Previous work has identified ARTD10 as mono-ADP-ribosyltransferase but has provided no physiological substrates so far apart from histones and automodification (Kleine et al., 2008), leaving open a lot of questions concerning the reported mono-ADP-ribosylation by ARTD10. Therefore a screening method to identify substrates in an unbiased manner was sought and found in the form of Invitrogens ProtoArrays. These arrays consist of nitrocellulose glass slides with approximately 8000 proteins spotted per slide. Optimization procedures are described in (Braczynsky, 2009), an example of which is shown in Figure 13A where nitrocellulose slides were loaded with ARTD10 or histones as positive controls and BSA or GST as negative controls (modified from (Braczynsky, 2009)). The nitrocellulose slides were incubated with tandem affinity purified (TAP)-ARTD10 and biotin-NAD⁺ or biotin-NAD⁺ only to test whether ARTD10 can modify immobilized substrates with biotin-NAD⁺ (Braczynsky, 2009).

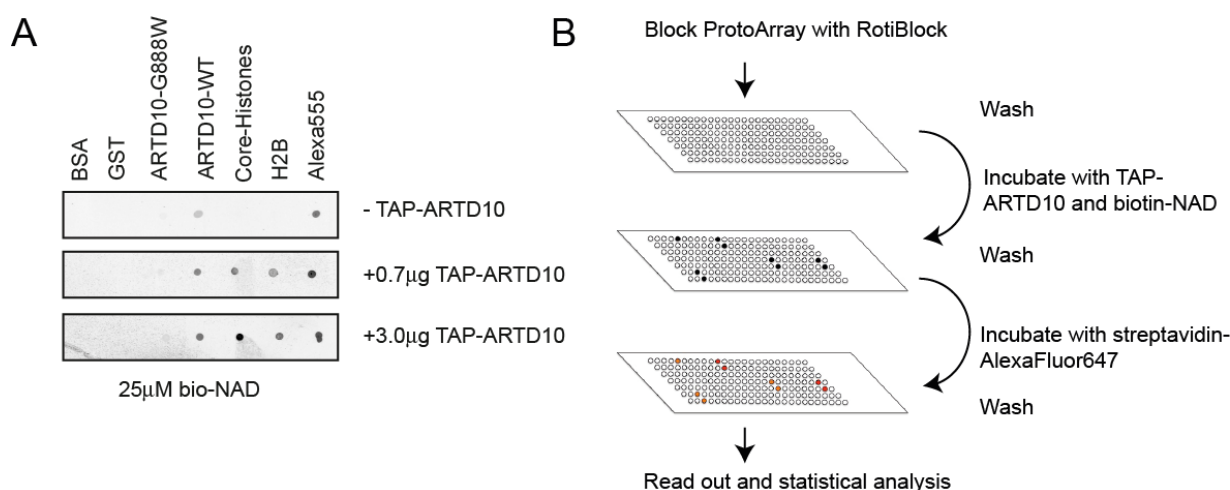


Figure 13 Overview of the ProtoArray approach. (A) Nitrocellulose membranes with spotted ARTD10, core histones, BSA and GST were employed by A. Braczynski to optimize array conditions. Modified from (Braczynsky, 2009). (B) Schematic representation of ProtoArray screens. Each array was incubated with ARTD10, ARTD8 or BSA and 25 μM biotin-β-NAD⁺ and visualized using streptavidin-AlexaFluor647.

These experiments indicate that ARTD10 is capable of modifying immobilized proteins with biotin-NAD⁺, since the positive control H2B is only modified in presence of TAP-ARTD10. ADP-ribosylation assays using biotin-NAD⁺ can thus be performed on these slides, upon which the incorporated mono-ADP-ribosylation can be detected by incubating with streptavidin-AlexaFluor647 (Figure 13B). A similar approach was used to investigate putative ARTD8 substrates. Instead of TAP-protein, baculo-derived ARTD8 was used.

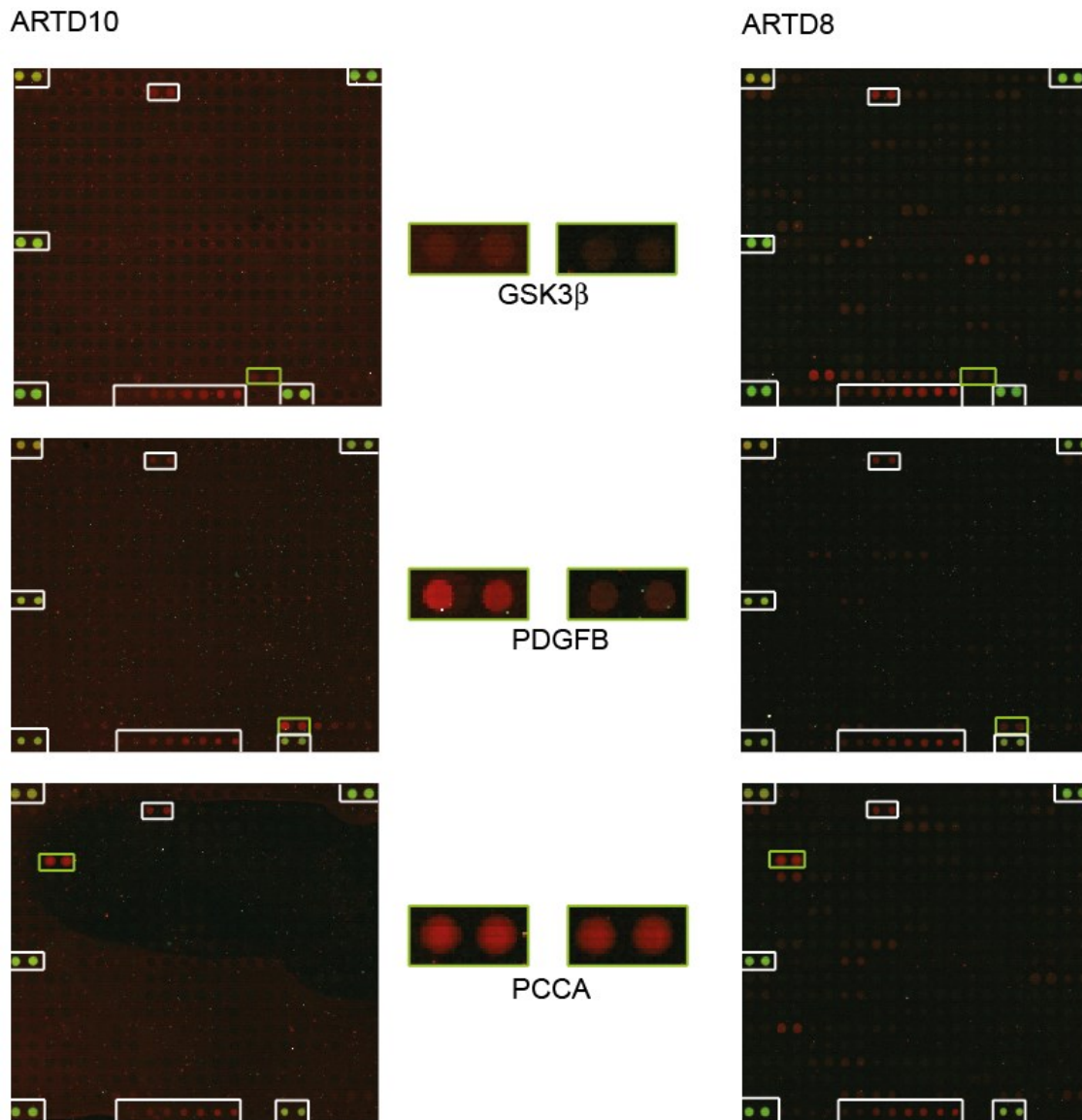


Figure 14 Sub-arrays showing individual hits for ARTD10 and ARTD8. The upper panels show the location of GSK3 β on both arrays, the middle panels show the modification of PDGFB on both arrays and the lower panels show PCCA on both arrays. In the middle a magnification of the relevant spots is shown.

Exemplary sub-arrays are displayed, with spotted controls highlighted in white (Figure 14). When investigating these sub-arrays, it becomes clear that ARTD10 is stickier than ARTD8 and thus causes a higher background signal. It only sticks to the array surface however and not to spotted proteins, since most spots on the ARTD10 array appear blacker than the surrounding background. One of the sub-arrays displayed here contains the growth factor PDGFB, which apparently is a good ARTD10 substrate. The modification of PCCA is also shown, which was identified on both arrays but is a biotin-binding enzyme, indicating that the signal is probably caused by biotin binding of PCCA and not by enzymatic modification by ARTD10 or ARTD8. GSK β is being modified by ARTD10, although it appears to be only marginally above background. When compared to surrounding non-modified spots instead of comparing to background levels however, the signal seems quite strong. To

be able to judge modification rates objectively, a Z-score is calculated for every protein. This Z-score is calculated by subtracting the population mean (μ) from the sample mean (χ), subsequently divided by the standard deviation of the population (σ). All proteins with Z-scores ≥ 2.5 are considered a hit and were taken into account for further analysis.

Table 1: Top 30 ARTD10 substrates

ProtoArray ID	Uniprot ID	Full name	Z-score
PHG0046	PDGFB_HUMAN	Platelet-derived growth factor subunit B	28.0
NM_000282.1	Q5JTW5_HUMAN	Propionyl coenzyme A carboxylase, alpha polypeptide	20.9
histone		Histone (unfractionated whole histone)	18.3
Histone_F2a2		Histones H2A and H4	9.8
PHC1244	CCL19_HUMAN	Chemokine (C-C motif) ligand 19	9.7
PHC0215	IL21_HUMAN	Interleukin-21	9.4
BC038838.1	PRR16_HUMAN	Proline-rich protein 16	7.5
BC012109.1	HOME2_HUMAN	Homer protein homolog 2	7.0
NM_020166.2	G5E9X5_HUMAN	Methylcrotonoyl-coenzyme A carboxylase 1 (alpha)	6.6
NM_004113.3	FGF12_HUMAN	Fibroblast growth factor 12	6
PV3612	STK6_HUMAN	Aurora kinase A	5.6
PV3353	NEK6_HUMAN	Serine/threonine-protein kinase Nek6	5.5
PV4877	ACVR1_HUMAN	Activin receptor type-1	5.3
PV3270	GSK3A_HUMAN	Glycogen synthase kinase alpha	5.1
BC030711.2		C2orf13	5.0
PV4883	ACVL1_HUMAN	Serine/threonine-protein kinase receptor R3	4.9
PV3501	PLK1_HUMAN	Polo-like kinase 1	4.8
NM_032459.1	EFS_HUMAN	Embryonal Fyn-associated substrate	4.8
PV3973	KGP2_HUMAN	cGMP-dependent protein kinase 2	4.8
NM_173597.1		Hypothetical protein FLJ37587	4.8
PV3878	MARK2_HUMAN	Serine/threonine-protein kinase MARK2	4.7
PV3688	EPHA2_HUMAN	Ephrin type-A receptor 2	4.7
PHC1346	SDF1_HUMAN	Stromal cell-derived factor 1 (CXCL12)	4.6
PV3665	KC1D_HUMAN	Casein kinase I isoform delta	4.6
P2287	KPCD_HUMAN	Protein kinase C delta type	4.6
PHC1055	CCL5_HUMAN	C-C motif chemokine 5 (RANTES)	4.5
PV3826	CLK3_HUMAN	Dual specificity protein kinase CLK3	4.4
PHC0045	IL4_HUMAN	Interleukin-4	4.4
BC025700.1	AFF4_HUMAN	AF/FMR2 family, member 4	4.2
PV3365	GSK3B_HUMAN	Glycogen synthase kinase beta	4.2

In Table 1, a summary of the top hits identified on the ARTD10 arrays is given. After taking a first glance at the results, what becomes obvious is the presence of core histones amongst the top hits, thereby validating the previous studies and giving a first impression of reliability of the arrays.

Secondly, the presence of biotin-binding enzymes such as propionyl coenzyme A carboxylase alpha polypeptide (PCCA) and methylcrotonoyl-Coenzyme A carboxylase 1 alpha (MCCA) (Figure 14) among the top-hits implies that the spotted proteins are in a native state and able to bind biotin-NAD⁺. The measured signal for ARTD7 is probably automodification. Interesting is also that 3 of the proteins within the top 20, namely Never in mitosis A-related kinase 6 (NEK6), Aurora kinase A and Polo-like kinase (PLK1), are mitosis-related, implying that ARTD10 could regulate mitosis through these substrates. The growth arresting effect of ARTD10 in colony formation assays might be caused by modification of these substrates, possibly leading to disturbed mitosis. Before speculating on possible functions of the substrates identified however, it has to be validated that these proteins can indeed be modified by ARTD10 and ARTD8 in *in vitro* ADP-ribosylation assays and not merely represent some kind of artifact.

To validate the results shown in Table 1, several substrates were tested in independent ADP-ribosylation assays. Protein bought from Invitrogen was tested, IKKε and P-TEFb among the proteins tested as well as the cyclin-dependent kinase CDK5 (Figure 15A and B). Unfortunately, the P-TEFb protein preparation by Invitrogen proved insufficiently pure to distinguish whether CDK9 or Cyclin T is being modified by ARTD10. It is tempting to speculate that Cyclin T is substrate, since the protein band is not visible in coomassie staining but nevertheless a relatively strong ADP-ribosylation signal is present (Figure 15A). Alternatively, both might be modified by ARTD10, which has to be cleared in future studies with better protein preparations. Furthermore a panel of kinases, kindly provided by Stefan Knapp (Structural Genomics Consortium, Oxford, UK), was tested (Figure 15C). Interestingly, some of these proteins had a Z-score below 2.5, namely DYRK1, FES and SRPK2, which in this *in vitro* assay could be modified by ARTD10 nevertheless. This implies that by lowering the ProtoArray hit threshold from $Z \geq 2.5$ to for instance $Z \geq 2.0$, one could even increase the list of potential substrates. The kinase domain of cytoplasmic tyrosine-protein kinase BMX is not substrate, indicating that the modification site of this protein lies outside of the kinase domain. The growth factor PDGF-B was previously validated, as well as the kinase GSK3α (Feijs, 2009). Modification of the voltage-gated channel KCNAB1 immunoprecipitated from HeLa cells also takes place (Figure 15D) although to a lower extent and barely visible without enhancing contrast.

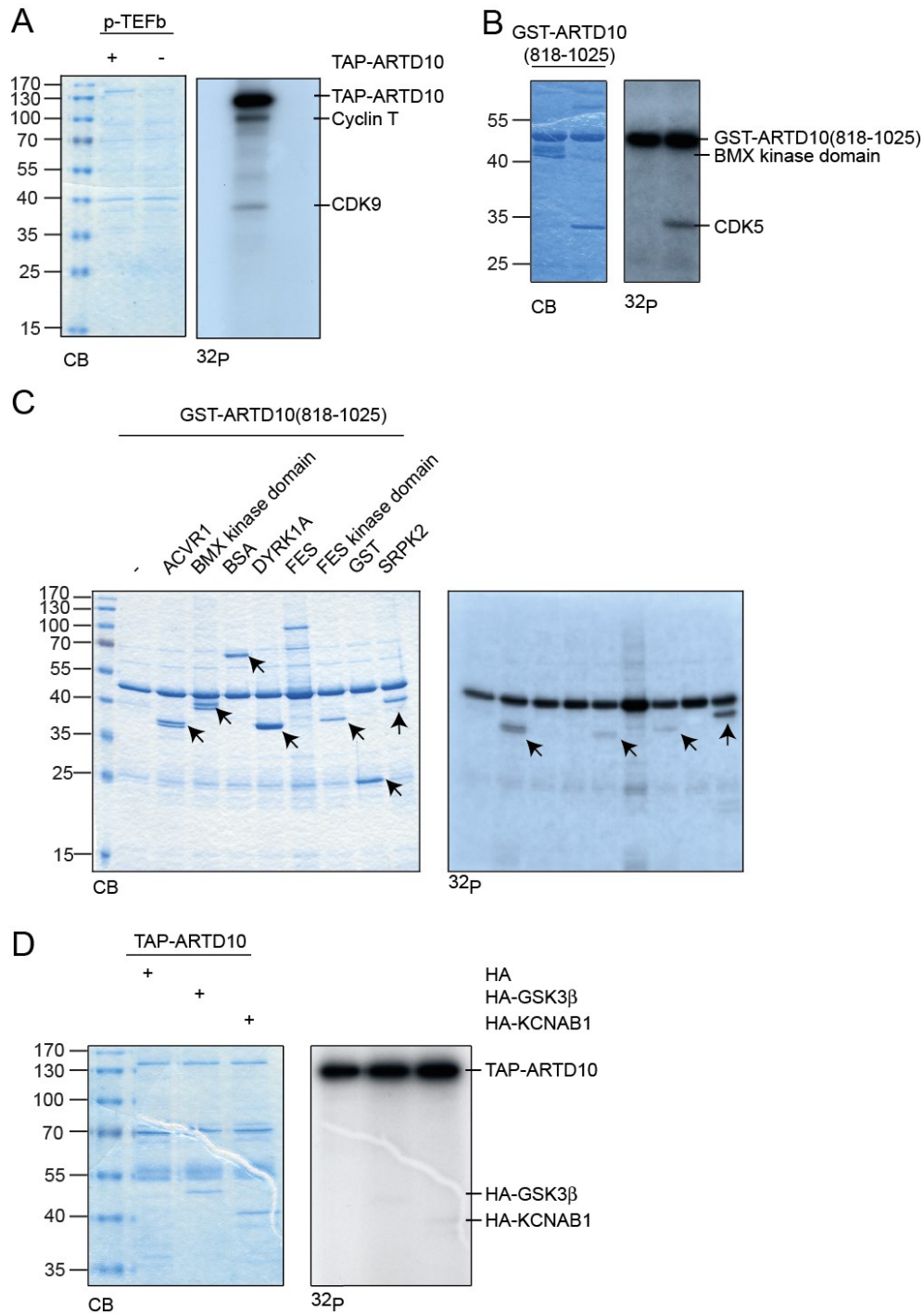


Figure 15 Validation of ProtoArray results. ADP-ribosylation assays were performed on (A) recombinant P-TEFb (B) recombinant BMX kinase domain and CDK5 (C) recombinant ACVR1, BMX kinase domain, BSA, DYRK1A, FES, FES kinase domain, GST and SRPK2 (D) immunoprecipitated HA-GSK3β and HA-KCNAB1 from transiently transfected HeLa cells

This might possibly be due to endogenous mono-ADP-ribosylation of the protein that currently cannot be assessed because of lacking tools to detect mono-ADP-ribosylation. Once hydrolases are identified that remove mono-ADP-ribose from substrates, one could treat immunoprecipitated proteins with these hydrolases to remove all possible endogenous mono-ADP-ribosylation and test whether

immunoprecipitated proteins become a better substrate then. Alternatively, there could be other posttranslational modifications present that block efficient ADP-ribosylation by ARTD10. The last possibility might also be interference of the immunoprecipitation procedure with subsequent ADP-ribosylation assays, where for instance the antibody might get in the way.

The modification of proteins from different sources however excludes the possibility of false positive hits due to the technical artifacts in Invitrogen's protein purifications. Since all tested full-length proteins could be verified as substrate, it can be assumed that the arrays are valid and the proteins identified true substrates, at least in *in vitro* assays.

To analyze the similarities between the ARTD10 and ARTD8 substrate sets, a Venn diagram was made which shows that there is some overlap between ARTD10 and ARTD8 substrates, although both have a substantial amount of unique substrates (Figure 16A). This hints at roles in some different processes for the two enzymes although partially redundant. That only a relatively small amount of the 8000 proteins on the array could be modified by ARTD8 and ARTD10 indicates that these enzymes are rather specific and probably function only partially redundant whilst having unique roles in certain processes.

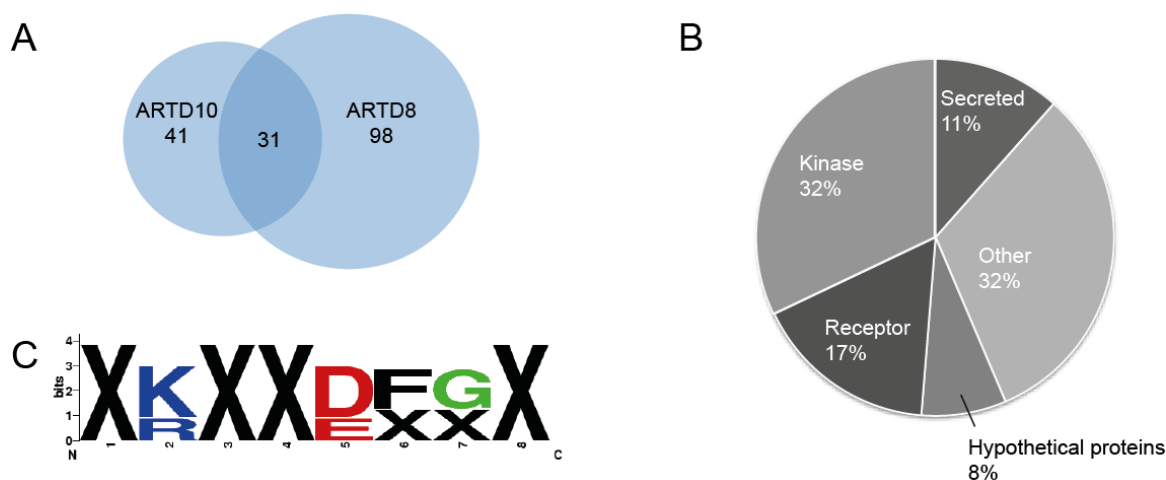


Figure 16 Analysis identified ARTD8 and ARTD10 substrates. (A) Venn diagram showing the overlap between the ARTD8 and the ARTD10 substrate sets. (B) ARTD10 substrates sorted according to function (C) Bioinformatical analysis revealed that the displayed motif appears more often in the positive hits than in the negative proteins (in collaboration with A. Schuppert).

ARTD8 activates STAT-dependent gene expression upon IL-4 stimulation (Goenka and Boothby, 2006; Goenka et al., 2007; Mehrotra et al., 2011) and it also protects B-cells from apoptosis by regulating key players in apoptosis, such as caspase-3 (Cho et al., 2009). Recently ARTD8 was described to be necessary for full pro-survival signaling by IL-4 in B-cells. Inhibition of AMP-activated protein kinase (AMPK) disturbed IL-4 induced cell survival and glycolysis, activation of AMPK in *Artd8*-null cells sufficed to restore IL-4 mediated signaling (Cho et al., 2011). Together,

these reports hint at a role of ARTD8 in lymphoma survival and regulation of cellular metabolism and glycolysis. Gene ontology analysis of the ARTD8 substrates identified reveals that several substrates are involved in insulin signaling, such as insulin receptor substrate 1 (IRS1) and protein kinase c zeta (PRKCZ), through which glycolysis can be influenced. Death-associated protein kinase 1 and 3 (DAPK1 and DAPK3) are two of the identified substrates that directly link ARTD8 with apoptosis. So far, the role of ARTD8 in apoptosis and metabolism has been investigated mainly in a descriptive manner. The underlying mechanisms might be uncovered by further analysis of the substrates described here.

We focused on the ARTD10 substrate-set for further analysis and summarized the functions of the identified proteins (Figure 16B). It becomes apparent that the kinases seem to be overrepresented as substrate, as well as secreted factors. The high amount of growth factors as well as the top outlier being a growth factor might urge to further investigate the functional consequence of mono-ADP-ribosylation for this subclass of ARTD10 substrates. At the moment it is however not clear where and when ARTD10 and those growth factors could get in near proximity in cells. It is not possible yet to distinguish whether the identified growth factors are an artifact caused by the non-physiological conditions of the arrays, in which ARTD10 is capable of modifying any residues sticking out far enough or whether there are as yet unknown physiological processes wherein ARTD10 modifies growth factors. ARTD10 could for example have a role to play in non-conventional protein secretion such as an autophagy-based secretion pathway (Dupont et al., 2011), especially considering the fact that ARTD10 interacts with autophagy-adaptor protein p62 (Kleine et al., 2012). Or ARTD10 might be released into the extracellular matrix itself, perhaps from dying cells, or maybe even in a more regulated manner after inflammasome activation (Gross et al., 2011). Evidence for extracellular ART activity already exists in the form of release of other enzymatically active ADP-ribosyltransferases from activated T-cells (Kahl et al., 2000). It is a fascinating question nevertheless what happens to these growth factors once modified. Are they still able to bind to their receptors or is their receptor affinity changed? It has already been described that extracellular arginine-ADP-ribosylation of PDGF-B by ARTC1 leads to a reduced receptor binding capacity (Saxty et al., 2001).

ARTD10 apparently has quite strict substrate preferences, since it only modifies a small percentage of the 8000 proteins present on the ProtoArrays. We therefore asked whether there is a similarity between the positive hits that appears less frequent in the negative proteins. Informatics students without extensive molecular biology knowledge performed this bioinformatical analysis, thereby making this study completely unbiased (Bayer et al., 2011). Several motifs could be identified that are enriched in the positive hits and that can be summarized as K/RxxE/DxG (Figure 16C). Interestingly, the DFG-motif was identified before as general kinase motif, containing residues essential for catalytic activity (Kornev et al., 2006). It is not clear whether this motif was identified here because of the high

representation of kinases within the substrate group or because ARTD10 modifies one of the residues in this motif, thereby causing so many kinases to be substrate. The high presence of kinases and associated kinase motifs might actually mask the presence of other motifs that might be more relevant for ARTD10 substrate recognition. If on the other hand ARTD10 recognizes and modifies amino acids in this motif, then mono-ADP-ribosylation could represent an important general regulator of kinase activity.

Since it is currently not clear whether ARTD10 can modify growth factors in cells, we decided to focus on the large substrate class of kinases and selected GSK3 β as model kinase for tests of the functional consequences of mono-ADP-ribosylation. Through GSK3 β a link is also established to the protein that ARTD10 originally was purified with, MYC (Yu et al., 2005). Phosphorylation of MYC on T58 by GSK3 β leads to its activation, but also ubiquitination and subsequent degradation as reviewed in (Adhikary and Eilers, 2005; Vervoorts et al., 2006). Finally, GSK3 β was not a substrate of ARTD8 on the ProtoArrays, making it more likely that putative functional consequences are really due to ARTD10 catalyzed mono-ADP-ribosylation and not to ARTD8.

mono-ADP-ribosylation of GSK3 β regulates kinase activity

Bacterially purified GST-GSK3 β was tested as substrate (data not shown) and could be verified although weakly, but these protein preparations showed high amounts of breakdown products. Using the GateWay cloning technology, expression vectors suitable for the baculoviral system were created with as starting point the pcDNA3.1-HA-GSK3 β acquired from Addgene (He et al., 1995). The pBAC-GST-GSK3 β vector was transfected into SF9 cells, subsequent rounds of virus amplification were performed until the virus titer was suitable for final infection and protein purification. Staining with a specific antibody revealed that the protein binding to the beads indeed is GSK3 β and that only small amounts of protein are lost during purification (Figure 17A).

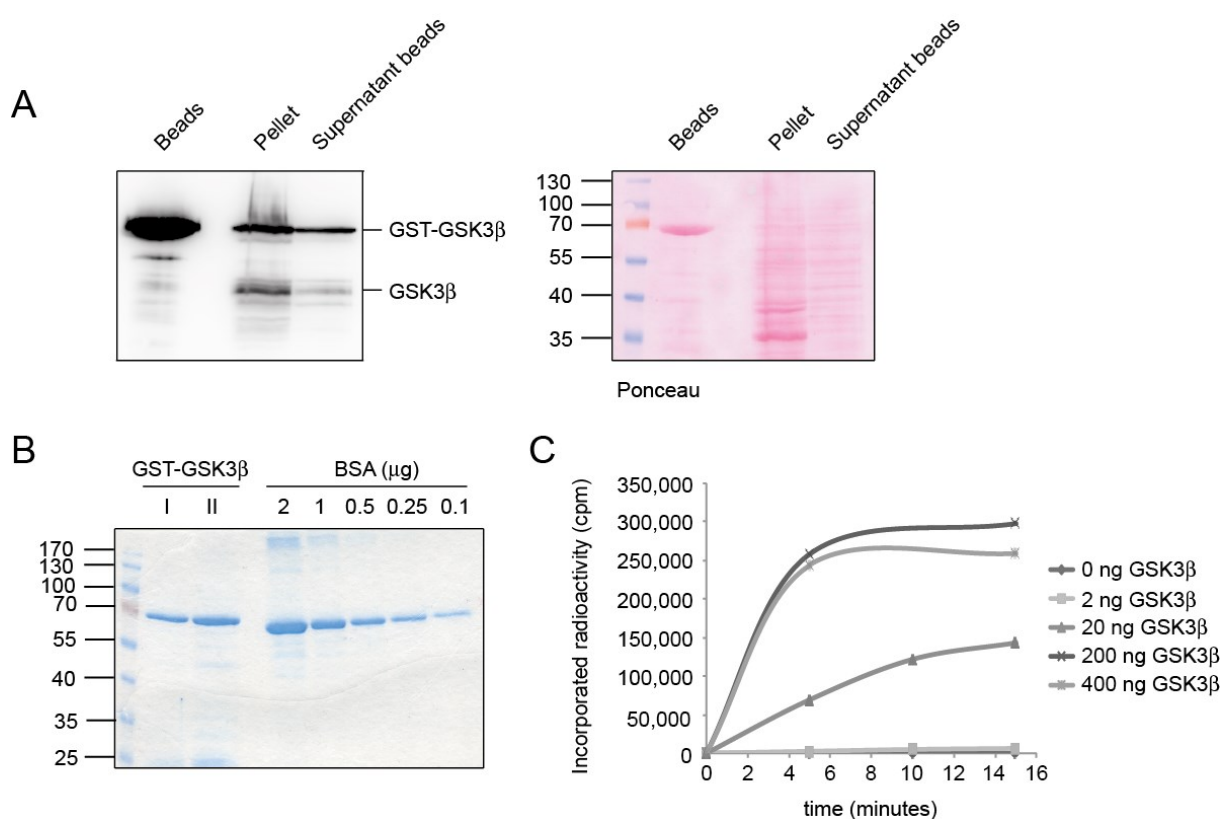


Figure 17 Purification and characterization GST-GSK3 β . (A) Small-scale GST-purification, where boiled GST-beads, pellet and supernatant of pellet incubation were tested in WB for GSK3 β presence. Left panel; specific α -GSK3 β staining, right; Ponceau staining. (B) Coomassie staining of a large-scale purification, with a BSA standard ranging from 2 μ g to 0.1 μ g. (C) Increasing amounts of GSK3 β were titrated in an *in vitro* kinase assay, incorporated radioactivity was assessed by scintillation counting.

The quality and quantity of the protein in the two elution fractions was analyzed by coomassie blue staining (Figure 17B). Additionally, mass spec analysis (data not shown) also confirmed the purified protein as GSK3 β . Lastly, its kinase activity was determined using kinase assays with radioactively labeled ATP and a primed substrate peptide (Figure 17C), where it becomes clear that the purified

protein is highly active and that small kinase amounts are best for enzymatic assays, as not to reach saturation too quickly.

When tested in an ADP-ribosylation assay with TAP-ARTD10, baculo-purified GST-GSK3 β could indeed be mono-ADP-ribosylated, whereas the negative control, GST could not (Figure 18A). An interesting side note is that ARTD10 seems to have differing affinities for GSK3 β purified from different sources. The most intense signal is achieved in an ADP-ribosylation assay with baculo-derived GST-GSK3 β , whereas GST-tagged GSK3 β purified from *E.coli* is modified less well. GST-GSK3 β purified from *E.coli* has kinase activity, although to a lower extent, so apparently it is folded correctly. It is tempting to speculate that baculo-derived GSK3 β carries some modification that increases the affinity of ARTD10 towards it. Examples of enzymes only recognizing proteins when these have certain PTMs already exist, such as described above for the E3 ligases Iduna or SCF^{FBW7}. HA-GSK3 β immunoprecipitated from HeLa cells is also a rather weak substrate (Figure 15D), indicating that the protein already is mono-ADP-ribosylated, lacks the right PTM or maybe carries a PTM that blocks efficient ADP-ribosylation by ARTD10.

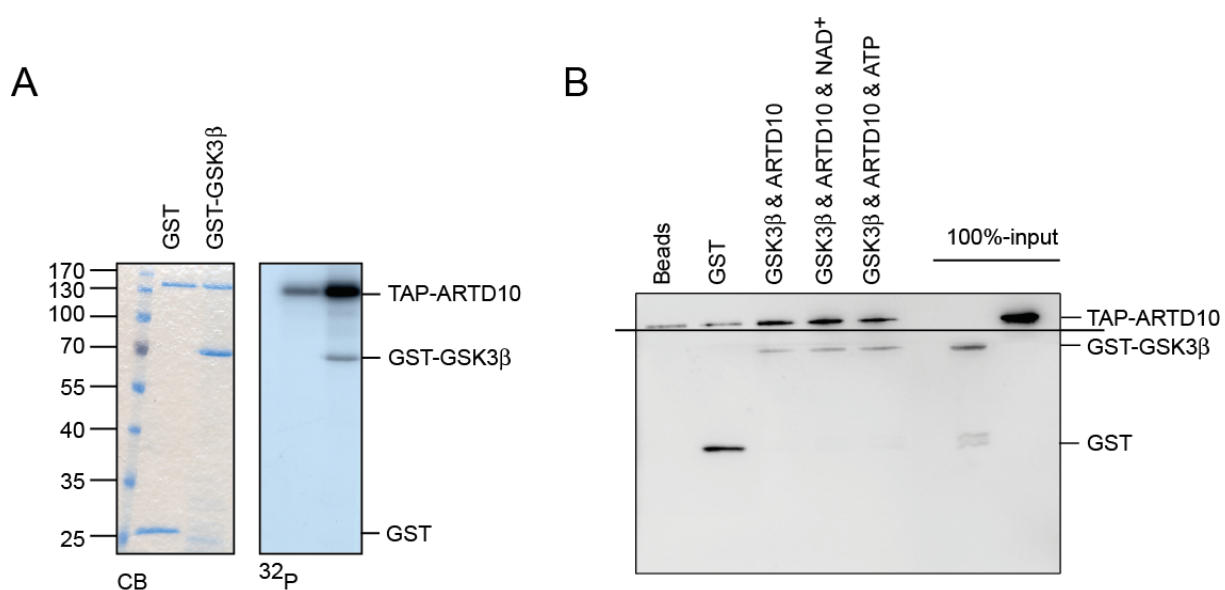


Figure 18 GSK3 β is mono-ADP-ribosylated by ARTD10 and interacts with ARTD10. (A) ADP-ribosylation assay with TAP-ARTD10 and GST-GSK3 β or GST, analyzed by coomassie and autoradiography. (B) GST-pull down experiment between TAP-ARTD10 and GST-GSK3 β . The blot was cut in two, the upper piece was incubated with an ARTD10 antibody, the lower part was incubated with a GST antibody.

GST-pull down experiments show a weak interaction between TAP-ARTD10 and GST-GSK3 β although above background, that is not dependent on ATP or NAD⁺ (Figure 18B).

Next we addressed whether mono-ADP-ribosylation in any way influences the enzymatic activity of GSK3 β , although no direct effects of mono- or poly-ADP-ribosylation have been described for

proteins modified by eukaryotic enzymes so far. For this purpose GST-GSK3 β was mono-ADP-ribosylated by TAP-ARTD10 and then tested in an *in vitro* kinase assay using a synthetic peptide carrying a priming phosphate. The kinase activity of mono-ADP-ribosylated GSK3 β activity was significantly reduced, in contrast to incubation of GSK3 β with TAP-ARTD10 in the absence of β -NAD⁺ or with the catalytically inactive mutant ARTD10-G888W, which resulted in a small increase in activity (Figure 19A).

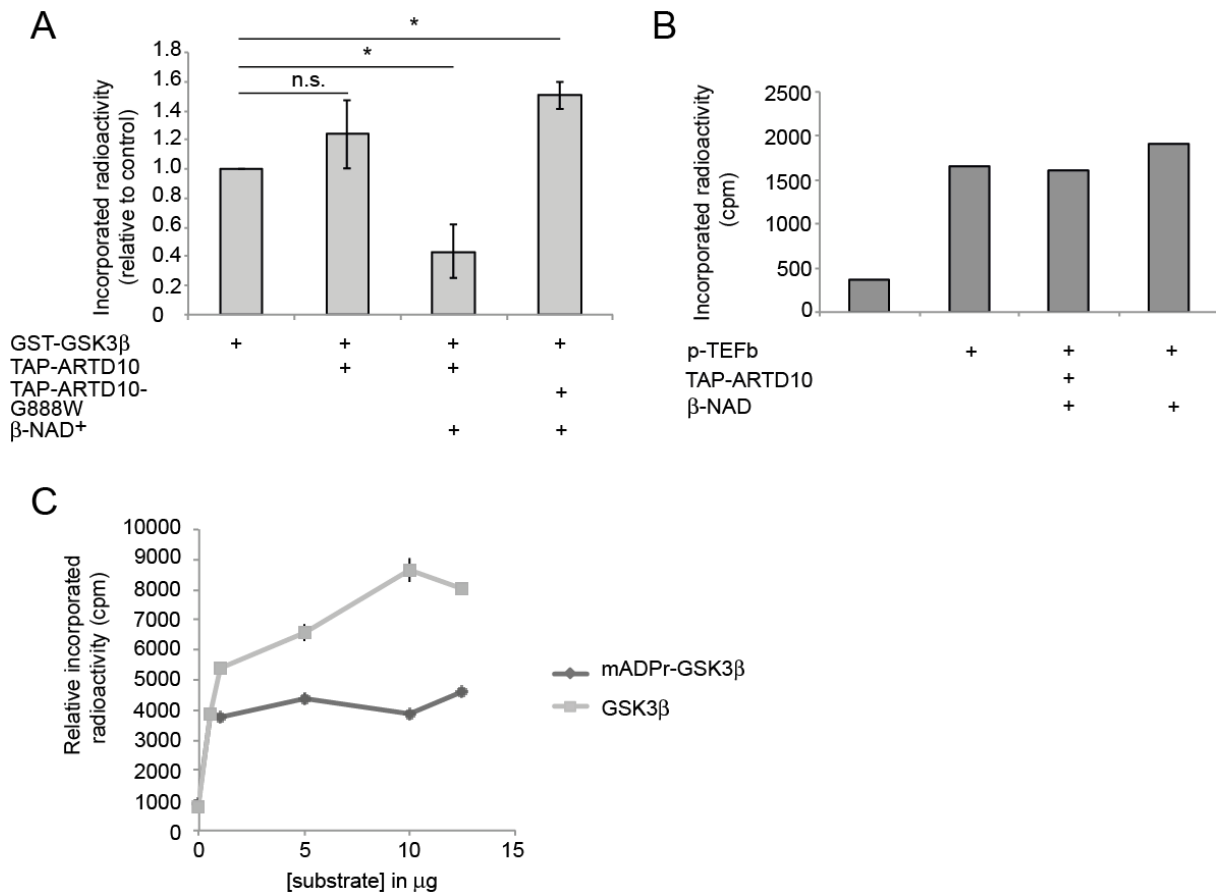


Figure 19 Mono-ADP-ribosylation inhibits GSK3 β activity *in vitro* but not P-TEFb activity. (A) GSK3 β was mono-ADP-ribosylated with β -NAD⁺ and subsequently activity was assessed in a kinase assay with a substrate peptide and [³²P]- γ -ATP. Incorporated radioactivity was determined by scintillation counting. Data are represented as mean \pm SD of a representative experiment with triplicate measurements. (B) Assays performed as in (A) but with P-TEFb instead of GSK3 β . Preliminary data from one experiment are displayed. (C) Increasing amounts of substrate were titrated in an *in vitro* kinase assay with untreated or mono-ADP-ribosylated GSK3 β , incorporated radioactivity was assessed by scintillation counting. Error bars represent SD of quadruplicate measurements a representative experiment is shown.

Phosphorylations in the activation loop determine the structural localization of the aspartate of the DFG motif, necessary for an active kinase (Kornev et al., 2006). If ARTD10 modifies a site in this area, ADP-ribosylation might thus prevent the proper conformation and thereby block catalytic activity. Moreover, since the kinase purified from *E.coli* will lack the phosphorylation at this site and thus have the DFG-motif in a closed conformation already, this might be the wrong conformation to allow efficient modification by ARTD10 and thereby explain why GSK3 β from SF9 cells is a better

substrate than GSK3 β . The differences between the GSK3 β from different sources could be tested using mass spec to investigate whether there indeed are different PTMs that might influence recognition by ARTD10.

In contrast, when subjecting P-TEFb to similar experiments, no effect on kinase activity could be measured in a preliminary experiment (Figure 19B), implying that either modification is not taking place efficiently enough or that mono-ADP-ribosylation has a different effect on this cyclin/CDK complex. This could be due to the fact that the cyclin subunit might be modified and not the kinase, which has to be clarified in future studies, where it for instance could also be addressed whether mono-ADP-ribosylation of P-TEFb influences binding of the different subunits to each other or to different proteins like MYC, which it has been shown to bind to (Kanazawa et al., 2003). Alternatively, intracellular localization of the P-TEFb subunits might be influenced by mono-ADP-ribosylation, as has been described for other PTMs of P-TEFb (Dow et al., 2010).

Serine 9 phosphorylation of GSK3 β functions as competitive inhibitor of enzymatic activity (Frame et al., 2001), since the tail folds back onto the kinase domain as pseudo-substrate and blocks the catalytic site in this manner (Figure 1). To investigate whether mono-ADP-ribosylation functions in a manner comparable to serine 9 phosphorylation, substrate amounts were titrated in *in vitro* kinase assays. In the case of competitive inhibition, sufficient amounts of substrate will lead to increased kinase activity despite inhibitor since the substrate will then effectively compete with the pseudo-substrate for binding in the catalytic center. The graph in Figure 19C shows that initially non-modified GSK3 β shows a higher activity than mono-ADP-ribosylated GSK3 β as expected. The increasing amounts of substrate do not suffice to abolish the inhibitory effect of mono-ADP-ribosylation, as even high amounts of substrate do not restore kinase activity to a level comparable to non-modified GSK3 β , indicating a non-competitive inhibitory mechanism. Since serine 9 phosphorylation functions as competitive inhibitor, the here reported inhibitory mechanism is proposed to be distinct from the inhibition caused by serine 9 phosphorylation and thus represents a novel regulatory mechanism.

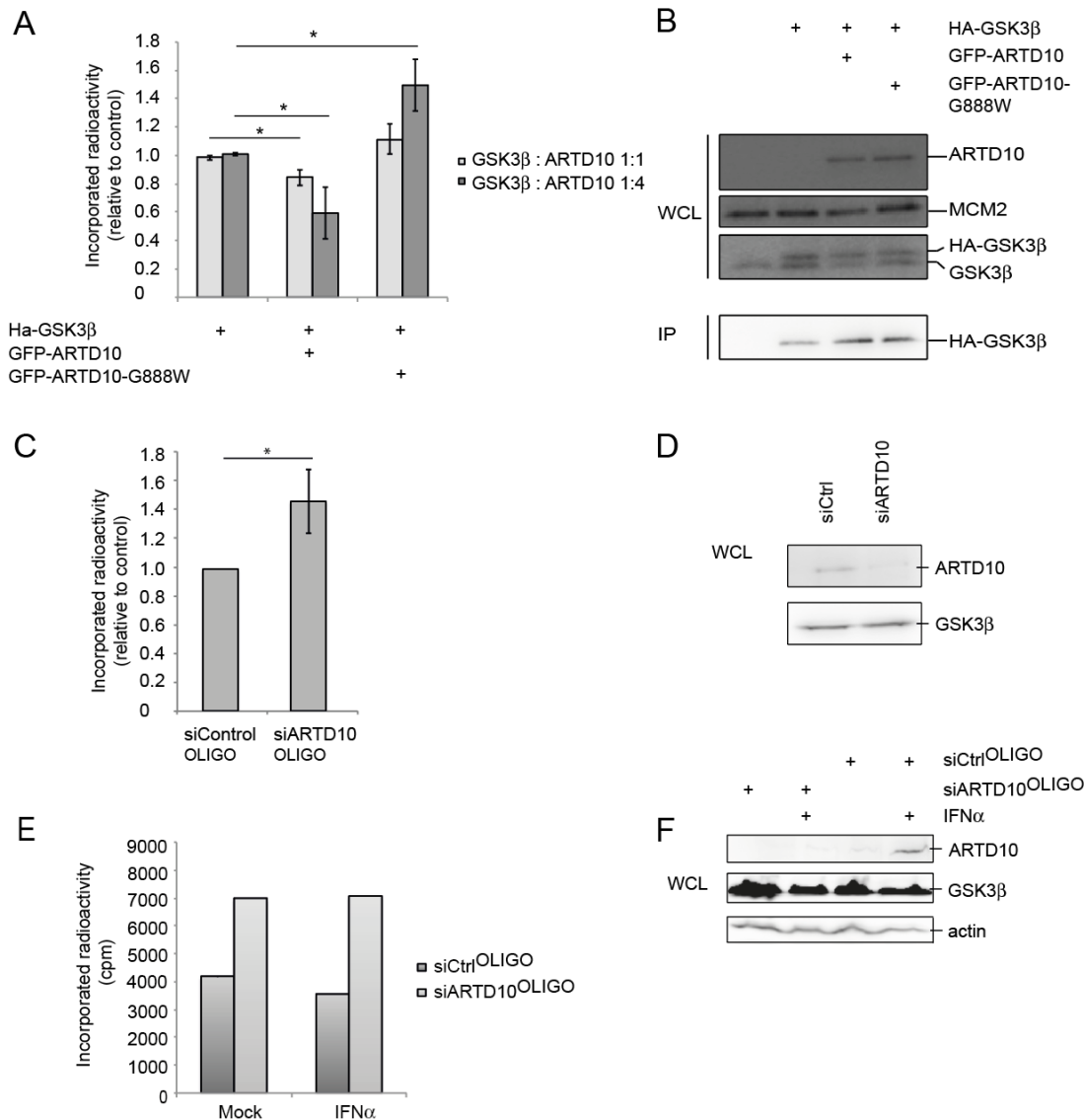


Figure 20 Mono-ADP-ribosylation inhibits GSK3 β activity in cells. (A) GFP-ARTD10 or the inactive mutant GFP-ARTD10-G888W were co-expressed with HA-GSK3 β in U2OS cells. Immunoprecipitated GSK3 β was subsequently subjected to an *in vitro* kinase assay. Data are represented as mean \pm SEM of biological triplicates. (B) Input controls for (A). (C) U2OS cells were treated with siARTD10 or siControl pools, endogenous GSK3 β was immunoprecipitated, subjected to kinase assays and evaluated with scintillation counting. Data are represented as mean \pm SEM of biological triplicates. (D) Input controls for (C). (E) U2OS cells transfected with siRNA pools were mock- or IFN α -treated 24 hours after transfection, lysed after 48 hours, endogenous GSK3 β was immunoprecipitated, subjected to kinase assays and evaluated with scintillation counting. Preliminary data from one experiment are shown. (F) Input controls for (E).

Previous studies using colony formation assays have revealed that overexpression of ARTD10, but not ARTD10-G888W, interferes with cell proliferation (Kleine et al., 2008), suggesting that mono-ADP-ribosylation occurs in cells and is vital for normal cell physiology. To expand on this observation, we co-expressed GFP-ARTD10 or GFP-ARTD10-G888W together with HA-GSK3 β in U2OS cells and subsequently determined kinase activity of immunoprecipitated GSK3 β . Kinase activity was decreased with co-expression of ARTD10 compared with control-transfected cells (Figure 20A), indicating that ARTD10 indeed intracellularly mono-ADP-ribosylates GSK3 β . In contrast, co-expression of

ARTD10-G888W induced kinase activity, which might be due to a dominant-negative effect of the catalytically inactive ARTD10 and thus hints at the presence of endogenous mono-ADP-ribosylation of GSK3 β . The effects were not the result of altered GSK3 β expression or of different immunoprecipitation efficiencies (Figure 20B).

To exclude artifacts caused by protein overexpression, we additionally knocked down ARTD10 with siRNA SMARTpools in U2OS cells, immunoprecipitated endogenous GSK3 β and tested kinase activity. Knockdown of ARTD10 was efficient and indeed led to a significant increase in kinase activity (Figure 20C), thereby again hinting at endogenous ADP-ribosylation. The differences in kinase activity were not caused by influences of siRNA on GSK3 β levels, since the input blots show comparable levels of GSK3 β in siControl and siARTD10 treated cells (Figure 20D).

To test in a preliminary experiment whether IFN α indeed induces ARTD10 expression as reported, cells transfected with siControl or siARTD10 were stimulated with IFN α for 24 hours, as ARTD10 was indicated as late-response gene (Mahmoud et al., 2011). ARTD10 protein expression is only upregulated in the siControl-transfected cells and not in the siARTD10-transfected cells, indicating that IFN α indeed upregulates ARTD10 gene transcription (Figure 20F). Moreover, IFN α seems to have an inhibitory effect on GSK3 β activity, indicating that upon upregulation of ARTD10, it modifies a larger amount of GSK3 β and thereby blocks kinase activity (Figure 20E). IFN α has no effect on GSK3 β activity in the siControl-transfected cells.

Further validating these findings, we measured the phosphorylation of p65 RELA at S468, a known GSK3 β target as schematically represented in Figure 21A (Buss et al., 2004). ARTD10-G888W overexpression and knockdown of endogenous ARTD10 by shRNA enhanced p65-S468 phosphorylation (Figure 21B), supporting the concept that mono-ADP-ribosylation of GSK3 β by ARTD10 inhibits kinase activity in cells. Overexpressed HA-GSK3 β is efficiently phosphorylated at serine 9, explaining why overexpression of HA-GSK3 β does not suffice to induce p65-S468 phosphorylation to the same extent.

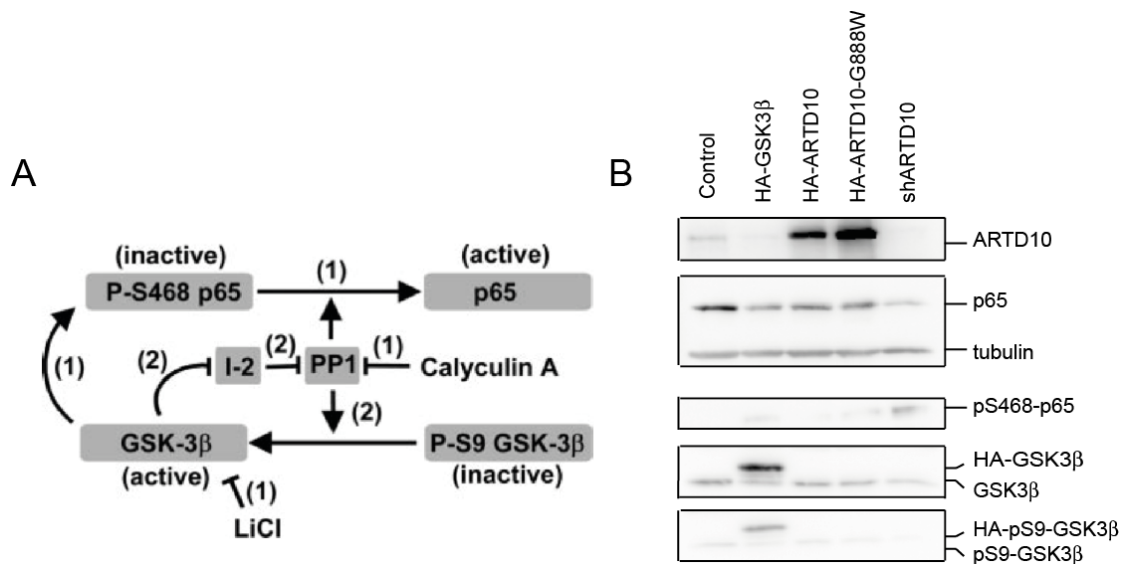


Figure 21 Mono-ADP-ribosylation influences GSK3 β downstream signaling. (A) Schematic representation of GSK3 β and p65 inhibitory phosphorylations. Modified from (Buss et al., 2004). (B) ARTD10 was knocked-down using shRNA or overexpressed in U2OS cells, as well as ARTD10-G888W or HA-GSK3 β . 48 hours after transfection cells were lysed and the proteins analyzed on Western Blot. A representative blot is shown.

Although this is only indirect proof of intracellular mono-ADP-ribosylation, because of the lack of antibodies or other detection tools, this is currently the best evidence of intracellular ARTD10 activity that can be achieved. That mono-ADP-ribosylation can directly influence the activity of a substrate implies a functional difference between poly- and mono-ADP-ribosylation, because poly-ADP-ribosylation so far has mainly been reported to influence signaling events through recruitment of other proteins, such as ubiquitin E3 ligases (Gibson and Kraus, 2012), but not through a direct regulation of enzymatic activity of substrate proteins. PAR chains might actually also be capable of influencing proteins directly, but we might just not be aware of it yet. In contrast to serine 9 phosphorylation, this inhibitory mechanism seems to be non-competitive and thereby opens a novel dimension in GSK3 β regulation. It is tempting to speculate that different stimuli might lead to different ways of inhibition of GSK3 β , thereby directing GSK3 β activity to certain pathways under specific circumstances, as has been described before in e.g. regulation of Wnt signaling (McNeill and Woodgett, 2010).

The transcription factor MYC should also be influenced by altered GSK3 β activity, as schematically summarized in Figure 22A. Decreased phosphorylation by GSK3 β should lead to decreased ubiquitination and increased stability of MYC, because the recognition site for SCF^{FBW7} is dependent on this phosphorylation as described in the introduction. *In vivo* ubiquitination experiments reveal no such effect on MYC ubiquitination, which seems to be not influenced by ARTD10 co-expression (Figure 22B). However, these experiments were performed in the absence of any proteasome inhibitor, which should lead to a degradation of the K48-linked MYC modified by SCF^{FBW7}, indicating that it likely is K63-linked polyubiquitin that is present in the pull-down. Any effects on K48-linked ubiquitination could be masked by strong K63-linked ubiquitin signals. Experiments performed with a

proteasomal inhibitor have a similar outcome, which may indeed be caused by a strong K63-linked polyubiquitination (data not shown). To avoid the difficulties with K63-linked ubiquitin masking K48-linked ubiquitin signals, MYC activity was next tested in reporter gene assays. Here it could indeed be shown that ARTD10 co-expression negatively influences MYC activity (Figure 22C), which is in accordance with lower kinase activity and thus less T58 phosphorylation, which is not only a signal for degradation through ubiquitination but also for activation (Vervoorts et al., 2006). It is however also possible that ARTD10 affects MYC activity not through GSK3 β , but via one of its other substrates, such as P-TEFb (Gargano et al., 2007; Kanazawa et al., 2003), or also directly through the protein-protein interaction published before (Yu et al., 2005).

HECTH9 is an E3-ligase ubiquitinating MYC with K63-linked polyubiquitin, not leading to degradation of MYC but to activation (Adhikary et al., 2005). In the reporter gene assay, overexpressed MYC can indeed be further activated by co-expression of HECTH9 (Figure 22C). ARTD10 and the inactive mutant ARTD10-G888W are capable of repression also in the presence of HECTH9. A double mutant, where the UIMs are inactivated and catalytic activity is blocked, ARTD10-G888WdUIM, has no repressive effect anymore, suggesting that ARTD10 might be recruited through its UIMs and inhibit MYC by binding to it in addition to the necessity of catalytic activity. *In vitro* pull-down assays were used to narrow-down the region of MYC interaction within ARTD10, but due to stickiness of *in vitro* translated MYC, MYC signals were present after incubation with 5 different ARTD10 fragments (data not shown) and since this was not the main focus of the study presented here, further attempts at unraveling the relation between MYC and ARTD10 were abandoned for the time being.

However, future experiments could address the role of endogenous ARTD10 in MYC regulation by inducing ARTD10 expression by IFN α and assessing endogenous MYC-responsive genes by rt-PCR or in reporter gene assays.

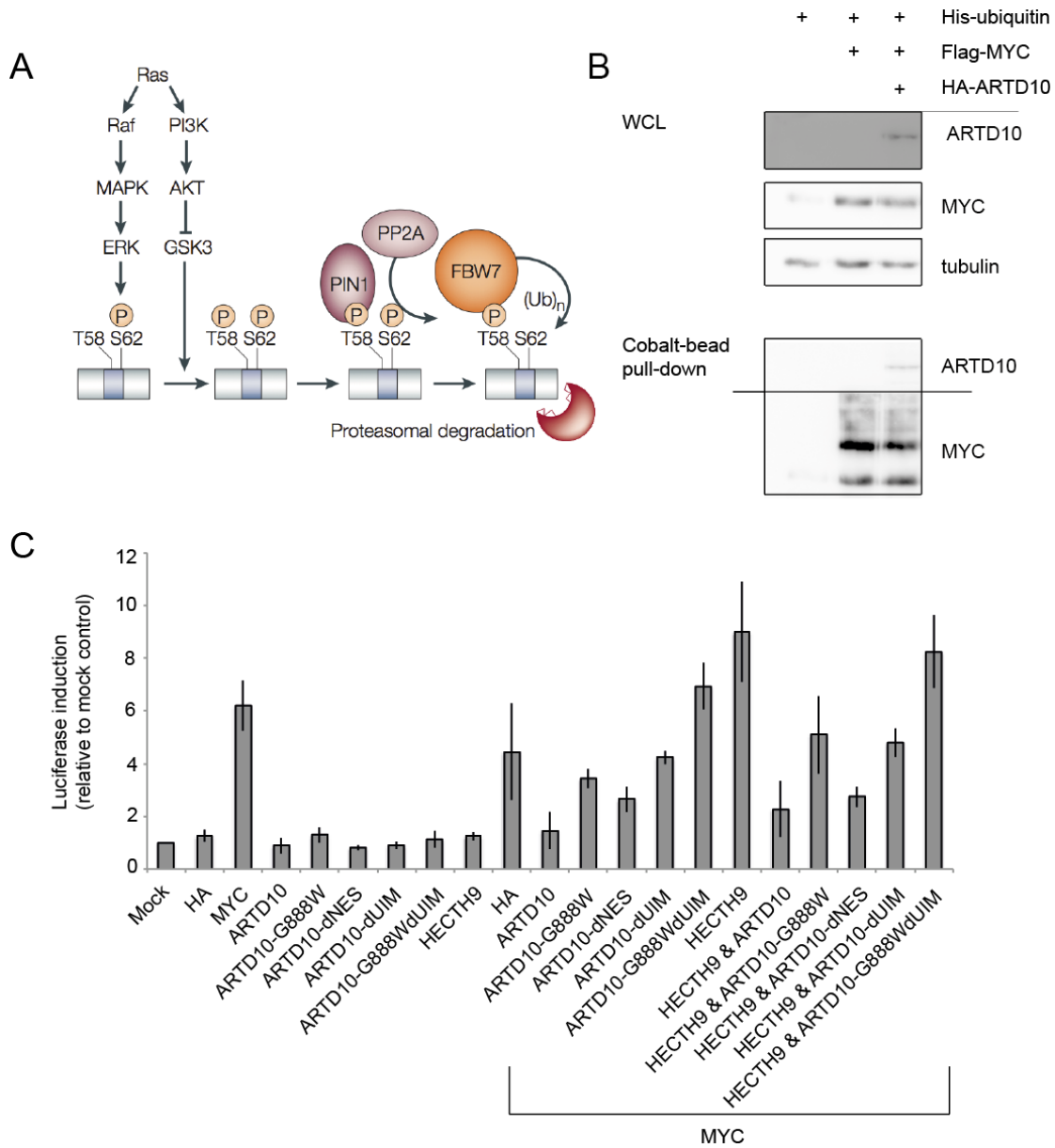


Figure 22 ARTD10 has no influence on MYC ubiquitination but represses reporter gene activity. (A) Schematical representation of the different signals leading to MYC phosphorylation and ubiquitination. Modified from (Adhikary and Eilers, 2005). (B) U2OS cells were transfected with His-ubiquitin, Flag-MYC and HA-ARTD10. Upon urea lysis, a pull-down was performed with TALON™ Metal Affinity Resin followed by a WB. Upper panel displays the input controls, lower panel displays the pull-down, where the upper part was incubated with an ARTD10 antibody and the lower part with an MYC antibody. A representative blot is shown. (C) Reporter gene assay in U2OS cells, where the influence of indicated proteins was tested on an artificial luciferase construct with multiple MYC-binding sites ($n \geq 3$).

An interesting additional observation in the *in vivo* ubiquitin assays is that ARTD10 itself is also pulled-out with TALON™ Metal Affinity Resin from cells containing His₆-ubiquitin, indicating that ARTD10 is also ubiquitinated under these circumstances (Figure 22B). This is probably also not K48-linked ubiquitin, since the protein carrying this would have been degraded quickly in the absence of proteasome inhibitor.

These findings highlight the possible effects of mono-ADP-ribosylation on GSK3 β activity towards its substrates in cells, the full extent to which GSK3 β 's activity is altered towards its vast array of substrates remains to be assessed. Since GSK3 β has already been described to be present in different intracellular pools depending on different stimuli (Taelman et al., 2010), it might well be that substrates of one GSK3 β pool are influenced whereas others are not. This could be an explanation of the negative influence of ARTD10 on p65 phosphorylation but the lack of effect on MYC ubiquitination. If ARTD10 mono-ADP-ribosylates only cytoplasmic GSK3 β , then it might be expected that phosphorylation of MYC by GSK3 β is not influenced. Another key aspect in this regard is the priming phosphate preference of GSK3 β that might actually be more limiting in some cases than GSK3 β activity itself. It could theoretically happen that GSK3 β becomes more active after inhibition of ARTD10, but if priming phosphates are lacking then increased GSK3 β activity will not be seen on these substrates. Future research will have to reveal which GSK3 β substrates can be influenced through manipulation of ARTD10.

Since multiple reports agree on a growth-inhibitory effect of ARTD10 (Chou et al., 2006; Kleine et al., 2008), colony formation assays were performed to test whether overexpression of the hyperactive mutant HA-GSK3 β -S9A can restore proliferation rates of cells with increased ARTD10 levels.

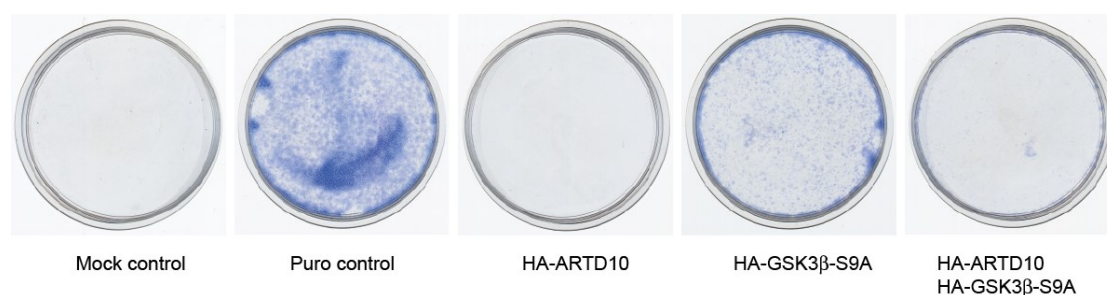


Figure 23 Colony formation assay with HA-ARTD10 and HA-GSK3 β -S9A. HA-ARTD10 and HA-GSK3 β -S9A were transfected into HeLa cells in addition to a puromycin control vector, transfected cells were selected by puromycin treatment. A representative experiment is shown.

HA-ARTD10 inhibits cell proliferation in this assay in accordance with published findings, however HA-GSK3 β -S9A co-expression does not suffice to restore the colony formation potential (Figure 23). This indicates that probably other ARTD10 substrates are responsible for the growth inhibitory phenotype or alternatively that the overexpressed S9A-mutant can also be mono-ADP-ribosylated very efficiently and thus is not able to overcome the inhibition of activity induced by ARTD10. Alternatively, the overexpression of an hyperactive GSK3 β mutant itself might inhibit proliferation, as colony formation seems to be reduced compared to control cells.

de-ADP-ribosylation by MDO2 restores GSK3 β activity

Regarding the impact of mono-ADP-ribosylation on GSK3 β , it can be hypothesized that this modification is reversible, comparable with e.g. reversibility of phosphorylation mediated by phosphatases. To test this hypothesis, GSK3 β was first mono-ADP-ribosylated *in vitro* and subsequently subjected to treatment with diverse potentially de-ADP-ribosylating enzymes.

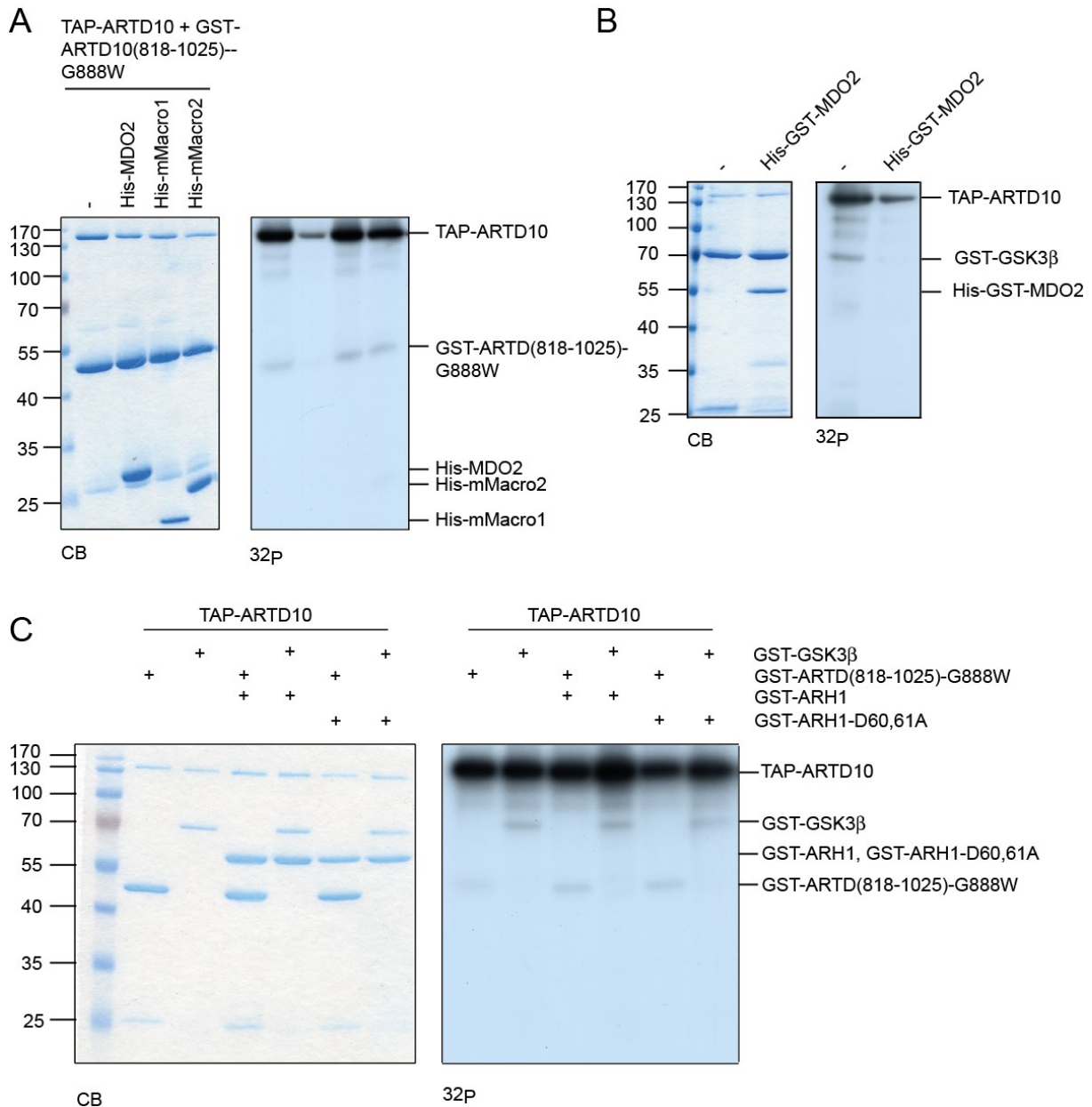


Figure 24 ARTD10 and GSK3 β can be de-ADP-ribosylated by MDO2 but not mMacro1, mMacro2 or ARH1. (A) Mono-ADP-ribosylated TAP-ARTD10 and GST-ARTD10-G888W were subjected to MDO2, Macro1 and Macro2 treatment. (B) Mono-ADP-ribosylated TAP-ARTD10 and GST-GSK3 β were subjected to His-MDO2 treatment. (C) Mono-ADP-ribosylated TAP-ARTD10, GST-GSK3 β and GST-ARTD10-G888W were subjected to ARH1 or ARH1D60, 61A treatment.

As expected, Macro1 and Macro2 of Artd8 cannot hydrolyze mono-ADP-ribose (Figure 24A), which also fits with the description of these Macrodomains as mono-ADP-ribose binding modules (Forst et al., manuscript in revision). His-purified His-GST-MDO2 however is capable of removing the ADP-ribose moiety from GSK3 β and also from ARTD10 itself (Figure 24B). This is quite surprising, as MDO2 has previously been described to hydrolyze *O*-acetyl-ADP-ribose only (Chen et al., 2011). No hydrolase activity of MDO2 towards ADP-ribosylated proteins has been shown before. In contrast to this, the arginine-specific ARH1 (kind gift from J. Moss, NIH, Bethesda, USA) is also not capable of removing ADP-ribose from either ARTD10 itself or from GSK3 β as expected (Figure 24C). Since the described substrate preference for ARH1 are mono-ADP-ribosylated arginines (Takada et al., 1993), this would also fit to the model of substrate-assisted catalysis wherein acidic residues form the acceptor site. Modeling suggests that MDO2 can only remove ADP-ribose from acidic residues (Rosenthal, Feijs et al., manuscript in revision), implying that GSK3 β is indeed modified on a glutamate or aspartate, as the current model of substrate-assisted catalysis also suggests.

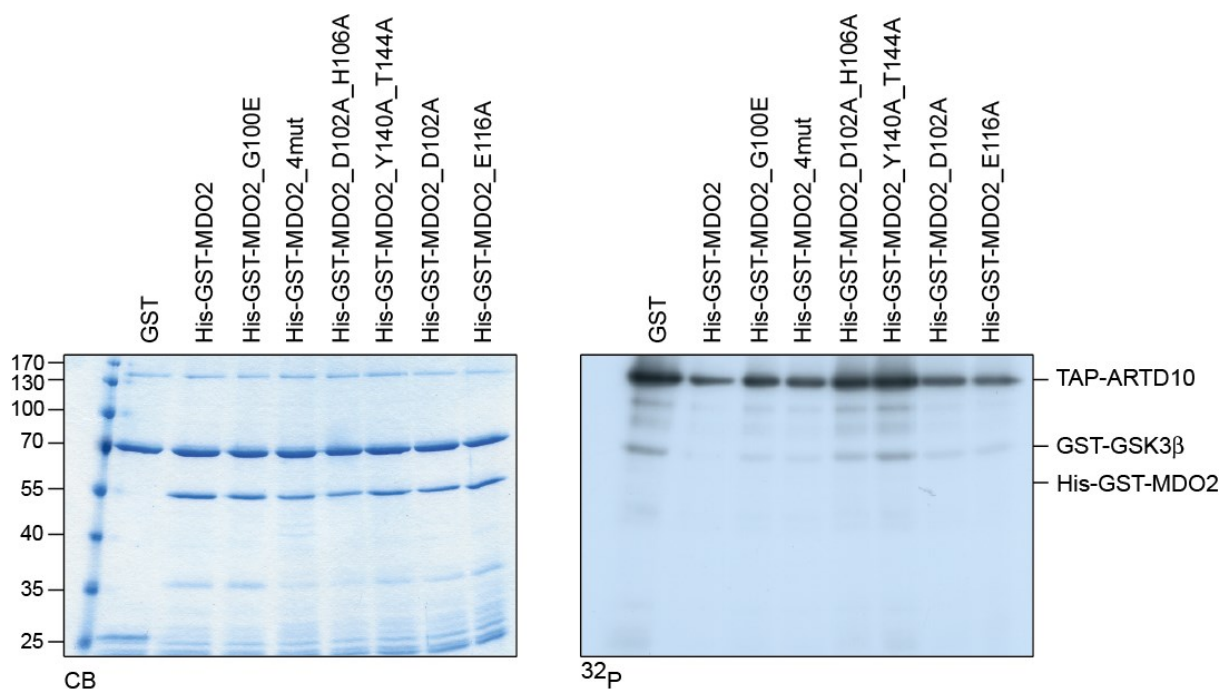


Figure 25 MDO2 mutants have different catalytic activities. GST-GSK3 β was coupled to beads and ADP-ribosylated, followed by an incubation with indicated MDO2 proteins and analysis by SDS-PAGE and autoradiography.

These models imply that at least 4 residues, D102, H106, Y140 and T144, in MDO2 are necessary for binding of the ADP-ribose and are potentially involved in hydrolysis. The activity of these mutants towards TAP-ARTD10 and GST-GSK3 β was tested and indeed, those mutants display a lower hydrolyzing activity in a preliminary experiment (Figure 25). However, extensive kinetics are needed to assess the exact influence of each mutation on activity.

To narrow down the range of possible amino acids that are modified by ARTD10 and thereby support the generated models of MDO2 de-ADP-ribosylating acidic residues and the substrate-assisted catalysis of ARTD10 using glutamates (Kleine et al., 2008), HA-ARTD10- Δ K was overexpressed in HeLa cells. ARTD10- Δ K is a mutant in which all lysines are substituted with arginines. Lysines were considered as acceptor site because lysines have been identified as ARTD1 automodification site (Altmeyer et al., 2009) and also as acceptor site in histones (Messner et al., 2010). The underlying hypothesis for the ARTD10-catalyzed modification would be that the substrates' glutamate or aspartate stabilizes the oxocarbenium transition state as described in the introduction, but that a neighboring lysine would serve as final acceptor. This has not been shown so far, but would theoretically be a possibility. HA-ARTD10- Δ K was immunoprecipitated and subsequently subjected to an ADP-ribosylation assay with radioactively labeled NAD⁺. After extensive washing of the beads with immunoprecipitated material, incubation with MDO2 followed. The automodification potential of this ARTD10 mutant is significantly lower than *wildtype* activity (Figure 26A) and it also modifies substrates to a much lower extent, as exemplified with GST-GSK3 α modification (Figure 26B). This could possibly be due to the fact that two of the mutated lysines are directly at the catalytic cleft, where even a single point mutation might render the protein less active or even inactive. Modification of ARTD- Δ K by GST-ARTD10(818-1025) takes place at a rate comparable with modification of the inactive ARTD10-G888W mutant, indicating that the overall structure of the protein is still intact (Figure 26A). It can still automodify to a certain extent and importantly, *wildtype* MDO2 can remove this modification (Figure 26C). The point mutant MDO2-G100E represents a typical Macrodomain mutant in which the catalytic site is blocked, thereby making hydrolysis impossible. This mutant is indeed not capable of removing the mono-ADP-ribose from HA-ARTD10- Δ K. These data indicate that MDO2 indeed de-ADP-ribosylates other amino acids than lysines. This makes it highly unlikely that ARTD10 modifies lysines, especially when taking into account that no dual specificities have been reported for ARTDs or hydrolases yet. Moreover, these data support the generated models of MDO2 as ADP-ribosylglutamate hydrolase.

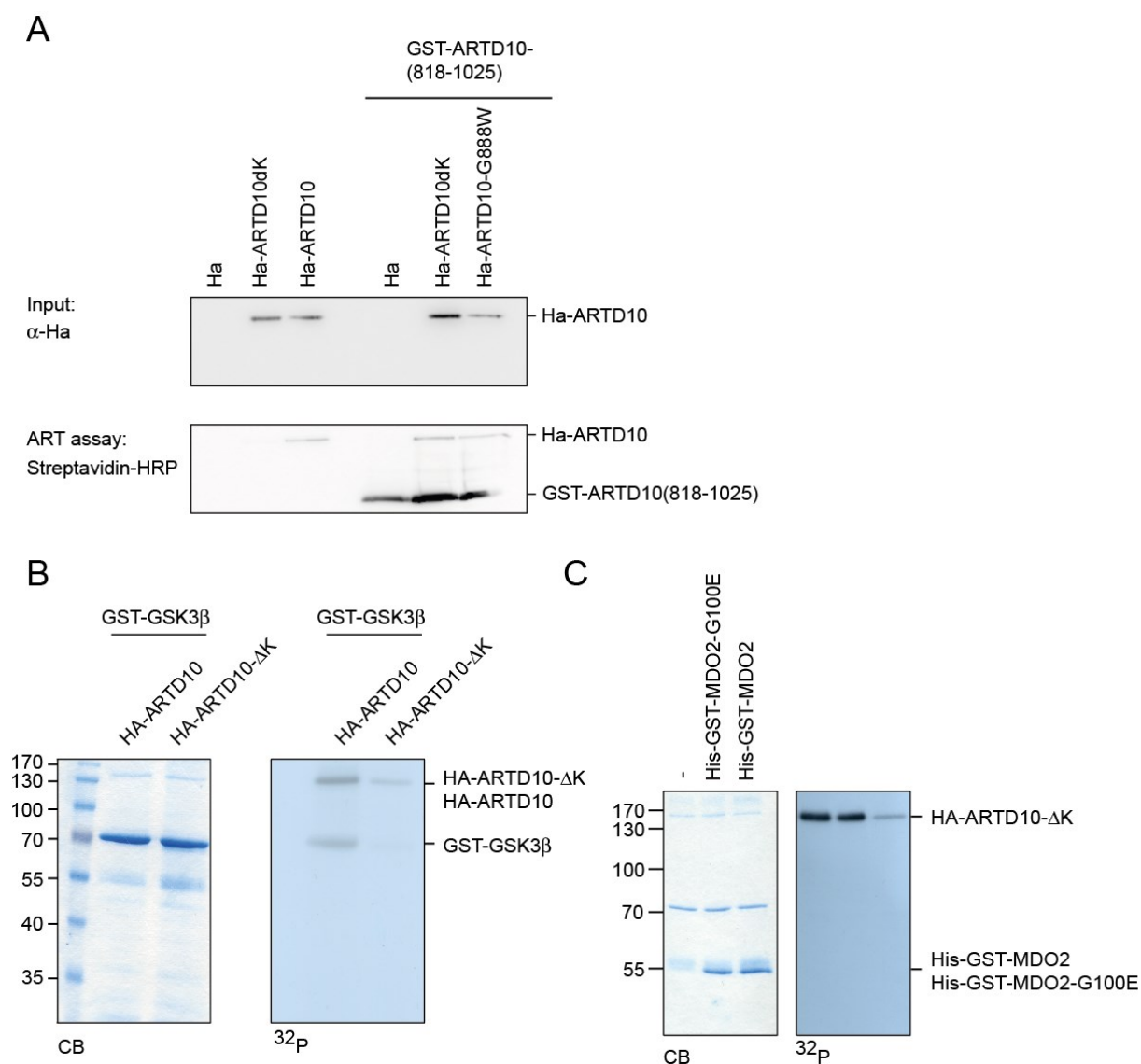


Figure 26 MDO2 de-ADP-ribosylates ARTD10- Δ K. (A) HA-ARTD10, HA-ARTD- Δ K and HA-ARTD10-G888W were overexpressed in HeLa cells and immunoprecipitated. Subsequently ADP-ribosylation assays were performed to test automodification (left) or with addition of GST-ARTD10(818-1025) to test *trans*-modification. (B) HA-ARTD10 and HA-ARTD10- Δ K were overexpressed in HeLa cells, immunoprecipitated and used to modify GSK3 β in an ADP-ribosylation assay. (C) HA-ARTD10- Δ K was overexpressed in HeLa cells and immunoprecipitated. Subsequently ADP-ribosylation assays were performed, followed by washing of the beads and incubation with His-GST-MDO2 or His-GST-MDO2-G100E.

These findings led us to test whether removal of mono-ADP-ribose by MDO2 is sufficient to restore GSK3 β kinase activity. Mono-ADP-ribosylated GSK3 β was incubated with MDO2 followed by a kinase assay. In this *in vitro* assay, de-ADP-ribosylation of GSK3 β by MDO2 sufficed to restore kinase activity to levels comparable with unmodified control GSK3 β (Figure 27). These findings imply that mono-ADP-ribosylation of GSK3 β does not induce irreversible conformational changes.

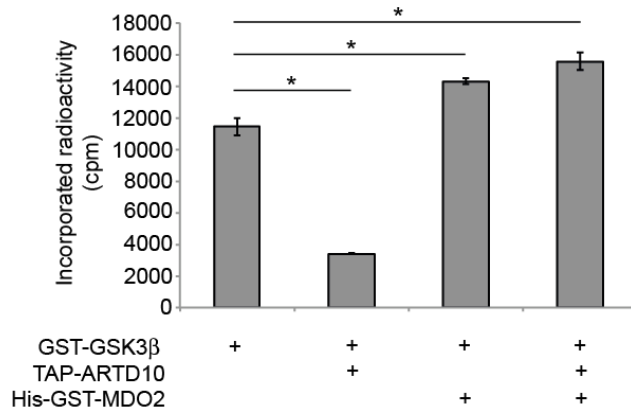


Figure 27 de-ADP-ribosylation by MDO2 suffices to restore GSK3 β activity *in vitro*. Mono-ADP-ribosylated GSK3 β was incubated with MDO2, kinase activity was subsequently assessed in kinase assays. Incorporated radioactivity was determined by scintillation counting. Data are represented as mean \pm SD of 3 measurements, a representative experiment is shown.

Next, we tested whether MDO2 also counteracts ARTD10 in cells. HA-GSK3 β was co-expressed with dsRed-ARTD10 alone or together with GFP-MDO2 and subsequently kinase assays were performed with the immunoprecipitated GSK3 β . Overexpression of MDO2 itself stimulated kinase activity (Figure 28A), compatible with the experiments shown before using either ARTD10-G888W or shRNA against ARTD10, supporting the notion that GSK3 β is mono-ADP-ribosylated in cells by endogenous ARTD10. Moreover MDO2 antagonized the activity of co-transfected ARTD10, without affecting protein expression as is shown in the input blot (Figure 28B). These effects seem rather small, possibly caused by lacking stimuli or by a suboptimal ratio of ADP-ribosyltransferase versus ADP-ribosylhydrolase and could possibly be further optimized.

Co-expression of His-tagged ARH1 in contrast had no influence on GSK3 β activity in a preliminary experiment (Figure 28C), as might be expected from the negative results in the *in vitro* assays. The overexpression levels are equal and do not lead to altered GSK3 β levels (Figure 28D). This indicates that specific catalytic hydrolase activity is necessary to restore GSK3 β to its non-ADP-ribosylated kinase activity and not merely some ADP-ribose hydrolyzing enzyme.

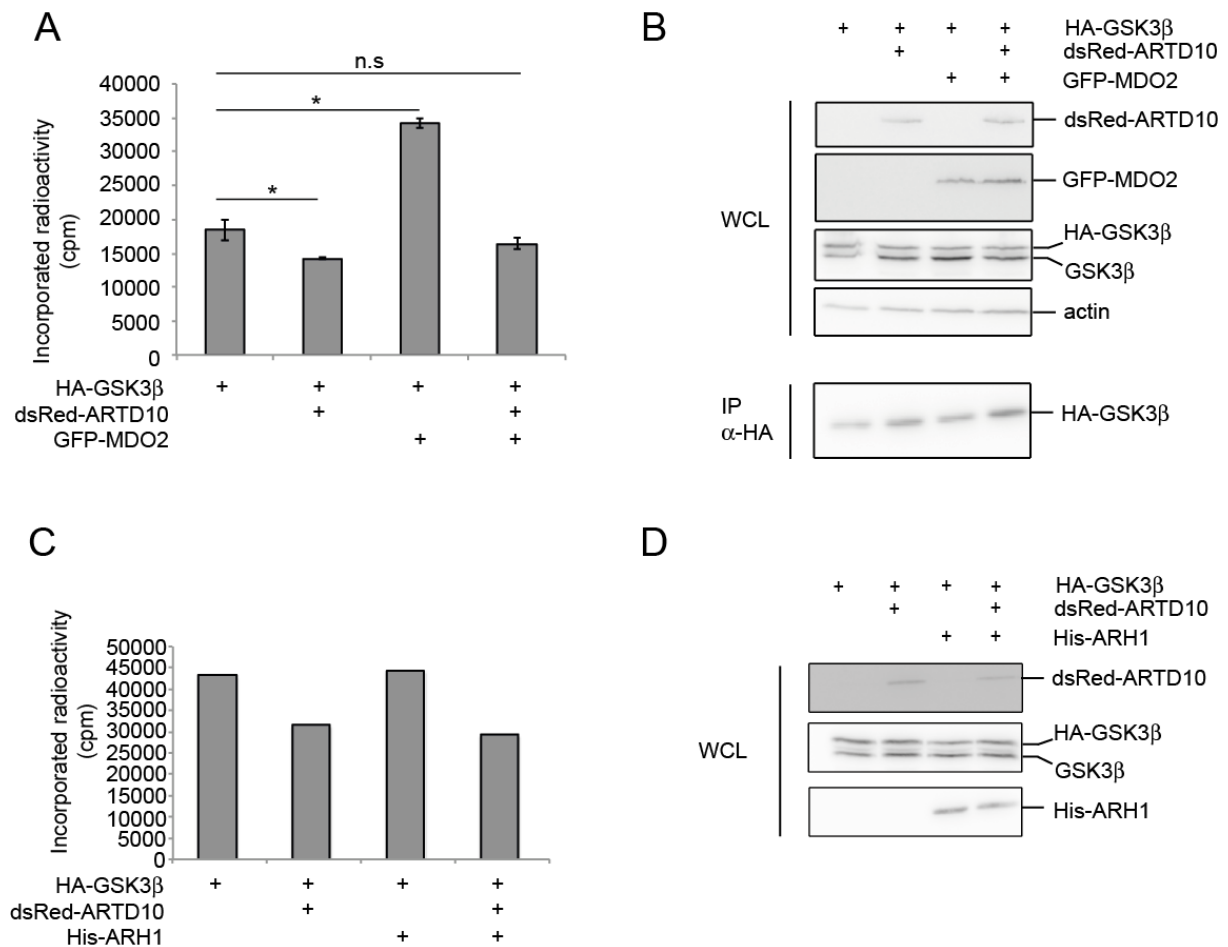


Figure 28 MDO2, but not ARH1 overexpression restores GSK3 β activity. (A) dsRed-ARTD10 and GFP-MDO2 were co-expressed with HA-GSK3 β in U2OS cells. Immunoprecipitated GSK3 β was subsequently subjected to a kinase assay and analyzed by scintillation counting. Data are represented as mean \pm SD of three measurements, a representative experiment is shown. (B). Input controls for (A). (C) dsRed-ARTD10 and His-ARH1 were co-expressed with HA-GSK3 β in U2OS cells. Immunoprecipitated GSK3 β was subsequently subjected to a kinase assay and analyzed by scintillation counting. Preliminary data from one experiment are shown. (D) Input controls for (C).

These results indicate that de-ADP-ribosylation of GSK3 β is sufficient to restore kinase activity, meaning that ADP-ribosylation can function as on/off-switch for GSK3 β . Multiple additional questions arise. When is GSK3 β ADP-ribosylated in cells, is some signal required to activate ARTD10 or to get the two proteins together under physiological conditions, without overexpressed protein? If e.g. IFN α can lead to increased ARTD10 protein expression (Figure 20F), will this then automatically lead to GSK3 β inhibition or are additional signals necessary to bring the two proteins in the correct spatial vicinity? Or do the cells have high enough steady-state levels of MDO2 to efficiently counteract ARTD10?

Since overexpression of HA-GSK3 β -S9A fails to restore colony formation potential, colony formation assays were performed to test if co-expression of MDO2 suffices to restore the normal growth behavior of cells with overexpressed ARTD10. HA-ARTD10 leads to decreased colony formation as

expected from previous results, whereas HA-MDO2 does not influence cell proliferation in this type of assay (Figure 29).

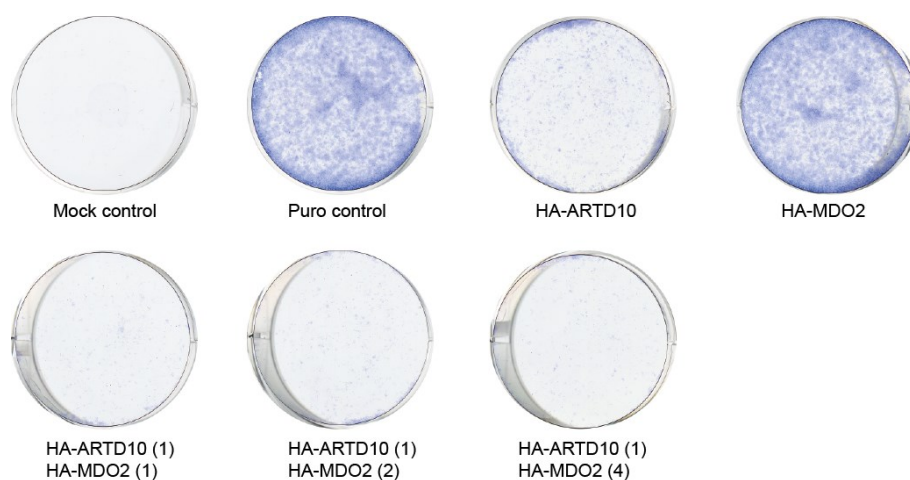


Figure 29 Colony formation assay with HA-ARTD10 and HA-MDO2. HA-ARTD10 and HA-MDO2 were transfected into HeLa cells in addition to a puromycin control vector, transfected cells were selected by puromycin treatment. Numbers in brackets indicate the relative amounts of DNA transfected. A representative experiment is shown.

HA-MDO2 was titrated in the indicated amounts in addition to unchanged HA-ARTD10 transfection. None of the transfected amounts of HA-MDO2 can reverse the inhibitory effect of ARTD10, indicating that the relevant substrates are not accessible to HA-MDO2 or that the stalled cell growth is caused independent of catalytic activity. It is however highly unlikely that this effect is independent of catalytic activity because several inactive ARTD10 mutants do not cause this proliferation arrest (Schuchlantz, 2008). Since nothing is known about the intracellular localization of MDO2 yet, it is imaginable that for example the mitosis-related kinases such as NEK6 and PLK1 are modified by ARTD10 in a distinct cellular compartment, thereby influencing mitotic progression but being inaccessible for MDO2 because it does not localize to this compartment. To be able to investigate these different possibilities in more detail, His-GST-MDO2 was used as antigen to create antibodies, which are currently being tested (in collaboration with E. Kremmer). These antibodies will aid in future studies to answer questions concerning e.g. MDO2 localization.

Taken together, these results indicate that mono-ADP-ribosylation is a PTM that can directly influence the modified proteins and that can be reversed *in vitro* as well as in cells. One of the questions that can be asked next, when considering the impact mono-ADP-ribosylation has on GSK3 β kinase activity, is how ARTD10 activity is regulated in cells.

Phosphorylation of ARTD10 by GSK3 β

No regulatory mechanisms have been identified for ARTD10 so far, it is currently unknown when the protein localizes to which cellular compartment, when it is active or when it is degraded. Taking a closer look at the identified substrates however (Table 1), it becomes apparent that the modification of so many different proteins has to be regulated tightly. In support of this notion is the severe effect that ARTD10 knockdown or overexpression has on cell proliferation (Chou et al., 2006; Feijs, 2009; Kleine et al., 2008). Upon entering of the ARTD10 sequence into the ELM Database (Dinkel et al., 2012), multiple interesting eukaryotic linear motifs (ELM) can be identified (Figure 30). The ELM Database currently contains 1800 linear motifs and additionally provides the user with structural information on the entered sequence. Additionally, it can be assessed whether motifs identified are conserved throughout the species. A higher conserved motif has a higher likelihood of being relevant. These motifs can provide first hints at the diverse proteins binding to or modifying ARTD10.

There are diverse motifs for kinases that can be identified in ARTD10 such as protein kinase A (PKA) and PLK1 motifs. This hints for instance at a reciprocal interaction between ARTD10 and PLK1, because PLK1 was identified in the ProtoArrays as ARTD10 substrate. Of particular interest are also the SCF^{FBW7}, TRAF2 and TRAF6 motifs depicted, since ARTD10 is ubiquitinated in cells by an unknown E3 ligase and with thus far unknown consequence (Figure 22B) and is involved in NF- κ B signaling (Verheugd et al., manuscript in revision). Considering the fact that TAP-ARTD10 becomes much less active upon dephosphorylation (Schuchlantz, 2008), the phosphatase motifs present in the catalytic domain could also prove to be important for regulation of ARTD10 activity. The areas marked in red are globular domains and thus less likely to be modified than the unstructured regions marked in green because many PTMs occur in unstructured regions, although for example acetylation does not occur more often in unstructured protein regions than in structured regions (Gao and Xu, 2012). Moreover, SMART/Pfam domain analysis is integrated in this analysis. Interestingly, the ART domain is not recognized although 3 potential ubiquitin interaction motifs are found.

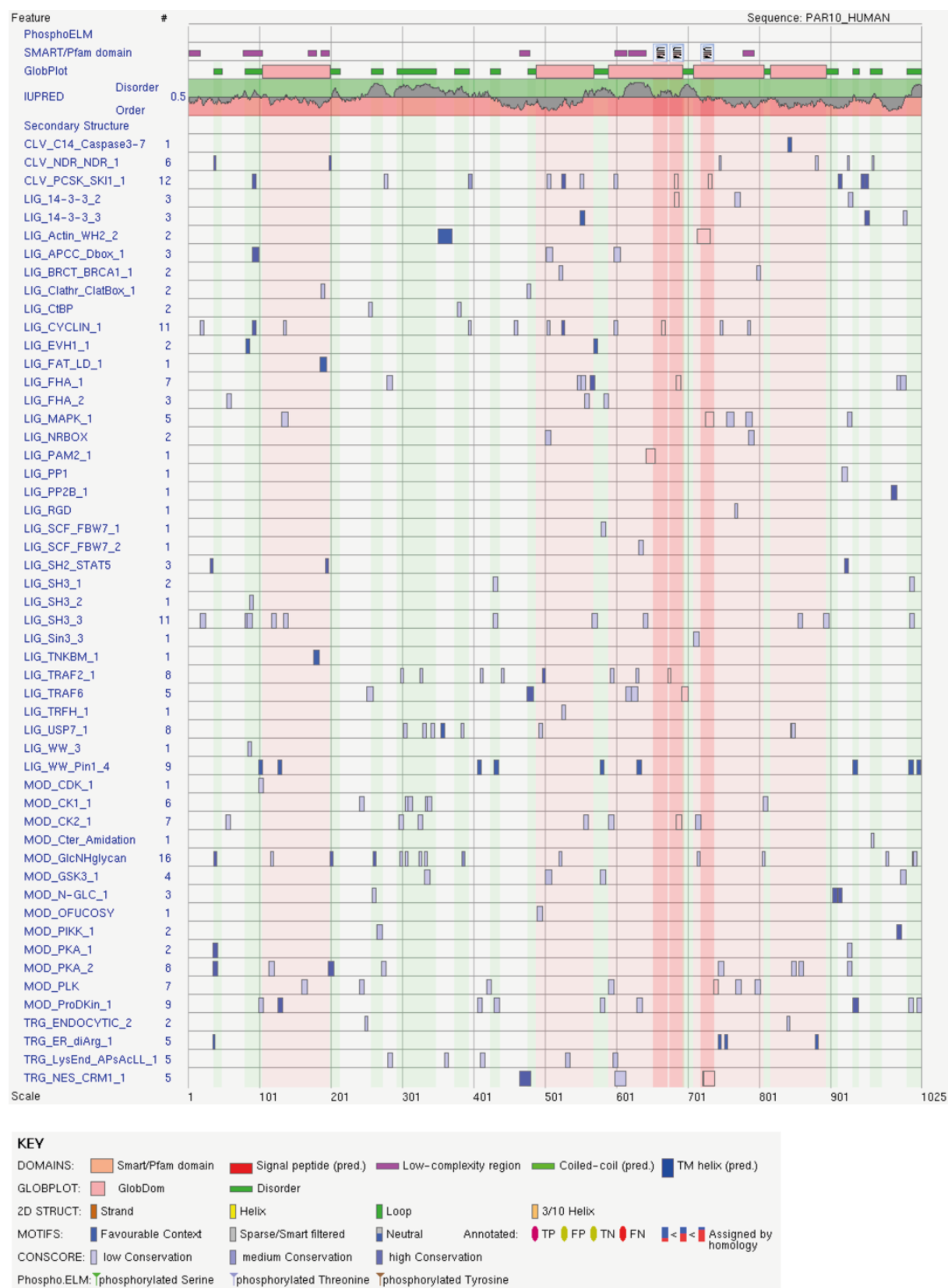


Figure 30 Overview of diverse linear motifs present in ARTD10. Sequence analysis was performed with the online ELM Database, which predicted the depicted eukaryotic linear motifs in ARTD10. A detailed description of the diverse motifs and their implications can be found at <http://elm.eu.org>

There are also putative GSK3 β modification sites present in ARTD10, however one must keep in mind that the consensus motif for GSK3 β is a very general one, S/T x x x pS/pT, and identified ELMs in a sequence might thus only be artificial. Over the years, the ELM Database has been improved to remove possibly artificial motifs (Dinkel et al., 2012; Gould et al., 2010) but nevertheless there are several GSK3 β motifs present. GSK3 β also phosphorylates other ARTD family members, such as ARTD5 (Yeh et al., 2006).

To examine whether GSK3 β is indeed capable of modification of ARTD10, a kinase assay was performed with GST-GSK3 β , BSA as negative control or baculo-derived p65 (a kind gift from M.O. Hottiger, ETH Zurich, Switzerland) as positive control to optimize reaction conditions (data not shown). Autoradiography shows that GSK3 β can modify TAP-ARTD10 under these circumstances (Figure 31A), implying that priming phosphorylations are either already present on the protein or that a non-primed phosphorylation site is being modified. To narrow down the area of modification, different overlapping GST-tagged fragments of ARTD10 (Figure 31B) were used in a kinase assay, where it becomes apparent that only fragment 3 can be modified in this *in vitro* assay (Figure 31C), indicating that the modification site lies between amino acids 459 and 600. Since these proteins were purified from *E.coli*, it can be assumed that no priming phosphorylation is present and this site thus represents a non-primed site. Mass spectrometry analysis of the phosphorylated fragment indicates threonine 553 as modification site, labeled in red in the surrounding sequence (Figure 31D). Marked in blue is a 14-3-3 binding motif identified using the ELM database, implying that phosphorylation by GSK3 β might regulate 14-3-3 binding. Of course, this is very hypothetical as yet. It would have to be verified first that GSK3 β can modify ARTD10 in cells and moreover no interaction of ARTD10 with 14-3-3 proteins has been described yet. Additionally, intracellular GSK3 β possibly modifies ARTD10 at the sites indicated in Figure 30, for which the priming phosphorylations lack in the *E.coli* purified protein.

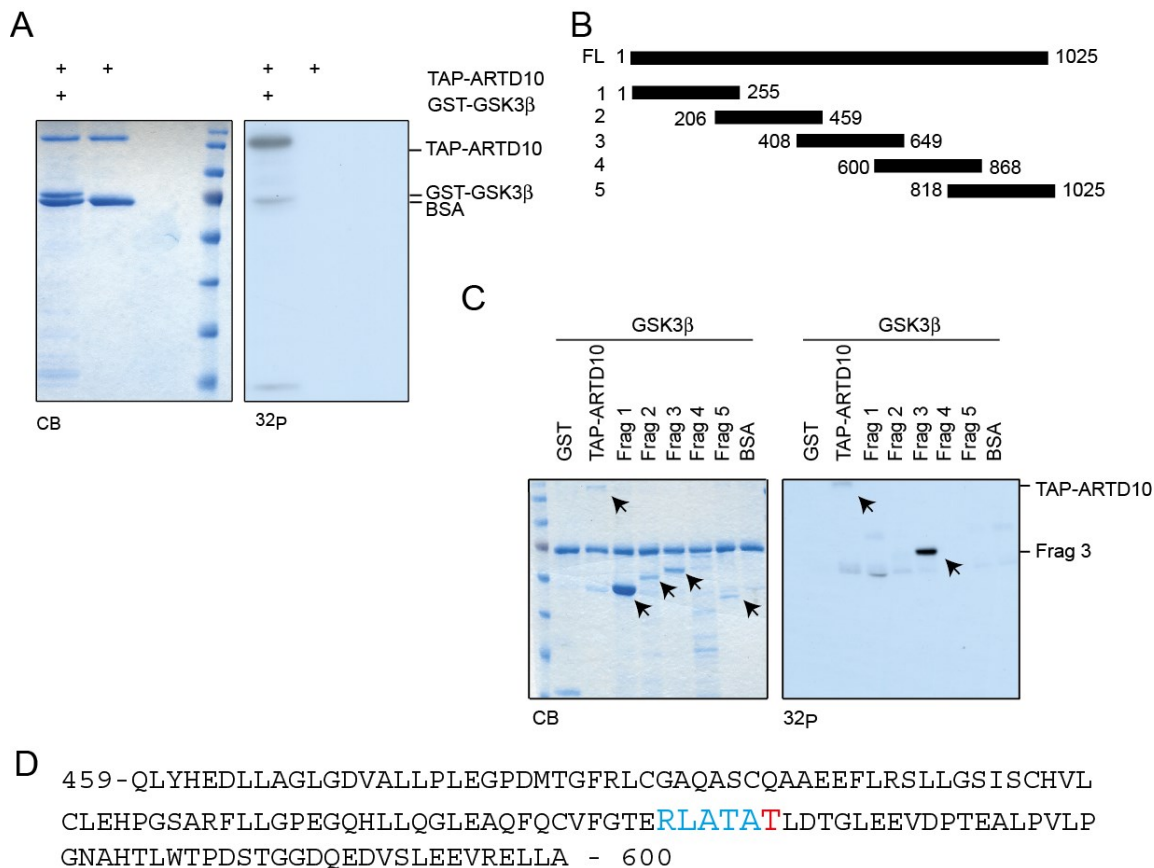


Figure 31 GSK3β phosphorylates ARTD10 at T553. (A) A kinase assay was performed with GST-GSK3β and TAP-ARTD10 or BSA. (B) Schematic representation of the different ARTD10 fragments generated to map the modification site in (C) A kinase assay was performed with GSK3β on TAP-ARTD10 and GST-fragments. (D) Mass spec analysis of phosphorylated fragment three revealed the presence of one phosphorylated peptide, the putatively modified threonine is marked in red. Depicted in blue is a putative 14-3-3 interaction motif.

To test whether this phosphorylation influences ARTD10 activity, ARTD10 was phosphorylated with non-labeled ATP and subsequently tested in an ADP-ribosylation assay. Automodification is not altered by phosphorylation of threonine 553 by GSK3β in a preliminary experiment (data not shown), leaving the functional consequence of this phosphorylation open at the moment. GST-pull down experiments indicate that ATP and NAD⁺ are not absolutely necessary for the interaction of the two proteins (Figure 18B). Binding of GSK3β to ARTD10 seems to be relevant for catalytic activity in an as yet unexplained manner, causing us to further investigate the interaction between the two proteins.

Previous experiments have already revealed the presence of multiple phosphorylation sites in ARTD10 (Schmitz, 2010), serine 324 was found to be phosphorylated in the G₁-phase of the cell cycle by high-throughput mass spec analysis (Gnad et al., 2011; Olsen et al., 2010), ubiquitination of ARTD10 is taking place (Figure 22B) and acetylation of ARTD10 has been detected at lysine 916 also in proteome-wide high-throughput screening approaches (Choudhary et al., 2009). Future experiments will have to reveal not only the responsible enzymes but also when these modifications occur and what the functional relevance thereof is.

Bioinformatical models of ARTD10 with NAD⁺ and GSK3 β

To further define the interaction between ARTD10 and GSK3 β , bioinformatical models were created (in collaboration with V. Lossaso and Prof. P. Carloni, GRS, Jülich, Germany). Since the only available crystal structure of the catalytic domain of ARTD10 contains the NAD⁺ analogue 3-AB but not NAD⁺ itself, models had to be made to assess how NAD⁺ docks into the catalytic center of ARTD10. First, it was determined which residues of ARTD10 interact with 3-AB in the crystal structure, as summarized in Table 2. In the first column it is listed which atom from which amino acid in ARTD10 interacts with which atom in 3-AB. This information is not only useful when planning docking studies, but should also be considered when for example mutating amino acids from this list as they will most likely result in an inactive enzyme. Phosphorylations occur on tyrosines 919 and 932 as measured by mass spectrometry (Schmitz, 2010) and are thus highly likely to regulate catalytic activity by interfering with the NAD⁺ interaction.

Table 2 Interactions between ARTD10 and 3-AB (V.Losasso)

	ARTD10 (Residue, atom)	3-AB (atom)
Hydrogen bonds	Ser927, OG	O7N
	Gly888, N	O7N
	Gly888, O	N7N
Hydrophobic interactions	Leu926, CD2	C5N
	Tyr932, CZ	N1N
	Tyr932, CE2	N1N, C2N
	Tyr932, CD2	C2N
	Tyr919, CB	C2N, N1N, C6N
	Tyr919, CD1	N1N, C6N

NAD⁺ actually exists in several hundreds of possible conformations, but a recent publication has revealed that most NAD⁺-consuming enzymes use NAD in the so-called “scorpion motif” (Lee et al., 2010). In this publication, 8 different enzymes utilizing NAD⁺ with solved crystal structures are analyzed. When superimposing the NAD⁺-conformation in these enzymes, it becomes apparent that they are indeed very similar (Figure 32A). All 8 of these were docked into ARTD10, with the best result obtained when using the NAD⁺-conformation from the ARTC2.2-NAD⁺ crystal, PDB-accession number 1OG3 (Figure 32B). When looking at a mesh figure of ARTD10 with NAD⁺, which displays what the model would look like when water would run over, it becomes apparent that with this docking the NAD⁺ indeed disappears in the catalytic cleft, but the C1-atom of NAD⁺ is facing outward, ready to be attached onto a substrate (Figure 32C).

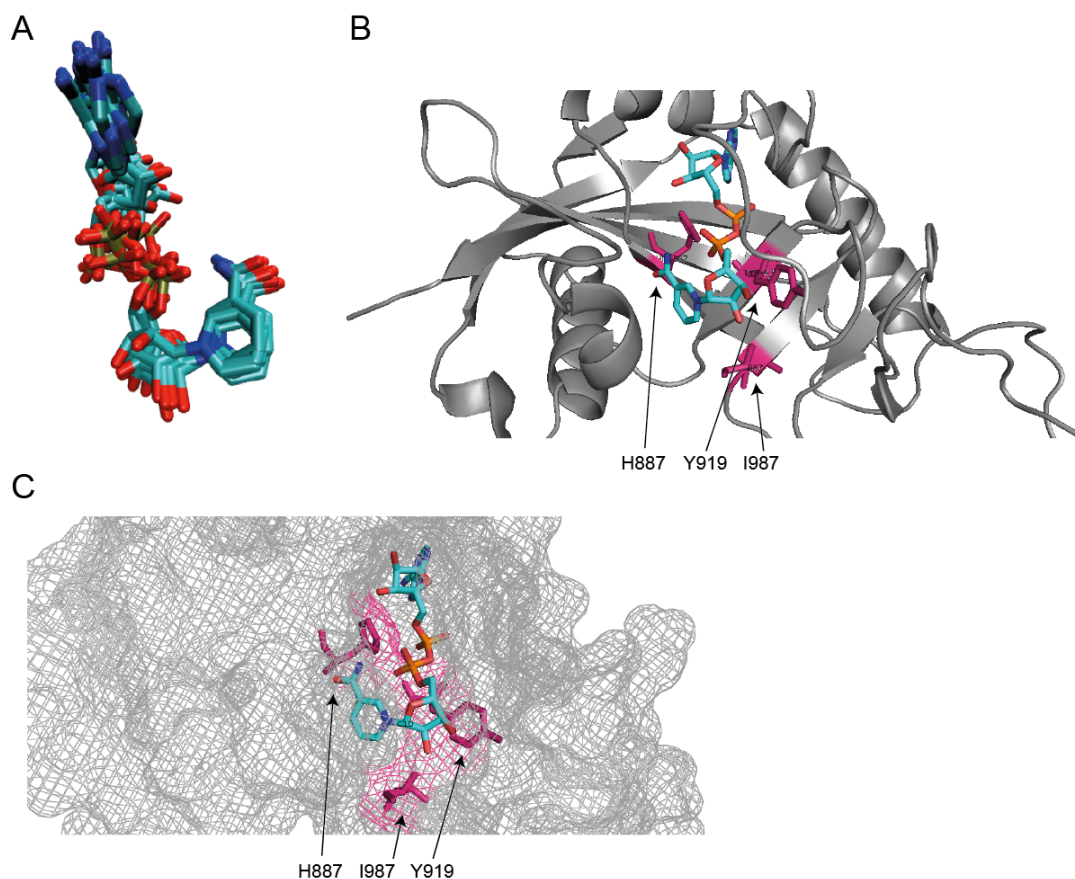


Figure 32 Docking of NAD in scorpion formation into the catalytic cleft of ARTD10. (A) Overlay of the conformation of NAD⁺ in different NAD⁺-consuming enzymes (V. Losasso). (B) Docking of NAD⁺ into the catalytic site of ARTD10 (V. Losasso). (C) Mesh figure of (B), showing how NAD⁺ disappears into the catalytic cleft of ARTD10.

Next, models were made of ARTD10-NAD⁺ and GSK3β to further investigate the interaction between ARTD10 and GSK3β. For these models to be as accurate as possible, it is essential to gather as much experimental information as possible on the modeled proteins, so certain preliminary experiments were performed beforehand the modeling procedure was started. It was tested how temperature influences the catalytic reaction, by first incubating ARTD10 at 30° for 15 minutes, with and without [³²P]-NAD⁺ and GST-GSK3β (Figure 33A). Temperature itself does not disturb the reaction, as GST-GSK3β can still be modified after incubation of ARTD10 at 30°C without [³²P]-NAD⁺. When ARTD10 is incubated with [³²P]-NAD⁺ for 15 minutes at 30° C, subsequently added GST-GSK3β cannot be modified anymore, indicating that the automodification is inhibitory. Furthermore, the influence of MgCl₂/CaCl₂ present in the reaction buffer was tested (Figure 33B), as these may have considerable influence on the outcome of docking studies. However, these also do not influence ARTD10s activity. Lastly, it was tested whether the presence of GSK3β might also influence the modification of other proteins, such as Ran-GTP which was identified as ARTD10 substrate before (Schuchlantz, 2008). This was not the case however, both proteins are modified equally well when present alone or simultaneously in the ADP-ribosylation reaction (Figure 33C), the used Ran-GppNHp is a non-cleavable GTP analog.

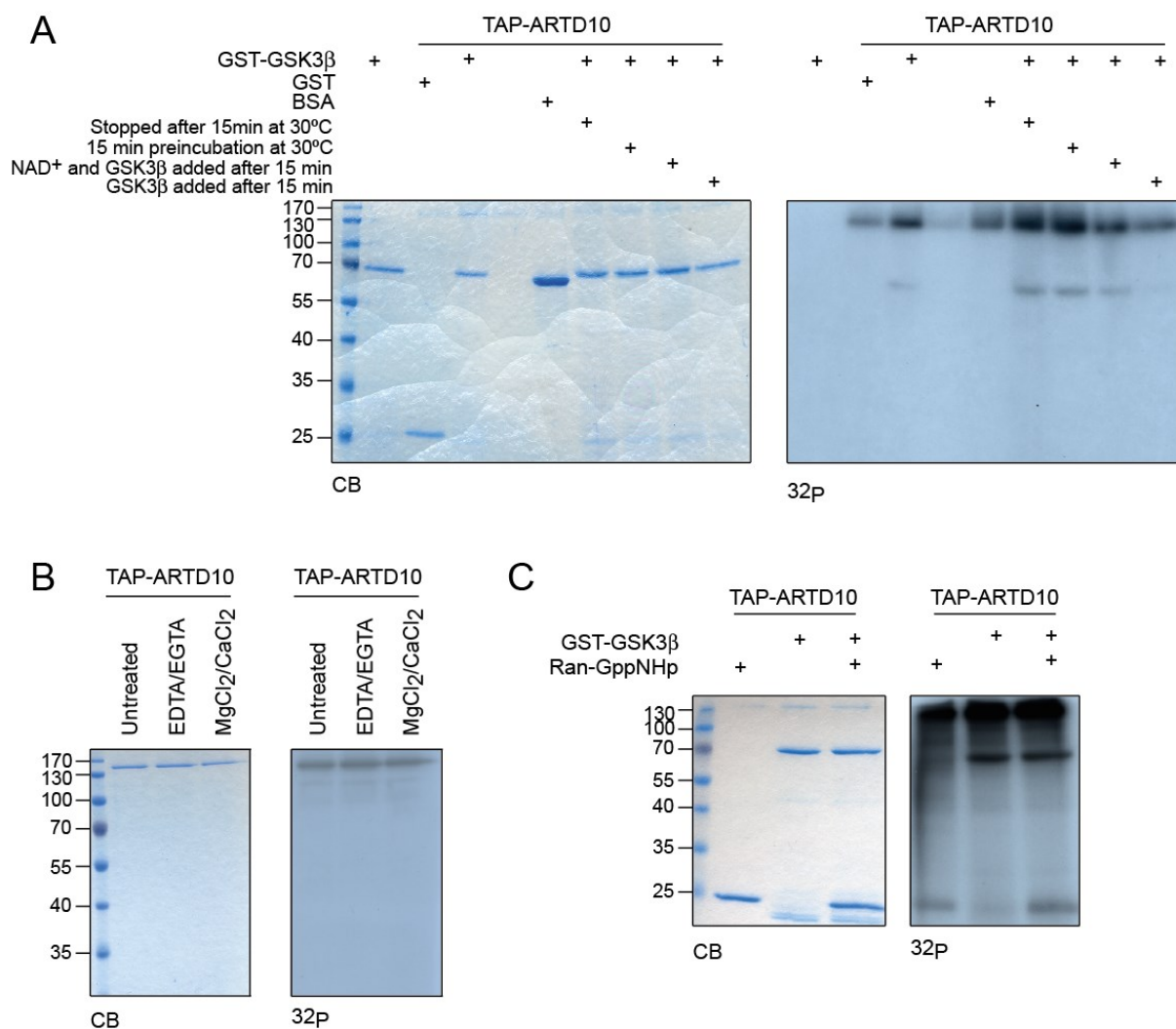


Figure 33 Assessment of the influence of different factors on ART activity. (A) TAP-ARTD10 was incubated with GST-GSK3β for 30 minutes at 30°C unless indicated otherwise. (B) TAP-ARTD10 was incubated in ADP-ribosylation buffer for 30 minutes at 30°C with addition of indicated components to the reaction buffer. (C) TAP-ARTD10 was incubated in an ADP-ribosylation assay with GST-GSK3β or Ran-GppNHp alone or together. Results from one preliminary experiment are shown.

Since addition of EDTA/EGTA or MgCl₂/CaCl₂ did not seem to have an influence on catalytic activity (Figure 33B), no ions were added as parameter in the docking studies. Several criteria were used to limit the search to the bare necessities, to avoid using more computer time than necessary. Because GSK3α was also identified as substrate on the ProtoArrays, only sites that are present in both GSK3α and GSK3β need to be considered. Initial docking studies were performed with only glutamates or aspartates of GSK3β as interacting residues according to the model of substrate-assisted catalysis, later on arginines and lysines were also considered because some of the ARTDs were described to modify lysines, as summarized in the introduction. Pairs of acidic and basic residues were also considered, to test the theory that the acidic residue might indeed serve to stabilize the reaction, in which however the neighboring basic residue would be the final acceptor, as described above. A summary of some of the candidate-modification sites for the analysis of single amino acids is given in Table 3.

Table 3 Summary of the docking study results (V. Losasso).

Residue	Solvent accessibility	HADDOCK scoring function	Interacting surface (Å ²)
GLU53	0.91	-84.3	540.6
ARG96	65.0	-105.25	567.4
GLU121	0.91	-80.4	513.4
ARG180	0.10	-101.3	938.8
LYS197	0.21	-86.9	1543.1
LYS205	0.10	-94.9	595.4
GLU211	0.60	-111.3	521.7
ASP264	0.56	-105.0	506.8
GLU279	0.71	-88.0	775.6
GLU290	1.00	-107.7	556.1

The solvent accessibility indicates how accessible the residue is, where a higher score means a higher solvent accessibility and thus higher likelihood of modification. The HADDOCK scoring function implements forces like van der Waals and electrostatic forces and should be low for good candidates. The interacting surface shows how big the area of the proteins is that is involved in the interaction, where a larger interacting area increases the probability of a real hit. It cannot easily be deduced from this information which site might be modified, because these scores cannot be combined into one score to create a list of potential modification sites ranging from the best possibilities to the weaker ones.

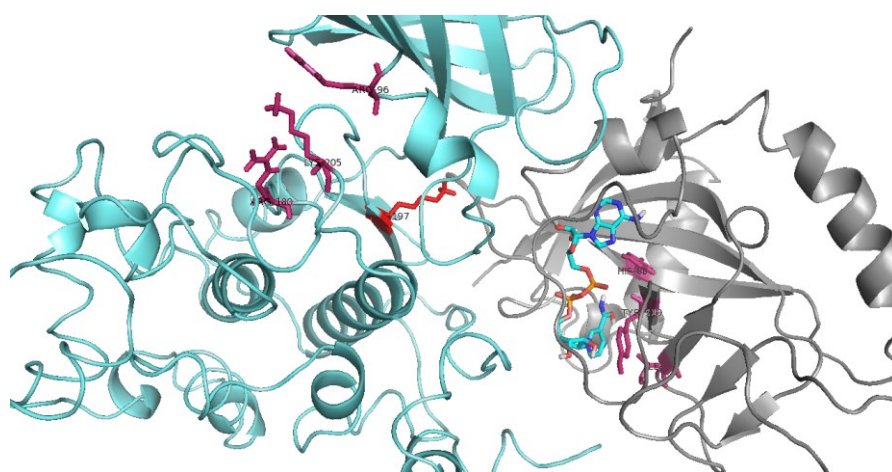


Figure 34 Model of the interaction between GSK3 β residue K197 and ARTD10. GSK3 β is displayed in light blue, the catalytic domain of ARTD10 in grey. Catalytic residues of both enzymes are shown in pink. K197, the putative modification site analyzed in this model is shown in red (V. Losasso).

In Figure 34 the interaction between GSK3 β 's residue K197 and ARTD10 is shown. GSK3 β is colored light blue, the catalytic domain of ARTD10 in grey. The residues most important for catalytic activity for both enzymes are shown as pink sticks. Labeled in red is K197 of GSK3 β . Although this residue had a quite high score, mainly because of the large interacting surface, it becomes apparent that this particular residue is actually pretty far away from the NAD⁺ moiety in the current model and thus unlikely to be modified.

Several of the residues listed in Table 3 were mutated and subsequently tested in independent ADP-ribosylation assays (Figure 35), but the relevant residue has not been identified yet, since all mutants tested could still be modified by ARTD10. The method employed here to study these mutants unfortunately displays limited sensitivity, as for instance in Figure 35A HA-GSK3 β -E53A_E121A seems to be no substrate anymore, whereas the triple mutant, HA-GSK3 β -E53A_E121A_E279A is substrate, indicating that both E53 and E121 are not the relevant site.

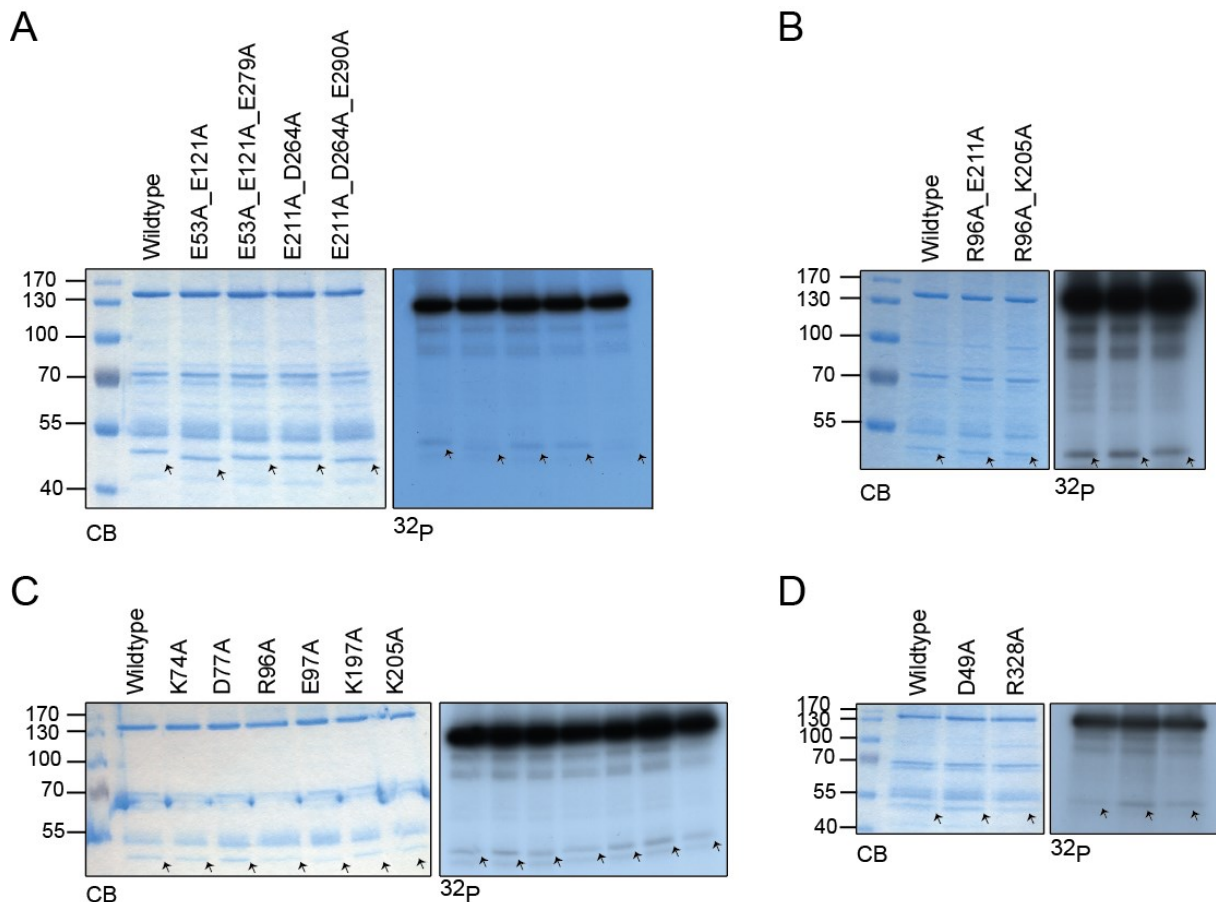


Figure 35 GSK3 mutants tested in ADP-ribosylation assays. Indicated GSK3 β mutants were overexpressed in HeLa cells, immunoprecipitated and tested in ADP-ribosylation assays with TAP-ARTD10.

To identify mono-ADP-ribosylation sites in GSK3 β , it might be better to analyze the ADP-ribosylation actually present on GSK3 β after an ADP-ribosylation assay than to mutate every putative modification site, as this might lead to false positive or false negative results. False positives might be caused by conformational changes due to the mutagenesis, thereby making a modification site inaccessible. Alternatively, the binding surface might be destroyed instead of the modification site, also leading to false positive results. False negatives could occur if the modification site indeed is mutated, but where a secondary modification site might arise due to the mutagenesis. To circumvent this problem, kinase assays were performed on GSK3 β that was immunoprecipitated from U2OS cells co-expressing ARTD10 or ARTD10-G888W. It is expected that the mutant in which the modification

site is mutated, will not be repressed by ARTD10 since it cannot be modified. Kinase activity should then be comparable for the mutant co-transfected with active or inactive ARTD10.

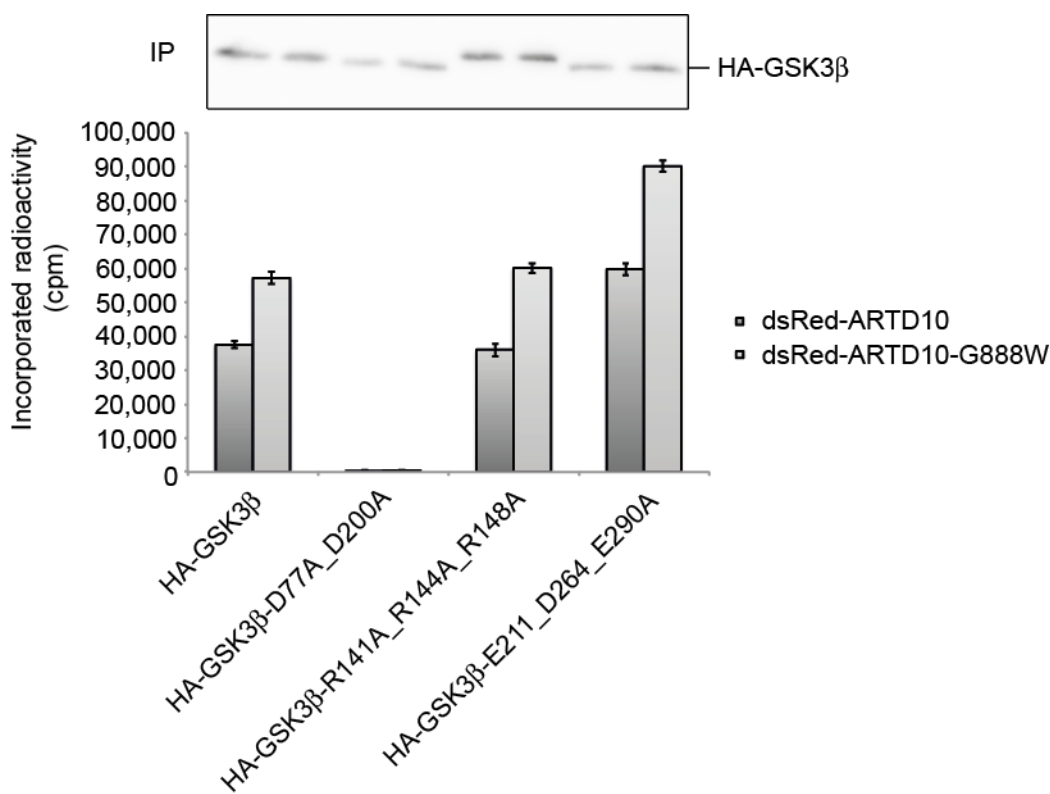


Figure 36 Activity of HA-GSK3 β mutants co-transfected with dsRed-ARTD10 or dsRed-ARTD10-G888W. U2OS cells were transfected with indicated GSK3 β plasmids and either active or inactive ARTD10. 24 hours after transfection, cells were lysed and GSK3 β immunoprecipitated. Immunoprecipitated material was used in kinase assays to determine activity, with an exemplary IP control blot shown. Data are represented as mean \pm SD of triplicate measurements of a representative experiment.

HA-GSK3 β *wildtype* was used as control and indeed, co-expression of dsRed-ARTD10-G888W leads to a higher kinase activity than co-expression of dsRed-ARTD10. The basal expression levels of the different mutants slightly differ, however co-expression of ARTD10 does not influence expression of these mutants, making it possible to compare co-expression of ARTD10 *wildtype* with ARTD10-G888W, but not between mutants (Figure 36). GSK3 β -D77A_D200A lacks activity, which might be expected since D200 is part of the DFG-motif, which is crucial for kinase activity (Kornev et al., 2006). Should one of these aspartic acid residues be the relevant amino acid for mono-ADP-ribosylation, then this will be missed in this type of assay. Both triple mutants tested here, HA-GSK3 β -R141A_R144A_R148 and HA-GSK3 β -E211A_D264A_E290A are active. Both have increased kinase activity when co-transfected with dsRed-ARTD10-G888W, comparable to the induction of *wildtype* GSK3 β , indicating that these 6 sites are not the mono-ADP-ribosylation sites and are not crucial for kinase activity. The triple mutant HA-GSK3 β _E53A_E121A_E279A behaves similar (data not shown), indicating that these three amino acids are also not the modification sites.

In future research, these bioinformatical models could be further refined and ideally describe the interaction of relevant residues within GSK3β with the NAD⁺ in the catalytic cleft, as this might be more important for catalysis than closeness to the residues of the catalytic triad. Alternatively, the distance between the relevant residue and the C1-atom of NAD⁺ that becomes attached to the substrates could be calculated, to implement the distance between those in the evaluation. This might lead to better fitting models that give better chances of identifying the relevant sites. Additionally, PTMs often occur on flexible protein regions (Gao and Xu, 2012). The flexible N-terminal extension is missing in the rigid crystal structure used for these docking studies and for example the DFG-motif is in a fixed state that is not reflective of its state in a watery environment, where multiple conformations are possible. It is possible that certain amino acids are weak candidates according to these models, but in truth are more flexible than the structure reveals and thus suited as modification site despite low score. Putative modification sites present in flexible regions might therefore be missed in these studies. Since these models could not provide a definite answer yet to the question which sites in GSK3β ARTD10 is modifying, we developed alternative methods based on mass spectrometry and peptide arrays to further analyze the different possibilities.

Mapping modification sites using mass spectrometry and peptide arrays

As mentioned in the introduction, mapping of ADP-ribosylation sites using conventional mass spectrometry methods is not trivial. Since the major problem is the instability of the linkage between ribose and substrate, regardless of the amino acid modified, methods were developed to circumvent this particular problem. Two similar approaches were employed simultaneously and optimized using the automodified catalytic domain of ARTD10. After ADP-ribosylation assays with or without β -NAD⁺ as control, in-solution trypsin digests were performed. Subsequently the samples were desalted and loaded onto different columns. To assess whether the conditions for trypsin digestion and subsequent desalting were optimal, tests were performed with digested and subsequently desalted material. As expected, no clear peaks corresponding to mono-ADP-ribosylated peptides could be detected (data not shown). Next, peptides mono-ADP-ribosylated with biotin-ADP-ribose were incubated with streptavidin-dynabeads, samples mono-ADP-ribosylated with regular β -NAD⁺ were incubated with ProSep BP essentially as described in (Rosenthal et al., 2011). After subsequent washing steps, bound peptides were eluted and when necessary desalted again, before drying and subsequent analysis by mass spec. Different washing conditions were tested especially for the streptavidin-dynabeads since high background binding was present without stringent washing of the beads (data not shown). Due to the highly stable interaction between streptavidin and biotin, harsh washing conditions, such as RIPA lysis buffer, could be chosen for further experiments to reduce background signals without disturbing the specific interaction. The advantage of this method is that only the mono-ADP-ribosylated peptides should be present in the final mass spectrometric spectrum, so it should not matter if the ADP-ribose is cleaved during the ionization procedure. Input samples were measured from all samples analyzed, containing 10% of the total amount of material. To generate enough material for mass spec analysis, 5 ADP-ribosylation assays were performed in parallel for each sample and added to one column of beads after digestion. Unfortunately, contradicting the earlier report introducing this method for ADP-ribosylation performed by ARTD1, we were not able to consistently measure a peptide specifically binding to the columns that could correspond to a modified peptide.

The next step could be the treatment of trypsin digested mono-ADP-ribosylated samples with MDO2 to remove the ADP-ribose completely before mass spec analysis. That should take care of the ADP-ribose and render identifiable peaks in the spectra. Alternatively, digested mono-ADP-ribosylated samples treated with PDE should render peptides with an identifiable modification, the phospho-ribose. By comparing non-modified peptides with PDE-treated peptides and mono-ADP-ribosylated peptides, it should be possible to define which peptides are modified by ARTD10 and how mono-ADP-ribose is cleaved off exactly during MALDI analysis. Of course, the other possibility would be to try to tackle this problem with other mass spec methods such as ETD.

One-dimensional chromatography ADP-ribosylation maps

An alternative method that might allow for better recovery of mono-ADP-ribosylated peptides and to reduce background is chromatography. This method has been used to map phosphorylation of peptides (Luscher and Eisenman, 1992; van der Geer and Hunter, 1994), before mass spectrometry became a common method. First, ARTD10 was mono-ADP-ribosylated with radioactively labeled NAD^+ and loaded on SDS-PAGE. To assess the incorporated radioactivity, the gel was exposed to X-ray film at RT (Figure 37A).

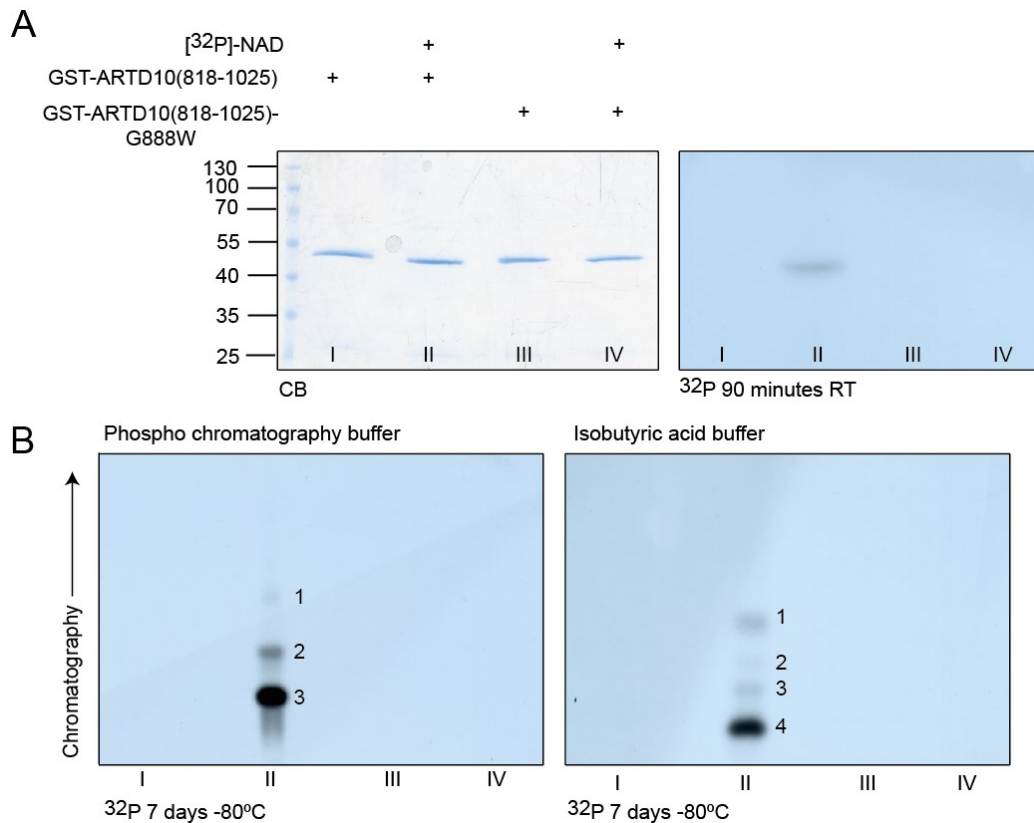


Figure 37 1D chromatography of mono-ADP-ribosylated GST-ARTD10(818-1025). (A) GST-ARTD10(818-1025) or GST-ARTD10(818-1025)-G888W were used in ADP-ribosylation assays with [^{32}P]-NAD and analyzed by coomassie. The wet gel was exposed to film at RT for 90 minutes. (B) The coomassie bands from (A) were extracted from the gel and digested with trypsin. Digested peptides were loaded on cellulose plates and separated by chromatography in 1 direction. Two different chromatography buffers were tested.

The corresponding coomassie band was cut out to enable in-gel digestion of the relevant proteins. Digested peptides were then spotted on cellulose chromatography plates in pH 1.9 buffer as described before (van der Geer and Hunter, 1994). After a chromatography run of approximately 12 hours, plates were exposed to X-ray film at -80°C (Figure 37B). It becomes apparent that there is only one major automodification peptide within GST-ARTD10(818-1025) and that there are either less-well modified second sites or that the trypsin digest was incomplete. Two different chromatography buffers were employed, phosphochromatography buffer and isobutyric acid buffer to be able to separate also

peptides running very similar in one buffer (van der Geer and Hunter, 1994). The two buffers gave similar patterns, with one major automodification site present and some minor modification sites. This method can now be repeated for other substrates in order to analyze how many modification sites are present. Moreover, material can be eluted from these plates and measured with mass spec, to identify the peptides that modified. Alternatively, partial trypsin digests could be performed on protein modified with [^{32}P]-NAD $^{+}$. After SDS-PAGE separation, the radioactive bands correspond to the area wherein the modification takes place. Those can subsequently be identified by regular MALDI analysis. Narrowing down the area of interest will make mass spec analysis of mono-ADP-ribosylated samples using the methods described above less complex.

Peptide arrays to define consensus motifs

Since it is not known yet what preferences ARTD10 has in its substrates or whether there might be some consensus motif, we decided to screen peptide libraries for good substrate peptides. For this purpose peptide arrays from JPT (Berlin) were employed, wherein peptides are spotted directly on a glass surface. The method used to probe these arrays is similar to the method described above for the ProtoArrays, allowing a fluorescent readout due to the binding of streptavidin-AlexaFluor647 to biotin-ADP-ribose containing peptides. Since ARTD10 mono-ADP-ribosylates core histones, it is expected that certain peptides derived from core histones should be modified. Two different sets of arrays were probed. The first set contained histone tail peptides, in which all of the different currently known PTMs were present but only histone peptides with known posttranslational modifications were spotted, indicating that not the entire histones are present on these arrays. The PTMs on these histones are quite interesting, as it was reported before that acetylated histones carry more ADP-ribose than their non-acetylated versions (Golderer and Grobner, 1991). Indeed, ARTD10 modifies the first stretch of amino acids of H4 best when acetylated at lysine 5, 8 and/or 16, although the overall incorporated signal is relatively weak. Modification of K20 by methylation or acetylation seems to inhibit modification (Figure 38). Curiously, the first peptide of H4, with the sequence SGRGKGGKGLGKGGAKRHRK, does not contain any glutamic or aspartic acid. It is possible that because no specific modification site is available in those peptides, ARTD10 becomes unspecific and modifies other residues with very low kinetics, hence the low signals. This is a known problem for example for GSK3 β , that is also known to be promiscuous in *in vitro* assays, but which has a lot higher specificity in cells due to spatial and temporal restrictions (Sutherland, 2011).

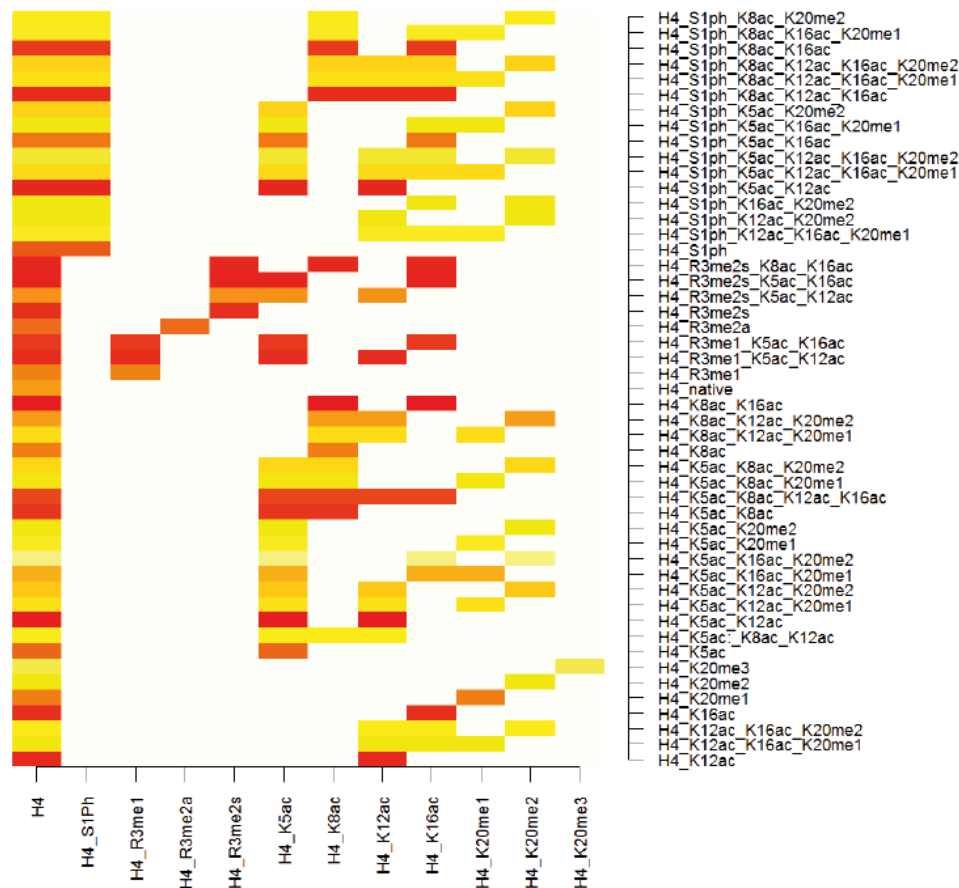


Figure 38 Overview of the mono-ADP-ribosylation of an H4-peptide carrying different other PTMs. Histone-tail arrays were incubated with TAP-ARTD10 and bio-NAD⁺. A heat-map was generated to visualize the relative modification of each peptide. Red reflects well-modified peptides, the weaker modified peptides are indicated in yellow.

The second set of arrays used thus contained peptides covering the entire histone tails, divided in overlapping peptides of 20 amino acids. Additionally, peptides are spotted with all known modifications that occur on histone tails, such as methylation and acetylation. It is expected that better hits can be identified on these arrays, since now the histones are covered completely. It should be possible to verify at least glutamate 2 of H2B (Moyle and Muir, 2010) as modification site for instance, moreover it would be interesting to identify the relevant amino acids on the other histones as well. Finally, it should be possible to narrow down the site of modification to a few amino acids, since multiple overlapping peptides should be identified for each modification site.

When incubating these arrays with 1 μ g TAP-ARTD10 and 25 μ M bio-NAD⁺, no peptide seems to be modified above background level (Figure 39A). We thus decided to use double amounts of these reagents to increase signal strength (Figure 39B). Apparently, bio-NAD⁺ can bind to these peptides non-enzymatically, perhaps through glycation, since under these conditions signals are also present in the BSA only control slide. Moreover, these amounts of TAP-ARTD10 seem to stick to the array surface quite efficiently, thereby causing substantial overall background signals.

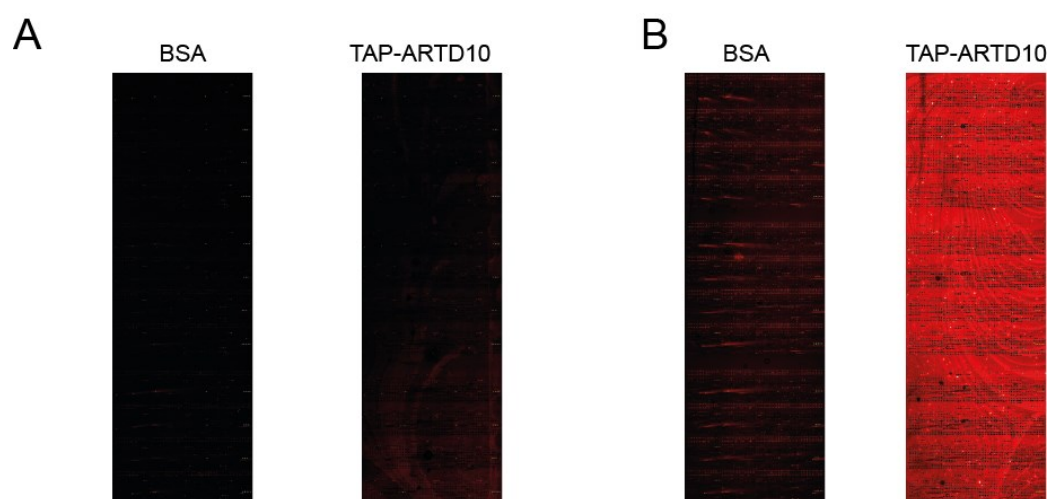


Figure 39 Scans of PepStar Histone Tail Arrays. Peptide arrays were incubated with (A) 1 μg TAP-ARTD10 or BSA as indicated and 25 μM bio-NAD⁺ or (B) 2 μg TAP-ARTD10 or BSA as indicated and 50 μM bio-NAD⁺.

By manually comparing each spot, positive hits could be identified nevertheless. Interestingly, of the peptides derived from H4, the peptide with the highest relative signal when comparing intensities of ARTD10 and control incubation, is again the first peptide containing the first 20 amino acids, even though as mentioned this peptide lacks acidic amino acids. For H3, peptides overlapping with the IRRYQKSTELLIRKLPFQRL-peptide that contained the STE-motif were best modified by ARTD10. This would be potentially more interesting and should be followed-up on, by trying to modify these peptides in *in vitro* assays in solution to verify this result.

Additionally two peptides derived from GSK3 β , 71-YQAKLCDSGELV and 194-AVLKLCDFGSAK, containing the K/RxxD/ExG motif, were used to test if these amino acids are the modification site in GSK3 β . These sites could not be tested as modification site in kinase assays with GSK3 β mutants, since these mutants per se are devoid of kinase activity (Figure 36). Unfortunately, these peptides could not be modified in *in vitro* ADP-ribosylation assays (data not shown). They also had no inhibitory effect on ADP-ribosylation assays on GST-GSK3 β , indicating that these peptides do not compete for modification and thus are not being modified (data not shown). This might imply that ARTD10 cannot modify peptides, either because it needs a certain structure for catalysis, or maybe it needs an increased binding surface. For the GSK3 β peptides analyzed, it is also likely that they do not contain the modification site and are thus negative in ADP-ribosylation assays. The peptides present on the peptide arrays should contain modification sites however, as ARTD10 was reported before to modify glutamate 2 of H2B (Moyle and Muir, 2010), supporting the notion that ARTD10 needs more than just a small stretch of amino acids to be capable of catalysis. This means that peptide arrays are not suited to study the ADP-ribosylation reaction by ARTD10 and that alternative methods have to be employed to possibly define a consensus motif for ARTD10 substrates. This challenge has not been undertaken for any of the ARTD or ARTC enzymes so far.

Conclusions

“As our circle of knowledge expands,
so does the circumference of darkness surrounding it.”

A. Einstein

ProtoArrays are a highly useful tool to identify ARTD substrates

The results of the screen for ARTD10 substrates presented here have been thoroughly validated. All full-length proteins that were tested, no matter how they were purified, could be confirmed as ARTD10 substrate, indicating that the identified hits are real substrates at least in *in vitro* assays. These kind of arrays can now be used to screen for substrates of the other ARTD or also ARTC enzymes and thus represent a novel method to approach this PTM. A valid question to be addressed next is whether all those proteins are also ARTD10 substrates in cells, to investigate whether the same is true as for GSK3 β , that some of the *in vitro* substrates are actually *in vitro* artifacts (Sutherland, 2011). The same is true for the identified ARTD8 substrates; those will have to be validated *in vitro* as well as in cells. The fact that many unique substrates were identified, indicates that these enzymes have unique roles in cellular processes and do not function completely redundant, in spite of a highly similar catalytic domain.

The percentages of kinases and secreted molecules are remarkably high. Future research will have to reveal whether mono-ADP-ribosylation takes place on a common motif of the kinases, such as the aforementioned DFG motif (Kornev et al., 2006) or on another conserved domain, thereby causing so many kinases to be substrate. Which in itself would be very interesting, as mono-ADP-ribosylation could then represent a general regulatory mechanism of kinases. Regarding the secreted factors, the obvious next step to take is the modification of a recombinant growth factor and test whether receptor binding capacities are impaired, such as reported before for PDGF-B (Saxty et al., 2001). Additionally, the question whether or not there is ARTD10 present in the extracellular matrix under certain circumstances or whether it may be involved in secretion pathways is very intriguing as well. HMGB1 was reported to be secreted highly poly-ADP-ribosylated from cells, so apparently a link already exists between ADP-ribosylation and secreted proteins, although this is not clear yet mechanistically (Davis et al., 2012).

Mono-ADP-ribosylation reversibly inhibits GSK3 β activity

This thesis is the first work that describes not only the mono-ADP-ribosylation of a kinase by an eukaryotic intracellular enzyme, but also that mono-ADP-ribosylation inhibits enzymatic activity. Such direct functional consequences have not been reported yet for any protein mono-ADP-ribosylated by ARTDs, but may actually be only the tip of the iceberg, if the other substrates identified are influenced likewise. A third novelty in this report is the description of MDO2 as de-ADP-ribosylating enzyme for GSK3 β and for ARTD10 itself. Until now, it was not clear which enzyme is responsible for the removal of the last ADP-ribose moiety. Because mono-ADP-ribosylation functions as a non-competitive inhibitor in contrast to the well-studied serine 9 phosphorylation (Dajani et al.,

2001; Frame et al., 2001), it is probable that different signals regulate GSK3 β in different manners, thereby perhaps modulating certain GSK3 β substrates without affecting others. These findings raise multiple additional questions. Does MDO2 also have some protein backbone specificity, or can it remove any ADP-ribose moiety? When are MDO2 and ARTD10 expressed, how is their activity regulated? Is overall mono-ADP-ribosylation in physiological conditions kept low in cells by MDOs, or are basal levels high? Is there a constant addition and removal of the mono-ADP-ribose, or are MDO2 and ARTD10 usually inactive in cells? All these questions have to be addressed in future studies to clear how mono-ADP-ribosylation is regulated in cells, under normal and pathological conditions. Currently, it is difficult to study regulation of ARTD10, since there are not many possible read-outs yet. Intracellular localization can be studied and *in vitro* activity can be tested, but further read-outs, such as assays to test ADP-ribosyltransferase activity in cells have to be developed still.

Reliable tools to study ADP-ribosylation sites are still lacking

The docking studies presented here are in principle useful to study the interaction between enzyme and substrate. The generated model between ARTD10 and NAD⁺ can be employed to study which residues in the catalytic cleft are important in the interaction of ARTD10 with NAD⁺. It is however difficult to obtain data with a high predictive power using this method, because the crystal structures used are confined in one conformation. The modification site might be in a flexible region that is captured in a non-favorable state in the crystal and thus be false negative in the docking studies. The attempts at site mapping that are described here, show that it is also not straightforward to directly measure mono-ADP-ribosylation, in agreement with earlier publications on this topic (Hengel and Goodlett, 2012). Mass spec methods regularly used for phosphorylation fail when applied to mono-ADP-ribosylation and even published methods that were developed to measure ADP-ribosylation could not be applied successfully. Furthermore, the obtained hints that ARTD10 cannot modify peptides further complicates matters, as peptide arrays commonly used to study other enzymes are of no use. Thus other methods have to be developed to define a putative consensus motif. Additionally, the generation of an antibody is difficult without a good substrate peptide that can be modified efficiently. To solve these difficulties, methods have to be developed to create mono-ADP-ribosylated antigen on large scale, which would ideally be modified chemically to strengthen the labile bonds such as the PDE-resistant NAD[S] (Meyer et al., 1984). Alternatively, one could develop antibodies using phage display, by first positively selecting binding-modules against mono-ADP-ribosylated proteins and subsequent negative selection against the unmodified protein.

Concluding remarks

This work shows that mono-ADP-ribosylation has the potential to become as important as better studied PTMs such as phosphorylation, especially considering the diversity of identified substrates, the impact on GSK3 β activity and the fact that it could be shown that this PTM is reversible. However, mono-ADP-ribosylation is probably not as widespread as some other PTMs, because there are not as many responsible enzymes. The current state of the field can probably be best compared with the phosphorylation field around 30 years ago, where people first came to realize that this modification could very well be important, but where sophisticated tools to study it were still lacking. This means that right now, the “old” tools used in the beginning of the phosphorylation era might be most useful to study ADP-ribosylation, such as partial trypsin digests and chromatography. However, in the long run someone has to invest in the creation of better-suited reagents to be able to fully comprehend the physiological relevance of the posttranslational modification mono-ADP-ribosylation.

References

“Lord Polonius: What do you read, my lord?

Hamlet: Words, words, words.

Lord Polonius: What is the matter, my lord?

Hamlet: Between who?

Lord Polonius: I mean, the matter that you read, my lord.”

William Shakespeare

References

- Adhikary, S., and Eilers, M. (2005). Transcriptional regulation and transformation by Myc proteins. *Nat Rev Mol Cell Biol* 6, 635-645.
- Adhikary, S., Marinoni, F., Hock, A., Hulleman, E., Popov, N., Beier, R., Bernard, S., Quarto, M., Capra, M., Goettig, S., *et al.* (2005). The ubiquitin ligase HectH9 regulates transcriptional activation by Myc and is essential for tumor cell proliferation. *Cell* 123, 409-421.
- Aguiar, R.C., Takeyama, K., He, C., Kreinbrink, K., and Shipp, M.A. (2005). B-aggressive lymphoma family proteins have unique domains that modulate transcription and exhibit poly(ADP-ribose) polymerase activity. *The Journal of biological chemistry* 280, 33756-33765.
- Aguiar, R.C., Yakushijin, Y., Kharbanda, S., Salgia, R., Fletcher, J.A., and Shipp, M.A. (2000). BAL is a novel risk-related gene in diffuse large B-cell lymphomas that enhances cellular migration. *Blood* 96, 4328-4334.
- Ahel, D., Horejsi, Z., Wiechens, N., Polo, S.E., Garcia-Wilson, E., Ahel, I., Flynn, H., Skehel, M., West, S.C., Jackson, S.P., *et al.* (2009). Poly(ADP-ribose)-dependent regulation of DNA repair by the chromatin remodeling enzyme ALC1. *Science* 325, 1240-1243.
- Ahel, I., Ahel, D., Matsusaka, T., Clark, A.J., Pines, J., Boulton, S.J., and West, S.C. (2008). Poly(ADP-ribose)-binding zinc finger motifs in DNA repair/checkpoint proteins. *Nature* 451, 81-85.
- Altmeyer, M., Messner, S., Hassa, P.O., Fey, M., and Hottiger, M.O. (2009). Molecular mechanism of poly(ADP-ribosylation) by PARP1 and identification of lysine residues as ADP-ribose acceptor sites. *Nucleic Acids Res* 37, 3723-3738.
- Amit, S., Hatzubai, A., Birman, Y., Andersen, J.S., Ben-Shushan, E., Mann, M., Ben-Neriah, Y., and Alkalay, I. (2002). Axin-mediated CKI phosphorylation of beta-catenin at Ser 45: a molecular switch for the Wnt pathway. *Genes Dev* 16, 1066-1076.
- Aravind, L. (2001). The WWE domain: a common interaction module in protein ubiquitination and ADP ribosylation. *Trends in biochemical sciences* 26, 273-275.
- Ashworth, A. (2008). A synthetic lethal therapeutic approach: poly(ADP) ribose polymerase inhibitors for the treatment of cancers deficient in DNA double-strand break repair. *J Clin Oncol* 26, 3785-3790.
- Atasheva, S., Akhrymuk, M., Frolova, E.I., and Frolov, I. (2012). New PARP Gene with an Anti-Alphavirus Function. *J Virol* 86, 8147-8160.
- Bauersachs, S., Mitko, K., Ulbrich, S.E., Blum, H., and Wolf, E. (2008). Transcriptome studies of bovine endometrium reveal molecular profiles characteristic for specific stages of estrous cycle and early pregnancy. *Exp Clin Endocrinol Diabetes* 116, 371-384.
- Bayer, I., Beyer, L., and Manodumrongthum, S. (2011). Analyse des Dockingverhalten von PARP10 und PARP14. In AICES (Aachen, RWTH Aachen University).
- Beurel, E., Michalek, S.M., and Jope, R.S. (2010). Innate and adaptive immune responses regulated by glycogen synthase kinase-3 (GSK3). *Trends in immunology* 31, 24-31.
- Bonicalzi, M.E., Haince, J.F., Droit, A., and Poirier, G.G. (2005). Regulation of poly(ADP-ribose) metabolism by poly(ADP-ribose) glycohydrolase: where and when? *Cell Mol Life Sci* 62, 739-750.
- Bosinger, S.E., Li, Q., Gordon, S.N., Klatt, N.R., Duan, L., Xu, L., Francella, N., Sidahmed, A., Smith, A.J., Cramer, E.M., *et al.* (2009). Global genomic analysis reveals rapid control of a robust innate response in SIV-infected sooty mangabeys. *J Clin Invest* 119, 3556-3572.
- Braczinsky, A.K. (2009). Development of novel tools to study PARP10-mediated ADP-ribosylation reactions (Aachen, RWTH University).

- Breddehorst, R., Wielckens, K., Gartemann, A., Lengyel, H., Klapproth, K., and Hilz, H. (1978). Two different types of bonds linking single ADP-ribose residues covalently to proteins. Quantification in eukaryotic cells. *Eur J Biochem* 92, 129-135.
- Bruzzone, S., Guida, L., Zocchi, E., Franco, L., and De Flora, A. (2001). Connexin 43 hemi channels mediate Ca²⁺-regulated transmembrane NAD⁺ fluxes in intact cells. *Faseb J* 15, 10-12.
- Burzio, L.O., Riquelme, P.T., and Koide, S.S. (1979). ADP ribosylation of rat liver nucleosomal core histones. *The Journal of biological chemistry* 254, 3029-3037.
- Buss, H., Dorrie, A., Schmitz, M.L., Frank, R., Livingstone, M., Resch, K., and Kracht, M. (2004). Phosphorylation of serine 468 by GSK-3 β negatively regulates basal p65 NF- κ B activity. *J Biol Chem* 279, 49571-49574.
- Caldes, C., Vilanova, B., Adrover, M., Munoz, F., and Donoso, J. (2011). Understanding non-enzymatic aminophospholipid glycation and its inhibition. Polar head features affect the kinetics of Schiff base formation. *Bioorg Med Chem* 19, 4536-4543.
- Callow, M.G., Tran, H., Phu, L., Lau, T., Lee, J., Sandoval, W.N., Liu, P.S., Bheddah, S., Tao, J., Lill, J.R., *et al.* (2011). Ubiquitin ligase RNF146 regulates tankyrase and Axin to promote Wnt signaling. *PLoS One* 6, e22595.
- Cervantes-Laurean, D., Jacobson, E.L., and Jacobson, M.K. (1996). Glycation and glycooxidation of histones by ADP-ribose. *The Journal of biological chemistry* 271, 10461-10469.
- Cervantes-Laurean, D., Loflin, P.T., Minter, D.E., Jacobson, E.L., and Jacobson, M.K. (1995). Protein modification by ADP-ribose via acid-labile linkages. *The Journal of biological chemistry* 270, 7929-7936.
- Chambon, P., Weill, J.D., and Mandel, P. (1963). Nicotinamide mononucleotide activation of new DNA-dependent polyadenylic acid synthesizing nuclear enzyme. *Biochemical and biophysical research communications* 11, 39-43.
- Chauvistré, H. (2008). Regulation von Poly-ADP-Ribose Polymerase 10 durch Ubiquitinierung (RWTH Aachen University).
- Chen, D., Vollmar, M., Rossi, M.N., Phillips, C., Kraehenbuehl, R., Slade, D., Mehrotra, P.V., von Delft, F., Crosthwaite, S.K., Gileadi, O., *et al.* (2011). Identification of macrodomain proteins as novel O-acetyl-ADP-ribose deacetylases. *The Journal of biological chemistry* 286, 13261-13271.
- Chen, G., Guo, X., Lv, F., Xu, Y., and Gao, G. (2008). p72 DEAD box RNA helicase is required for optimal function of the zinc-finger antiviral protein. *Proceedings of the National Academy of Sciences of the United States of America* 105, 4352-4357.
- Chen, Z.J., and Sun, L.J. (2009). Nonproteolytic functions of ubiquitin in cell signaling. *Molecular cell* 33, 275-286.
- Cho, S.H., Ahn, A.K., Bhargava, P., Lee, C.H., Eischen, C.M., McGuinness, O., and Boothby, M. (2011). Glycolytic rate and lymphomagenesis depend on PARP14, an ADP ribosyltransferase of the B aggressive lymphoma (BAL) family. *Proceedings of the National Academy of Sciences of the United States of America* 108, 15972-15977.
- Cho, S.H., Goenka, S., Henttinen, T., Gudapati, P., Reinikainen, A., Eischen, C.M., Lahesmaa, R., and Boothby, M. (2009). PARP-14, a member of the B aggressive lymphoma family, transduces survival signals in primary B cells. *Blood* 113, 2416-2425.
- Chou, H.Y., Chou, H.T., and Lee, S.C. (2006). CDK-dependent activation of poly(ADP-ribose) polymerase member 10 (PARP10). *J Biol Chem* 281, 15201-15207.
- Choudhary, C., Kumar, C., Gnad, F., Nielsen, M.L., Rehman, M., Walther, T.C., Olsen, J.V., and Mann, M. (2009). Lysine acetylation targets protein complexes and co-regulates major cellular functions. *Science* 325, 834-840.

- Cohen, P., and Frame, S. (2001). The renaissance of GSK3. *Nat Rev Mol Cell Biol* 2, 769-776.
- Collier, R.J. (2001). Understanding the mode of action of diphtheria toxin: a perspective on progress during the 20th century. *Toxicon* 39, 1793-1803.
- Cook, B.D., Dynek, J.N., Chang, W., Shostak, G., and Smith, S. (2002). Role for the related poly(ADP-Ribose) polymerases tankyrase 1 and 2 at human telomeres. *Mol Cell Biol* 22, 332-342.
- Cross, D.A., Alessi, D.R., Cohen, P., Andjelkovich, M., and Hemmings, B.A. (1995). Inhibition of glycogen synthase kinase-3 by insulin mediated by protein kinase B. *Nature* 378, 785-789.
- D'Alessandro, A., Righetti, P.G., and Zolla, L. (2010). The red blood cell proteome and interactome: an update. *J Proteome Res* 9, 144-163.
- D'Amours, D., Desnoyers, S., D'Silva, I., and Poirier, G.G. (1999). Poly(ADP-ribosylation) reactions in the regulation of nuclear functions. *Biochem J* 342 (Pt 2), 249-268.
- Dajani, R., Fraser, E., Roe, S.M., Young, N., Good, V., Dale, T.C., and Pearl, L.H. (2001). Crystal structure of glycogen synthase kinase 3 beta: structural basis for phosphate-primed substrate specificity and autoinhibition. *Cell* 105, 721-732.
- Dani, N., Stilla, A., Marchegiani, A., Tamburro, A., Till, S., Ladurner, A.G., Corda, D., and Di Girolamo, M. (2009). Combining affinity purification by ADP-ribose-binding macro domains with mass spectrometry to define the mammalian ADP-ribosyl proteome. *Proceedings of the National Academy of Sciences of the United States of America* 106, 4243-4248.
- Davis, K., Banerjee, S., Friggeri, A., Bell, C., Abraham, E., and Zerfaoui, M. (2012). Poly(ADP-ribosylation) of high mobility group box 1 (HMGB1) protein enhances inhibition of efferocytosis. *Mol Med* 18, 359-369.
- Denu, J.M. (2005). The Sir 2 family of protein deacetylases. *Curr Opin Chem Biol* 9, 431-440.
- Di Paola, S., Micaroni, M., Di Tullio, G., Buccione, R., and Di Girolamo, M. (2012). PARP16/ARTD15 Is a Novel Endoplasmic-Reticulum-Associated Mono-ADP-Ribosyltransferase That Interacts with, and Modifies Karyopherin-ss1. *PLoS One* 7, e37352.
- Diefenbach, J., and Burkle, A. (2005). Introduction to poly(ADP-ribose) metabolism. *Cell Mol Life Sci* 62, 721-730.
- Dinkel, H., Michael, S., Weatheritt, R.J., Davey, N.E., Van Roey, K., Altenberg, B., Toedt, G., Uyar, B., Seiler, M., Budd, A., *et al.* (2012). ELM--the database of eukaryotic linear motifs. *Nucleic Acids Res* 40, D242-251.
- Dolle, C., Niere, M., Lohndal, E., and Ziegler, M. (2010). Visualization of subcellular NAD pools and intra-organellar protein localization by poly-ADP-ribose formation. *Cell Mol Life Sci* 67, 433-443.
- Dominguez, C., Boelens, R., and Bonvin, A.M. (2003). HADDOCK: a protein-protein docking approach based on biochemical or biophysical information. *J Am Chem Soc* 125, 1731-1737.
- Dow, E.C., Liu, H., and Rice, A.P. (2010). T-loop phosphorylated Cdk9 localizes to nuclear speckle domains which may serve as sites of active P-TEFb function and exchange between the Brd4 and 7SK/HEXIM1 regulatory complexes. *J Cell Physiol* 224, 84-93.
- Dupont, N., Jiang, S., Pilli, M., Ornatowski, W., Bhattacharya, D., and Deretic, V. (2011). Autophagy-based unconventional secretory pathway for extracellular delivery of IL-1beta. *Embo J* 30, 4701-4711.
- Eide, B., Gierschik, P., and Spiegel, A. (1986). Immunochemical detection of guanine nucleotide binding proteins mono-ADP-ribosylated by bacterial toxins. *Biochemistry* 25, 6711-6715.
- Embi, N., Rylatt, D.B., and Cohen, P. (1980). Glycogen synthase kinase-3 from rabbit skeletal muscle. Separation from cyclic-AMP-dependent protein kinase and phosphorylase kinase. *Eur J Biochem* 107, 519-527.

- Fedorova, M., Frolov, A., and Hoffmann, R. (2010). Fragmentation behavior of Amadori-peptides obtained by non-enzymatic glycosylation of lysine residues with ADP-ribose in tandem mass spectrometry. *J Mass Spectrom* *45*, 664-669.
- Feijs, K.L.H. (2009). PARP10: Insights into its mono-ADP-ribosylation, nuclear import & cell proliferation (RWTH Aachen/University of Amsterdam).
- Firzlaff, J.M., Luscher, B., and Eisenman, R.N. (1991). Negative charge at the casein kinase II phosphorylation site is important for transformation but not for Rb protein binding by the E7 protein of human papillomavirus type 16. *Proceedings of the National Academy of Sciences of the United States of America* *88*, 5187-5191.
- Frame, S., and Cohen, P. (2001). GSK3 takes centre stage more than 20 years after its discovery. *Biochem J* *359*, 1-16.
- Frame, S., Cohen, P., and Biondi, R.M. (2001). A common phosphate binding site explains the unique substrate specificity of GSK3 and its inactivation by phosphorylation. *Molecular cell* *7*, 1321-1327.
- Gagne, J.P., Isabelle, M., Lo, K.S., Bourassa, S., Hendzel, M.J., Dawson, V.L., Dawson, T.M., and Poirier, G.G. (2008). Proteome-wide identification of poly(ADP-ribose) binding proteins and poly(ADP-ribose)-associated protein complexes. *Nucleic Acids Res* *36*, 6959-6976.
- Galland, F., Lacroix, L., Saulnier, P., Dessen, P., Meduri, G., Bernier, M., Gaillard, S., Guibourdenche, J., Fournier, T., Evain-Brion, D., *et al.* (2010). Differential gene expression profiles of invasive and non-invasive non-functioning pituitary adenomas based on microarray analysis. *Endocr Relat Cancer* *17*, 361-371.
- Gao, G., Guo, X., and Goff, S.P. (2002). Inhibition of retroviral RNA production by ZAP, a CCCH-type zinc finger protein. *Science* *297*, 1703-1706.
- Gao, J., and Xu, D. (2012). Correlation between posttranslational modification and intrinsic disorder in protein. *Pac Symp Biocomput*, 94-103.
- Gargano, B., Amente, S., Majello, B., and Lania, L. (2007). P-TEFb is a crucial co-factor for Myc transactivation. *Cell Cycle* *6*, 2031-2037.
- Gibson, B.A., and Kraus, W.L. (2012). New insights into the molecular and cellular functions of poly(ADP-ribose) and PARPs. *Nat Rev Mol Cell Biol* *13*, 411-424.
- Gnad, F., Gunawardena, J., and Mann, M. (2011). PHOSIDA 2011: the posttranslational modification database. *Nucleic Acids Res* *39*, D253-260.
- Goenka, S., and Boothby, M. (2006). Selective potentiation of Stat-dependent gene expression by collaborator of Stat6 (CoaSt6), a transcriptional cofactor. *Proceedings of the National Academy of Sciences of the United States of America* *103*, 4210-4215.
- Goenka, S., Cho, S.H., and Boothby, M. (2007). Collaborator of Stat6 (CoaSt6)-associated poly(ADP-ribose) polymerase activity modulates Stat6-dependent gene transcription. *The Journal of biological chemistry* *282*, 18732-18739.
- Golderer, G., and Grobner, P. (1991). ADP-ribosylation of core histones and their acetylated subspecies. *Biochem J* *277 (Pt 3)*, 607-610.
- Gottschalk, A.J., Timinszky, G., Kong, S.E., Jin, J., Cai, Y., Swanson, S.K., Washburn, M.P., Florens, L., Ladurner, A.G., Conaway, J.W., *et al.* (2009). Poly(ADP-ribosylation) directs recruitment and activation of an ATP-dependent chromatin remodeler. *Proceedings of the National Academy of Sciences of the United States of America* *106*, 13770-13774.
- Gould, C.M., Diella, F., Via, A., Puntervoll, P., Gemund, C., Chabanis-Davidson, S., Michael, S., Sayadi, A., Bryne, J.C., Chica, C., *et al.* (2010). ELM: the status of the 2010 eukaryotic linear motif resource. *Nucleic Acids Res* *38*, D167-180.

- Grabbe, C., Husnjak, K., and Dikic, I. (2011). The spatial and temporal organization of ubiquitin networks. *Nat Rev Mol Cell Biol* *12*, 295-307.
- Grimes, C.A., and Jope, R.S. (2001). The multifaceted roles of glycogen synthase kinase 3 β in cellular signaling. *Progress in neurobiology* *65*, 391-426.
- Gross, O., Thomas, C.J., Guarda, G., and Tschopp, J. (2011). The inflammasome: an integrated view. *Immunol Rev* *243*, 136-151.
- Guettler, S., LaRose, J., Petsalaki, E., Gish, G., Scotter, A., Pawson, T., Rottapel, R., and Sicheri, F. (2011). Structural basis and sequence rules for substrate recognition by Tankyrase explain the basis for cherubism disease. *Cell* *147*, 1340-1354.
- Guo, X., Carroll, J.W., Macdonald, M.R., Goff, S.P., and Gao, G. (2004). The zinc finger antiviral protein directly binds to specific viral mRNAs through the CCCH zinc finger motifs. *J Virol* *78*, 12781-12787.
- Ha, G.H., Kim, H.S., Go, H., Lee, H., Seimiya, H., Chung, D.H., and Lee, C.W. (2012). Tankyrase-1 function at telomeres and during mitosis is regulated by Polo-like kinase-1-mediated phosphorylation. *Cell Death Differ* *19*, 321-332.
- Haag, F., Adriouch, S., Brass, A., Jung, C., Moller, S., Scheuplein, F., Bannas, P., Seman, M., and Koch-Nolte, F. (2007). Extracellular NAD and ATP: Partners in immune cell modulation. *Purinergic Signal* *3*, 71-81.
- Haenni, S.S., Hassa, P.O., Altmeyer, M., Fey, M., Imhof, R., and Hottiger, M.O. (2008). Identification of lysines 36 and 37 of PARP-2 as targets for acetylation and auto-ADP-ribosylation. *Int J Biochem Cell Biol* *40*, 2274-2283.
- Haince, J.F., Ouellet, M.E., McDonald, D., Hendzel, M.J., and Poirier, G.G. (2006). Dynamic relocation of poly(ADP-ribose) glycohydrolase isoforms during radiation-induced DNA damage. *Biochimica et biophysica acta* *1763*, 226-237.
- Han, W., Li, X., and Fu, X. (2011). The macro domain protein family: structure, functions, and their potential therapeutic implications. *Mutat Res* *727*, 86-103.
- Hassa, P.O., Haenni, S.S., Elser, M., and Hottiger, M.O. (2006). Nuclear ADP-ribosylation reactions in mammalian cells: where are we today and where are we going? *Microbiol Mol Biol Rev* *70*, 789-829.
- Hassa, P.O., and Hottiger, M.O. (2002). The functional role of poly(ADP-ribose)polymerase 1 as novel coactivator of NF-kappaB in inflammatory disorders. *Cell Mol Life Sci* *59*, 1534-1553.
- Hassler, M., Jankevicius, G., and Ladurner, A.G. (2011). PARG: a macrodomain in disguise. *Structure* *19*, 1351-1353.
- Hayakawa, S., Shiratori, S., Yamato, H., Kameyama, T., Kitatsuji, C., Kashigi, F., Goto, S., Kameoka, S., Fujikura, D., Yamada, T., *et al.* (2011). ZAPS is a potent stimulator of signaling mediated by the RNA helicase RIG-I during antiviral responses. *Nat Immunol* *12*, 37-44.
- He, F., Tsuda, K., Takahashi, M., Kuwasako, K., Terada, T., Shirouzu, M., Watanabe, S., Kigawa, T., Kobayashi, N., Guntert, P., *et al.* (2012). Structural insight into the interaction of ADP-ribose with the PARP WWE domains. *FEBS Lett*.
- He, X., Saint-Jeannet, J.P., Woodgett, J.R., Varmus, H.E., and Dawid, I.B. (1995). Glycogen synthase kinase-3 and dorsoventral patterning in *Xenopus* embryos. *Nature* *374*, 617-622.
- Hengel, S.M., and Goodlett, D.R. (2012). A Review of Tandem Mass Spectrometry Characterization of Adenosine Diphosphate-Ribosylated Peptides. *Int J Mass Spectrom* *312*, 114-121.
- Hershko, A., and Ciechanover, A. (1998). The ubiquitin system. *Annu Rev Biochem* *67*, 425-479.

- Hottiger, M.O., Hassa, P.O., Luscher, B., Schuler, H., and Koch-Nolte, F. (2010). Toward a unified nomenclature for mammalian ADP-ribosyltransferases. *Trends Biochem Sci* 35, 208-219.
- Hsia, J.A., Tsai, S.C., Adamik, R., Yost, D.A., Hewlett, E.L., and Moss, J. (1985). Amino acid-specific ADP-ribosylation. Sensitivity to hydroxylamine of [cysteine(ADP-ribose)]protein and [arginine(ADP-ribose)]protein linkages. *J Biol Chem* 260, 16187-16191.
- Huang, S.M., Mishina, Y.M., Liu, S., Cheung, A., Stegmeier, F., Michaud, G.A., Charlat, O., Wiellette, E., Zhang, Y., Wiessner, S., *et al.* (2009). Tankyrase inhibition stabilizes axin and antagonizes Wnt signalling. *Nature* 461, 614-620.
- Jagtap, P., and Szabo, C. (2005). Poly(ADP-ribose) polymerase and the therapeutic effects of its inhibitors. *Nat Rev Drug Discov* 4, 421-440.
- Javle, M., and Curtin, N.J. (2011). The role of PARP in DNA repair and its therapeutic exploitation. *Br J Cancer* 105, 1114-1122.
- Johansen, T., and Lamark, T. (2011). Selective autophagy mediated by autophagic adapter proteins. *Autophagy* 7, 279-296.
- Juszczynski, P., Kutok, J.L., Li, C., Mitra, J., Aguiar, R.C., and Shipp, M.A. (2006). BAL1 and BBAP are regulated by a gamma interferon-responsive bidirectional promoter and are overexpressed in diffuse large B-cell lymphomas with a prominent inflammatory infiltrate. *Mol Cell Biol* 26, 5348-5359.
- Kahl, S., Nissen, M., Girisch, R., Duffy, T., Leiter, E.H., Haag, F., and Koch-Nolte, F. (2000). Metalloprotease-mediated shedding of enzymatically active mouse ecto-ADP-ribosyltransferase ART2.2 upon T cell activation. *Journal of immunology* 165, 4463-4469.
- Kanazawa, S., Soucek, L., Evan, G., Okamoto, T., and Peterlin, B.M. (2003). c-Myc recruits P-TEFb for transcription, cellular proliferation and apoptosis. *Oncogene* 22, 5707-5711.
- Kang, H.C., Lee, Y.I., Shin, J.H., Andrabi, S.A., Chi, Z., Gagne, J.P., Lee, Y., Ko, H.S., Lee, B.D., Poirier, G.G., *et al.* (2011). Iduna is a poly(ADP-ribose) (PAR)-dependent E3 ubiquitin ligase that regulates DNA damage. *Proceedings of the National Academy of Sciences of the United States of America* 108, 14103-14108.
- Kang, J.H., Ryu, H.S., Kim, H.T., Lee, S.J., Choi, U.K., Park, Y.B., Huh, T.L., Choi, M.S., Kang, T.C., Choi, S.Y., *et al.* (2009). Proteomic analysis of human macrophages exposed to hypochlorite-oxidized low-density lipoprotein. *Biochimica et biophysica acta* 1794, 446-458.
- Karki, S., Li, M.M., Schoggins, J.W., Tian, S., Rice, C.M., and MacDonald, M.R. (2012). Multiple interferon stimulated genes synergize with the zinc finger antiviral protein to mediate anti-alphavirus activity. *PLoS One* 7, e37398.
- Karlberg, T., Thorsell, A.G., Kallas, A., and Schuler, H. (2012). Crystal Structure of Human ADP-ribose Transferase ARTD15/PARP16 Reveals a Novel Putative Regulatory Domain. *The Journal of biological chemistry* 287, 24077-24081.
- Karras, G.I., Kustatscher, G., Buhecha, H.R., Allen, M.D., Pugieux, C., Sait, F., Bycroft, M., and Ladurner, A.G. (2005). The macro domain is an ADP-ribose binding module. *Embo J* 24, 1911-1920.
- Kato, J., Zhu, J., Liu, C., and Moss, J. (2007). Enhanced sensitivity to cholera toxin in ADP-ribosylarginine hydrolase-deficient mice. *Mol Cell Biol* 27, 5534-5543.
- Kato, J., Zhu, J., Liu, C., Stylianou, M., Hoffmann, V., Lizak, M.J., Glasgow, C.G., and Moss, J. (2011). ADP-ribosylarginine hydrolase regulates cell proliferation and tumorigenesis. *Cancer Res* 71, 5327-5335.
- Kelm, O., Wind, M., Lehmann, W.D., and Nigg, E.A. (2002). Cell cycle-regulated phosphorylation of the *Xenopus* polo-like kinase Plx1. *The Journal of biological chemistry* 277, 25247-25256.

- Kerns, J.A., Emerman, M., and Malik, H.S. (2008). Positive selection and increased antiviral activity associated with the PARP-containing isoform of human zinc-finger antiviral protein. *PLoS Genet* 4, e21.
- Kim, M.S., An, C.H., Kim, S.S., Yoo, N.J., and Lee, S.H. (2011). Frameshift mutations of poly(adenosine diphosphate-ribose) polymerase genes in gastric and colorectal cancers with microsatellite instability. *Hum Pathol* 42, 1289-1296.
- Kleine, H., Herrmann, A., Lamark, T., Forst, A.H., Verheugd, P., Luscher-Firzloff, J., Lippok, B., Feijs, K.L., Herzog, N., Kremmer, E., *et al.* (2012). Dynamic subcellular localization of the mono-ADP-ribosyltransferase ARTD10 and interaction with the ubiquitin receptor p62. *Cell Commun Signal* 10, 28.
- Kleine, H., and Luscher, B. (2009). Learning how to read ADP-ribosylation. *Cell* 139, 17-19.
- Kleine, H., Poreba, E., Lesniewicz, K., Hassa, P.O., Hottiger, M.O., Litchfield, D.W., Shilton, B.H., and Luscher, B. (2008). Substrate-assisted catalysis by PARP10 limits its activity to mono-ADP-ribosylation. *Mol Cell* 32, 57-69.
- Koch-Nolte, F., Adriouch, S., Bannas, P., Krebs, C., Scheuplein, F., Seman, M., and Haag, F. (2006). ADP-ribosylation of membrane proteins: unveiling the secrets of a crucial regulatory mechanism in mammalian cells. *Ann Med* 38, 188-199.
- Koh, D.W., Dawson, V.L., and Dawson, T.M. (2005). The road to survival goes through PARG. *Cell Cycle* 4, 397-399.
- Kornev, A.P., Haste, N.M., Taylor, S.S., and Eyck, L.F. (2006). Surface comparison of active and inactive protein kinases identifies a conserved activation mechanism. *Proceedings of the National Academy of Sciences of the United States of America* 103, 17783-17788.
- Krishnakumar, R., and Kraus, W.L. (2010). PARP-1 regulates chromatin structure and transcription through a KDM5B-dependent pathway. *Molecular cell* 39, 736-749.
- Krissinel, E., and Henrick, K. (2007). Inference of macromolecular assemblies from crystalline state. *J Mol Biol* 372, 774-797.
- Laing, S., Unger, M., Koch-Nolte, F., and Haag, F. (2011). ADP-ribosylation of arginine. *Amino Acids* 41, 257-269.
- Lee, Y.M., Babu, C.S., Chen, Y.C., Milcic, M., Qu, Y., and Lim, C. (2010). Conserved structural motif for recognizing nicotinamide adenine dinucleotide in poly(ADP-ribose) polymerases and ADP-ribosylating toxins: implications for structure-based drug design. *Journal of medicinal chemistry* 53, 4038-4049.
- Lesniewicz, K., Luscher-Firzloff, J., Poreba, E., Fuchs, P., Walsemann, G., Wiche, G., and Luscher, B. (2005). Overlap of the gene encoding the novel poly(ADP-ribose) polymerase Parp10 with the plectin 1 gene and common use of exon sequences. *Genomics* 86, 38-46.
- Levaot, N., Voytyuk, O., Dimitriou, I., Sircoulomb, F., Chandrakumar, A., Deckert, M., Krzyzanowski, P.M., Scotter, A., Gu, S., Janmohamed, S., *et al.* (2011). Loss of Tankyrase-mediated destruction of 3BP2 is the underlying pathogenic mechanism of cherubism. *Cell* 147, 1324-1339.
- Locht, C., Coutte, L., and Mielcarek, N. (2011). The ins and outs of pertussis toxin. *Febs J* 278, 4668-4682.
- Luscher, B., and Eisenman, R.N. (1992). Mitosis-specific phosphorylation of the nuclear oncoproteins Myc and Myb. *J Cell Biol* 118, 775-784.
- Ma, Q., Baldwin, K.T., Renzelli, A.J., McDaniel, A., and Dong, L. (2001). TCDD-inducible poly(ADP-ribose) polymerase: a novel response to 2,3,7,8-tetrachlorodibenzo-p-dioxin. *Biochemical and biophysical research communications* 289, 499-506.

- MacDonald, M.R., Machlin, E.S., Albin, O.R., and Levy, D.E. (2007). The zinc finger antiviral protein acts synergistically with an interferon-induced factor for maximal activity against alphaviruses. *J Virol* *81*, 13509-13518.
- Magni, G., Amici, A., Emanuelli, M., Orsomando, G., Raffaelli, N., and Ruggieri, S. (2004). Enzymology of NAD⁺ homeostasis in man. *Cell Mol Life Sci* *61*, 19-34.
- Mahmoud, L., Al-Saif, M., Amer, H.M., Sheikh, M., Almajhdi, F.N., and Khabar, K.S. (2011). Green fluorescent protein reporter system with transcriptional sequence heterogeneity for monitoring the interferon response. *J Virol* *85*, 9268-9275.
- Mann, M. (2006). Functional and quantitative proteomics using SILAC. *Nat Rev Mol Cell Biol* *7*, 952-958.
- Margarit, S.M., Davidson, W., Frego, L., and Stebbins, C.E. (2006). A steric antagonism of actin polymerization by a salmonella virulence protein. *Structure* *14*, 1219-1229.
- Massudi, H., Grant, R., Guillemin, G.J., and Braidy, N. (2012). NAD⁺ metabolism and oxidative stress: the golden nucleotide on a crown of thorns. *Redox Rep* *17*, 28-46.
- Matic, I., Ahel, I., and Hay, R.T. (2012). Reanalysis of phosphoproteomics data uncovers ADP-ribosylation sites. *Nat Methods* *9*, 771-772.
- Matthias, P., Muller, M.M., Schreiber, E., Rusconi, S., and Schaffner, W. (1989). Eukaryotic expression vectors for the analysis of mutant proteins. *Nucleic Acids Res* *17*, 6418.
- McLennan, A.G. (2006). The Nudix hydrolase superfamily. *Cell Mol Life Sci* *63*, 123-143.
- McNeill, H., and Woodgett, J.R. (2010). When pathways collide: collaboration and connivance among signalling proteins in development. *Nat Rev Mol Cell Biol* *11*, 404-413.
- Mehrotra, P., Riley, J.P., Patel, R., Li, F., Voss, L., and Goenka, S. (2011). PARP-14 functions as a transcriptional switch for Stat6-dependent gene activation. *The Journal of biological chemistry* *286*, 1767-1776.
- Melo, J.V. (1996). The molecular biology of chronic myeloid leukaemia. *Leukemia* *10*, 751-756.
- Menissier de Murcia, J., Ricoul, M., Tartier, L., Niedergang, C., Huber, A., Dantzer, F., Schreiber, V., Ame, J.C., Dierich, A., LeMour, M., *et al.* (2003). Functional interaction between PARP-1 and PARP-2 in chromosome stability and embryonic development in mouse. *Embo J* *22*, 2255-2263.
- Messner, S., Altmeyer, M., Zhao, H., Pozivil, A., Roschitzki, B., Gehrig, P., Rutishauser, D., Huang, D., Caflisch, A., and Hottiger, M.O. (2010). PARP1 ADP-ribosylates lysine residues of the core histone tails. *Nucleic Acids Res* *38*, 6350-6362.
- Meyer, T., and Hilz, H. (1986). Production of anti-(ADP-ribose) antibodies with the aid of a dinucleotide-pyrophosphatase-resistant hapten and their application for the detection of mono(ADP-ribosyl)ated polypeptides. *Eur J Biochem* *155*, 157-165.
- Meyer, T., Wielckens, K., Thiem, J., and Hilz, H. (1984). NAD[S], an NAD analogue with reduced susceptibility to phosphodiesterase. Chemical synthesis and enzymic properties. *Eur J Biochem* *140*, 531-537.
- Meyer-Ficca, M.L., Meyer, R.G., Coyle, D.L., Jacobson, E.L., and Jacobson, M.K. (2004). Human poly(ADP-ribose) glycohydrolase is expressed in alternative splice variants yielding isoforms that localize to different cell compartments. *Experimental cell research* *297*, 521-532.
- Milke, L. (2007). Biochemische und funktionelle Analyse der Ubiquitinierung und des Kerntransports von PARP10 (RWTH Aachen University).
- Mills, C.N., Nowsheen, S., Bonner, J.A., and Yang, E.S. (2011). Emerging roles of glycogen synthase kinase 3 in the treatment of brain tumors. *Front Mol Neurosci* *4*, 47.

- Minella, A.C., and Clurman, B.E. (2005). Mechanisms of tumor suppression by the SCF(Fbw7). *Cell Cycle* 4, 1356-1359.
- Mitko, K., Ulbrich, S.E., Wenigerkind, H., Sinowatz, F., Blum, H., Wolf, E., and Bauersachs, S. (2008). Dynamic changes in messenger RNA profiles of bovine endometrium during the oestrous cycle. *Reproduction* 135, 225-240.
- Montzka, K. (2006). Nucleo-cytoplasmatischer Transport von PARP10 (FH Aachen/RWTH Aachen University).
- Moorhead, G.B., Trinkle-Mulcahy, L., and Ulke-Lemee, A. (2007). Emerging roles of nuclear protein phosphatases. *Nat Rev Mol Cell Biol* 8, 234-244.
- Morgenstern, J.P., and Land, H. (1990). A series of mammalian expression vectors and characterisation of their expression of a reporter gene in stably and transiently transfected cells. *Nucleic Acids Res* 18, 1068.
- Moss, J., Yost, D.A., and Stanley, S.J. (1983). Amino acid-specific ADP-ribosylation. *The Journal of biological chemistry* 258, 6466-6470.
- Moyle, P.M., and Muir, T.W. (2010). Method for the synthesis of mono-ADP-ribose conjugated peptides. *J Am Chem Soc* 132, 15878-15880.
- Murawska, M., Hassler, M., Renkawitz-Pohl, R., Ladurner, A., and Brehm, A. (2011). Stress-induced PARP activation mediates recruitment of Drosophila Mi-2 to promote heat shock gene expression. *PLoS Genet* 7, e1002206.
- Nakayama, K.I., and Nakayama, K. (2006). Ubiquitin ligases: cell-cycle control and cancer. *Nat Rev Cancer* 6, 369-381.
- Niere, M., Mashimo, M., Agledal, L., Dolle, C., Kasamatsu, A., Kato, J., Moss, J., and Ziegler, M. (2012). ADP-ribosylhydrolase 3 (ARH3), not poly(ADP-ribose) glycohydrolase (PARG) isoforms, is responsible for degradation of mitochondrial matrix-associated poly(ADP-ribose). *The Journal of biological chemistry* 287, 16088-16102.
- Oka, S., Kato, J., and Moss, J. (2006). Identification and characterization of a mammalian 39-kDa poly(ADP-ribose) glycohydrolase. *The Journal of biological chemistry* 281, 705-713.
- Olsen, J.V., Vermeulen, M., Santamaria, A., Kumar, C., Miller, M.L., Jensen, L.J., Gnad, F., Cox, J., Jensen, T.S., Nigg, E.A., *et al.* (2010). Quantitative phosphoproteomics reveals widespread full phosphorylation site occupancy during mitosis. *Science signaling* 3, ra3.
- Ono, T., Kasamatsu, A., Oka, S., and Moss, J. (2006). The 39-kDa poly(ADP-ribose) glycohydrolase ARH3 hydrolyzes O-acetyl-ADP-ribose, a product of the Sir2 family of acetyl-histone deacetylases. *Proceedings of the National Academy of Sciences of the United States of America* 103, 16687-16691.
- Orlicky, S., Tang, X., Willems, A., Tyers, M., and Sicheri, F. (2003). Structural basis for phosphodependent substrate selection and orientation by the SCFCdc4 ubiquitin ligase. *Cell* 112, 243-256.
- Osago, H., Terashima, M., Hara, N., Yamada, K., and Tsuchiya, M. (2008). A new detection method for arginine-specific ADP-ribosylation of protein -- a combinational use of anti-ADP-ribosylarginine antibody and ADP-ribosylarginine hydrolase. *J Biochem Biophys Methods* 70, 1014-1019.
- Osago, H., Yamada, K., Shibata, T., Yoshino, K., Hara, N., and Tsuchiya, M. (2009). Precursor ion scanning and sequencing of arginine-ADP-ribosylated peptide by mass spectrometry. *Anal Biochem* 393, 248-254.
- Peterson, F.C., Chen, D., Lytle, B.L., Rossi, M.N., Ahel, I., Denu, J.M., and Volkman, B.F. (2011). Orphan macrodomain protein (human C6orf130) is an O-acyl-ADP-ribose deacylase: solution structure and catalytic properties. *The Journal of biological chemistry* 286, 35955-35965.

- Radich, J.P., Dai, H., Mao, M., Oehler, V., Schelter, J., Druker, B., Sawyers, C., Shah, N., Stock, W., Willman, C.L., *et al.* (2006). Gene expression changes associated with progression and response in chronic myeloid leukemia. *Proceedings of the National Academy of Sciences of the United States of America* *103*, 2794-2799.
- Riederer, B.M., Leuba, G., Vernay, A., and Riederer, I.M. (2011). The role of the ubiquitin proteasome system in Alzheimer's disease. *Exp Biol Med (Maywood)* *236*, 268-276.
- Rosenthal, F., Messner, S., Roschitzki, B., Gehrig, P., Nanni, P., and Hottiger, M.O. (2011). Identification of distinct amino acids as ADP-ribose acceptor sites by mass spectrometry. *Methods Mol Biol* *780*, 57-66.
- Salazar, J.C., Duhnam-Ems, S., La Vake, C., Cruz, A.R., Moore, M.W., Caimano, M.J., Velez-Climent, L., Shupe, J., Krueger, W., and Radolf, J.D. (2009). Activation of human monocytes by live *Borrelia burgdorferi* generates TLR2-dependent and -independent responses which include induction of IFN-beta. *PLoS Pathog* *5*, e1000444.
- Sandhu, S.K., Yap, T.A., and de Bono, J.S. (2011). The emerging role of poly(ADP-Ribose) polymerase inhibitors in cancer treatment. *Curr Drug Targets* *12*, 2034-2044.
- Sawyers, C.L., Hochhaus, A., Feldman, E., Goldman, J.M., Miller, C.B., Ottmann, O.G., Schiffer, C.A., Talpaz, M., Guilhot, F., Deininger, M.W., *et al.* (2002). Imatinib induces hematologic and cytogenetic responses in patients with chronic myelogenous leukemia in myeloid blast crisis: results of a phase II study. *Blood* *99*, 3530-3539.
- Saxty, B.A., Yadollahi-Farsani, M., Upton, P.D., Johnstone, S.R., and MacDermot, J. (2001). Inactivation of platelet-derived growth factor-BB following modification by ADP-ribosyltransferase. *Br J Pharmacol* *133*, 1219-1226.
- Schmitz, J. (2010). Charakterisierung der PARP10 Phosphorylierung (Aachen, RWTH Aachen University).
- Schoggins, J.W., Wilson, S.J., Panis, M., Murphy, M.Y., Jones, C.T., Bieniasz, P., and Rice, C.M. (2011). A diverse range of gene products are effectors of the type I interferon antiviral response. *Nature* *472*, 481-485.
- Schreiber, V., Ame, J.C., Dolle, P., Schultz, I., Rinaldi, B., Fraulob, V., Menissier-de Murcia, J., and de Murcia, G. (2002). Poly(ADP-ribose) polymerase-2 (PARP-2) is required for efficient base excision DNA repair in association with PARP-1 and XRCC1. *The Journal of biological chemistry* *277*, 23028-23036.
- Schreiber, V., Dantzer, F., Ame, J.C., and de Murcia, G. (2006). Poly(ADP-ribose): novel functions for an old molecule. *Nat Rev Mol Cell Biol* *7*, 517-528.
- Schuchlantz, H. (2005). Aufreinigung und Charakterisierung von Myc-Kofaktor-Komplexen (RWTH Aachen University).
- Schuchlantz, H. (2008). Mechanistic insights into the PARP10 mediated ADP-ribosylation reaction and analysis of PARP10's subcellular localization (RWTH Aachen University).
- Schwab, C.J., Colville, M.J., Fullerton, A.T., and McMahon, K.K. (2000). Evidence of endogenous mono-ADP-ribosylation of cardiac proteins via anti-ADP-ribosylarginine immunoreactivity. *Proc Soc Exp Biol Med* *223*, 389-396.
- Seman, M., Adriouch, S., Scheuplein, F., Krebs, C., Freese, D., Glowacki, G., Deterre, P., Haag, F., and Koch-Nolte, F. (2003). NAD-induced T cell death: ADP-ribosylation of cell surface proteins by ART2 activates the cytolytic P2X7 purinoceptor. *Immunity* *19*, 571-582.
- Shen, X., Wang, W., Wang, L., Houde, C., Wu, W., Tudor, M., Thompson, J.R., Sisk, C.M., Hubbard, B., and Li, J. (2012). Identification of genes affecting apolipoprotein B secretion following siRNA-mediated gene knockdown in primary human hepatocytes. *Atherosclerosis* *222*, 154-157.
- Slade, D., Dunstan, M.S., Barkauskaite, E., Weston, R., Lafite, P., Dixon, N., Ahel, M., Leys, D., and Ahel, I. (2011). The structure and catalytic mechanism of a poly(ADP-ribose) glycohydrolase. *Nature* *477*, 616-620.

- Smith, S., Gariat, I., Schmitt, A., and de Lange, T. (1998). Tankyrase, a poly(ADP-ribose) polymerase at human telomeres. *Science* *282*, 1484-1487.
- Stevens, L.A., Levine, R.L., Gochuico, B.R., and Moss, J. (2009). ADP-ribosylation of human defensin HNP-1 results in the replacement of the modified arginine with the noncoded amino acid ornithine. *Proceedings of the National Academy of Sciences of the United States of America* *106*, 19796-19800.
- Sun, L., Lv, F., Guo, X., and Gao, G. (2012). Glycogen Synthase Kinase 3beta (GSK3beta) Modulates Antiviral Activity of Zinc-finger Antiviral Protein (ZAP). *The Journal of biological chemistry* *287*, 22882-22888.
- Sutherland, C. (2011). What Are the bona fide GSK3 Substrates? *International journal of Alzheimer's disease* *2011*, 505607.
- Taelman, V.F., Dobrowolski, R., Plouhinec, J.L., Fuentealba, L.C., Vorwald, P.P., Gumper, I., Sabatini, D.D., and De Robertis, E.M. (2010). Wnt signaling requires sequestration of glycogen synthase kinase 3 inside multivesicular endosomes. *Cell* *143*, 1136-1148.
- Takada, T., Iida, K., and Moss, J. (1993). Cloning and site-directed mutagenesis of human ADP-ribosylarginine hydrolase. *The Journal of biological chemistry* *268*, 17837-17843.
- Tao, Z., Gao, P., and Liu, H.W. (2009). Identification of the ADP-ribosylation sites in the PARP-1 automodification domain: analysis and implications. *J Am Chem Soc* *131*, 14258-14260.
- Timinszky, G., Till, S., Hassa, P.O., Hothorn, M., Kustatscher, G., Nijmeijer, B., Colombelli, J., Altmeyer, M., Stelzer, E.H., Scheffzek, K., *et al.* (2009). A macrodomain-containing histone rearranges chromatin upon sensing PARP1 activation. *Nat Struct Mol Biol* *16*, 923-929.
- Tong, L., and Denu, J.M. (2010). Function and metabolism of sirtuin metabolite O-acetyl-ADP-ribose. *Biochimica et biophysica acta* *1804*, 1617-1625.
- Twomey, C., and McCarthy, J.V. (2006). Presenilin-1 is an unprimed glycogen synthase kinase-3beta substrate. *FEBS Lett* *580*, 4015-4020.
- van der Geer, P., and Hunter, T. (1994). Phosphopeptide mapping and phosphoamino acid analysis by electrophoresis and chromatography on thin-layer cellulose plates. *Electrophoresis* *15*, 544-554.
- Vervoorts, J., Luscher-Firzlaff, J., and Luscher, B. (2006). The ins and outs of MYC regulation by posttranslational mechanisms. *The Journal of biological chemistry* *281*, 34725-34729.
- Vucic, D., Dixit, V.M., and Wertz, I.E. (2011). Ubiquitylation in apoptosis: a post-translational modification at the edge of life and death. *Nat Rev Mol Cell Biol* *12*, 439-452.
- Wahlberg, E., Karlberg, T., Kouznetsova, E., Markova, N., Macchiarulo, A., Thorsell, A.G., Pol, E., Frostell, A., Ekblad, T., Oncu, D., *et al.* (2012). Family-wide chemical profiling and structural analysis of PARP and tankyrase inhibitors. *Nat Biotechnol* *30*, 283-288.
- Wang, N., Dong, Q., Li, J., Jangra, R.K., Fan, M., Brasier, A.R., Lemon, S.M., Pfeffer, L.M., and Li, K. (2010). Viral induction of the zinc finger antiviral protein is IRF3-dependent but NF-kappaB-independent. *The Journal of biological chemistry* *285*, 6080-6090.
- Wang, Z., Michaud, G.A., Cheng, Z., Zhang, Y., Hinds, T.R., Fan, E., Cong, F., and Xu, W. (2012). Recognition of the iso-ADP-ribose moiety in poly(ADP-ribose) by WWE domains suggests a general mechanism for poly(ADP-ribosyl)ation-dependent ubiquitination. *Genes Dev* *26*, 235-240.
- Webb, T.R., Cross, S.H., McKie, L., Edgar, R., Vizor, L., Harrison, J., Peters, J., and Jackson, I.J. (2008). Diphthamide modification of eEF2 requires a J-domain protein and is essential for normal development. *Journal of cell science* *121*, 3140-3145.

- Weissman, A.M., Shabek, N., and Ciechanover, A. (2011). The predator becomes the prey: regulating the ubiquitin system by ubiquitylation and degradation. *Nat Rev Mol Cell Biol* *12*, 605-620.
- Welcker, M., and Clurman, B.E. (2008). FBW7 ubiquitin ligase: a tumour suppressor at the crossroads of cell division, growth and differentiation. *Nat Rev Cancer* *8*, 83-93.
- Welcker, M., Orian, A., Jin, J., Grim, J.E., Harper, J.W., Eisenman, R.N., and Clurman, B.E. (2004). The Fbw7 tumor suppressor regulates glycogen synthase kinase 3 phosphorylation-dependent c-Myc protein degradation. *Proceedings of the National Academy of Sciences of the United States of America* *101*, 9085-9090.
- Welsby, I., Hutin, D., and Leo, O. (2012). Complex roles of members of the ADP-ribosyl transferase super family in immune defences: looking beyond PARP1. *Biochem Pharmacol* *84*, 11-20.
- Wu, D., and Pan, W. (2010). GSK3: a multifaceted kinase in Wnt signaling. *Trends in biochemical sciences* *35*, 161-168.
- Xu, P., Duong, D.M., Seyfried, N.T., Cheng, D., Xie, Y., Robert, J., Rush, J., Hochstrasser, M., Finley, D., and Peng, J. (2009). Quantitative proteomics reveals the function of unconventional ubiquitin chains in proteasomal degradation. *Cell* *137*, 133-145.
- Yeh, T.Y., Sbdio, J.I., and Chi, N.W. (2006). Mitotic phosphorylation of tankyrase, a PARP that promotes spindle assembly, by GSK3. *Biochemical and biophysical research communications* *350*, 574-579.
- Yu, M., Schreek, S., Cerni, C., Schamberger, C., Lesniewicz, K., Poreba, E., Vervoorts, J., Walsemann, G., Grotzinger, J., Kremmer, E., *et al.* (2005). PARP-10, a novel Myc-interacting protein with poly(ADP-ribose) polymerase activity, inhibits transformation. *Oncogene* *24*, 1982-1993.
- Yu, M., Zhang, C., Yang, Y., Yang, Z., Zhao, L., Xu, L., Wang, R., Zhou, X., and Huang, P. (2011). The interaction between the PARP10 protein and the NS1 protein of H5N1 AIV and its effect on virus replication. *Virology* *418*, 546.
- Zee, B.M., and Garcia, B.A. (2010). Electron transfer dissociation facilitates sequencing of adenosine diphosphate-ribosylated peptides. *Anal Chem* *82*, 28-31.
- Zhang, Y., Liu, S., Mickanin, C., Feng, Y., Charlat, O., Michaud, G.A., Schirle, M., Shi, X., Hild, M., Bauer, A., *et al.* (2011). RNF146 is a poly(ADP-ribose)-directed E3 ligase that regulates axin degradation and Wnt signalling. *Nat Cell Biol* *13*, 623-629.
- Zhao, K., Harshaw, R., Chai, X., and Marmorstein, R. (2004). Structural basis for nicotinamide cleavage and ADP-ribose transfer by NAD(+)-dependent Sir2 histone/protein deacetylases. *Proceedings of the National Academy of Sciences of the United States of America* *101*, 8563-8568.
- Ziegler, M. (2000). New functions of a long-known molecule. Emerging roles of NAD in cellular signaling. *Eur J Biochem* *267*, 1550-1564.
- Zocchi, E., Usai, C., Guida, L., Franco, L., Bruzzone, S., Passalacqua, M., and De Flora, A. (1999). Ligand-induced internalization of CD38 results in intracellular Ca²⁺ mobilization: role of NAD⁺ transport across cell membranes. *Faseb J* *13*, 273-283.

Attachments

Abbreviations.....	I
Layman’s summary.....	III
Scientific contributions	IV
Curriculum Vitae	VI
Eidesstattliche Erklärung.....	VII
Acknowledgements.....	VIII

Abbreviations

ADP:	adenosine diphosphate
ADPr:	adenosine diphosphate ribose
ATP:	adenosine triphosphate
ARH:	ADP-ribosylhydrolase
ART:	ADP-ribosyltransferase
ARTC:	ADP-ribosyltransferase cholera toxin like
ARTD:	ADP-ribosyltransferase diphtheria toxin like
BAL1-3:	B-aggressive lymphoma 1-3
BBAP:	B-cell aggressive lymphoma and BAL1 binding partner
BSA:	bovine serum albumin
CB:	coomassie blue
CDP:	Cdc4-phosphodegron
CID:	collision-induced dissociation
CoaSt6:	co-activator of STAT6
DAPK1/3	death associated protein kinase 1/3
DDX17:	p72 DEAD box RNA helicase
eEF2:	eukaryotic elongation factor 2
ELM:	eukaryotic linear motif
ETD:	electron-transfer dissociation
GSK3 β :	glycogen synthase kinase 3 β
GST:	glutathione S-transferase
IFN:	interferon
IKK ϵ :	inhibitor of nuclear factor kappa-B kinase subunit epsilon
IP:	immunoprecipitation
IRS1:	insulin receptor substrate 1
ISG:	interferon-stimulated gene
MALDI:	matrix-assisted laser desorption/ionization
Mass spec:	mass spectrometry
MCCA:	methylcrotonyl-Coenzyme A carboxylase 1 alpha
MDO2:	O-acetyl-ADP-ribose deacetylase MacroD2
MMLV:	Moloney murine leukaemia virus
NAD:	nicotinamid adenine dinucleotide
NAM:	nicotinamid
NEK6:	never in mitosis A-related kinase
NES:	nuclear export signal

NF- κ B	nuclear factor NF-kappa B
NICD:	NAD ⁺ -induced cell death
NLS:	nuclear localization signal
PAR:	poly-ADP-ribose
PARP:	poly-ADP-ribose polymerase
PARG:	poly-ADP-ribose glycohydrolase
PDB:	Protein Data Bank
PDE:	phosphodiesterase
PCCA:	propionyl coenzyme A carboxylase alpha polypeptide
PRKCZ:	protein kinase c zeta
P-TEFb:	positive transcription elongation factor b
RRM:	RNA recognition motif
RT:	room temperature
SCF:	SKP1-Cul1-RBX1
SINV:	Sindbis virus
SRPK2:	serine/arginine rich protein kinase 2
STAT:	signal transducer and activators of transcription
TAP:	tandem affinity purification
TFA:	trifluoroacetic acid
TOF:	time-of-flight
UBA:	ubiquitin activating enzyme
UBC:	ubiquitin conjugating enzyme
UIM:	ubiquitin interaction motif
VEEV:	Venezuelan equine encephalitis virus
WB:	Western blot
WCL:	whole cell lysate
ZAP:	zinc-finger antiviral protein
ZAPS:	zinc-finger antiviral protein short isoform

Layman's summary

Enzymes are molecules that catalyze a reaction without being used in that reaction themselves. In washing powder, there are for example enzymes that break down fat, the so-called lipases. They will do this over and over again, until all fat is gone. There are not only enzymes that destroy other molecules; there are also enzymes that can help build things. An example of this are the enzymes that work together to copy DNA, the material carrying the traits you inherited from your parents.

The cells that together form the human body contain thousands of enzymes per cell. For some of them, it is clear what they do, whereas for others it isn't. For some of the ones with known function, it is also known that they play a role in certain diseases and thus therapies have been developed to influence the function of those enzymes in cells. In certain types of breast cancer for example, there can be malfunctioning of DNA repair systems, allowing the cells to mutate. ARTD1, formerly called PARP1, is an enzyme that, amongst other functions, recognizes where the DNA is broken and attaches a flag onto those spots. Other enzymes will then come to those flags and repair the broken DNA. If one now blocks ARTD1 in certain types of cancer, the broken DNA will not be repaired anymore. The cancer cells will get so many breaks in their DNA that eventually they die. Healthy cells will not die as quickly as those cancer cells because of an additional DNA repair system that is still working in those healthy cells.

The aim of this work was to study an enzyme, ARTD10. Already known is that ARTD10 can also attach flags to other molecules, but different flags from the ones made by ARTD1. In this thesis it is described how we searched for molecules that receive flags from ARTD10. Subsequently I investigated how this flag influences the function of an exemplary molecule, the enzyme GSK3 β . It could be shown that GSK3 β cannot function anymore when it is carrying this flag. Furthermore it is shown that this reaction is reversible, as there is another enzyme, MDO2, which catalyzes the reverse reaction and removes the flag again. Lastly, tools were investigated that can be used to study these little flags, since there is nothing except radioactive labeling that currently allows us to see the flags. Once it is clear what the function of ARTD10 is, it might become a target for specialized therapies as well, but therefore we need to gain further understanding first.

Scientific contributions

Publications in scientific journals:

Feijs KLH, Kleine H, Braczynski A, Forst AH, Herzog N, Verheugd P, Linzen U, Kremmer E, Lüscher B. Identification of ARTD10 substrates and regulation of GSK3 β by mono-ADP-ribosylation. *Manuscript submitted*

Rosenthal F*, **Feijs KLH***, Bonalli M, Frugier E, Forst AH, Imhof R, Winkler HC, Caflisch A, Hassa PO, Lüscher B, Hottiger MO. Macrodomein-containing proteins are novel mono-ADP-ribosylhydrolases. *Nature Structural and Molecular Biology*, *manuscript in revision*

* these authors contributed equally

Verheugd P, Milke L, Herzog N, **Feijs KLH**, Forst AH, Kremmer E, Kleine H, Lüscher B. Regulation of NF- κ B signaling by the mono-ADP-ribosyltransferase ARTD10. *Nature Communications*, *manuscript in revision*

Herzog N, Hartkamp JDH, Verheugd P, Forst AH, **Feijs KLH**, Kremmer E, Kleine H, Lüscher B. Caspase-dependent cleavage of the mono-ADP-ribosyltransferase ARTD10 interferes with its pro-apoptotic function. *Manuscript submitted*

Venkannagari H, Fallarero A, **Feijs KLH**, Lüscher B, Lethiö L. Activity-based assay for human mono ADP-ribosyl transferases for screening and profiling inhibitors. *Manuscript in preparation*

Forst AH, Karlberg T, Herzog N, Thorsell AG, **Feijs KLH**, Verheugd P, Kursula P, Nijmeijer B, Lippok B, Kleine H, Kremmer E, Ladurner A, Lüscher B, Schüler H. Recognition of mono-ADP-ribosylated ARTD10 substrates by ARTD8 macrodomains. *Manuscript submitted*

Kleine H, Herrmann A, Lamark T, Forst AH, Verheugd P, Lüscher-Firzlauff J, Lippok B, **Feijs KLH**, Herzog N, Kremmer E, Johansen T, Müller-Newen G, Lüscher B. Dynamic subcellular localization of the mono-ADP-ribosyltransferase and interaction with the ubiquitin receptor p62. *Cell communication & signaling*, *manuscript in press*

Presentations at scientific meetings

Feijs KLH, Kleine H, Braczynski A and Lüscher B. Identification of ARTD10 substrates using protein microarrays and characterization of mono-ADP-ribosylation as inhibitory mechanism of GSK3 β . *Poster presented at the 4th EMBO Meeting, 22-25 September, Nice, France (2012).*

Feijs KLH, Kleine H, Braczynski A, Forst AH, Herzog N, Verheugd P, Kremmer E and Lüscher B. Modification of GSK3 β by ARTD10 inhibits kinase activity. *Talk given at the 6th PARPregio Meeting, 6-7 September, Aachen, Germany (2012).*

Feijs KLH, Herzog N, Verheugd P, Forst AH, Kleine H and Lüscher B. PARP10/ARTD10 controls cell physiology by modulating key cellular signaling pathways. *Talk given at the 18th International Conference on ADP-ribose metabolism, 18-21 August, Zurich, Switzerland (2010).*

Kleine H, Braczynski A, **Feijs KLH**, Linzen U, Hassa PO, Hottiger MO, Shilton BH, and Lüscher B. Characterization of mono-ADP-ribosylating poly-ADP-ribose-polymerases and unbiased identification of their substrates using protein microarrays. *Poster presented at the GBM Meeting "Signal Transduction and Disease", 27-30 September, Aachen, Germany (2009).*

Kleine H, Braczynski A, **Feijs KLH**, Linzen U, Hassa PO, Hottiger MO, Shilton BH, and Lüscher B. Characterization of mono-ADP-ribosylating poly-ADP-ribose-polymerases and unbiased identification of their substrates using protein microarrays. *Poster presented at the 1st EMBO Meeting, 29 August - 1 September, Amsterdam, the Netherlands (2009)*

Curriculum Vitae

Personal

Name: Karla Louisa Hendrika Feijs

Date of birth: 13.05.1986

Place of birth: Heerlen, the Netherlands

Nationality: Dutch

Education

2009 – 2012 PhD, RWTH Aachen University, DE

Additional courses attended at the Center for Doctoral Studies: “Higher Education Jobs”, “Applying for Research Grants or Funding”, “Professional Negotiations Module 1”, “Regeln guter wissenschaftlicher Praxis”, “Projektmanagement für Führungskräfte Modul 1” and “Growing through conflicts”.

2007 – 2009 Master Biomedical Sciences, University of Amsterdam, NL

Internships at the department of Molecular Carcinogenesis at the Netherlands Cancer Institute and at the Institute of Biochemistry at the University Hospital Aachen/RWTH Aachen University

2004 – 2007 Bachelor Molecular Life Sciences, Maastricht University, NL

Internships at the department of Immunology of Maastricht University and at the departments of Biochemistry of Maastricht University/Inner Medicine of the Academic Hospital Maastricht

1998 – 2004 High school College Rolduc Gymnasium, Kerkrade, NL

1990 – 1998 Primary school D’r Durpel, Kerkrade, NL

Certificates and courses

2010 Course “Exploring Modular Protein Architecture”, EMBL, Heidelberg (DE)

2008 Radionuclide Safety (Dutch level 5B), AvL, Amsterdam (NL)

2008 Experimental Animal Science (Dutch art. 9a), AMC, Amsterdam (NL)

2003 English language course (CAE, CEFR level C1), University of Cambridge (GB)

Eidesstattliche Erklärung

Ich erkläre eidesstattlich, dass ich die vorliegende Dissertation selbständig verfasst und alle in Anspruch genommenen Hilfen in der Dissertation angegeben habe. Des Weiteren erkläre ich, dass die vorliegende Dissertation nicht bereits als Diplomarbeit oder vergleichbare Prüfungsarbeit verwendet worden ist.

04.10.2012

Karla Feijs

Acknowledgements

I wouldn't have made it on my own. Therefore I would like to thank the following people:

Bernhard, it feels like yesterday that I first visited the Klinikum to ask for a research project on MYC. Even though I must admit I hesitated to accept a project on the exotic enzyme PARP10 instead of MYC, I am happy I did. Thanks for the interesting project that still seems to have unlimited possibilities, your enthusiasm and optimism throughout. Although we solved quite some questions, there are still so many more that need answering. Hopefully we will be able to solve some more in the years to come somehow!

To Professor Baumgartner I am indebted for the willingness to be co-examiner.

For the co-operation on the quest for the modification site in GSK3 β I'd like to thank Valeria Losasso and Paolo Carloni. Even though we haven't found what we are looking for yet, I'm still optimistic we will get an answer eventually. In that light I'd also like to thank Corinna Henkel and Christian Preisinger here in Aachen and Kristina Jurcic in Canada, I'm sure that all the mass spec optimization that somehow made so much time and materials disappear, will pay off in the end. We will get modification sites mapped eventually. MDO2 was brought to our attention by Michael Hottiger and Florian Rosenthal, which proved to be very interesting indeed. Next I want to thank Andreas Schuppert and his team of students for the bioinformatical analysis of our substrate sets. For the free peptide array samples, I'd like to thank the company JPT in Berlin and especially Ulf Reimer who performed the analysis of these arrays.

Im Allgemeinen möchte ich mich bei allen ehemaligen und jetzigen Mitgliedern der Lüscher Arbeitsgruppe bedanken für die tolle Atmosphäre. Im Einzelnen: Für die ProtoArray Vorarbeiten ein Dankeschön an Henning und Anne. Patrice, danke für die lustigen Trockeneisbomben, Flur-Kaffee-Partys und sonstige Späße. Ohne (Frust)Schoki, Kekse und Eis wäre das Leben im Labor viel unangenehmer gewesen. Die Zusammenarbeit im Labor war auch genial. Als letztes, danke für die Deutsch Korrekturen! Nico, ich bin noch immer Stolz auf unsere fast 100km Radtour in Zürich, vielleicht noch stolzer als auf meinem Vortrag dort. Auch die Technoparade war einzigartig ;). Deine Hilfe bei Computer-Problemen und auch bei Klonierungen war super. Danke! Jürgen, danke für 2 Sachen: ohne dich wäre mein deutsch nie so gut geworden. Okay, Grammatik kann ich noch immer nicht... Aber man kann mich inzwischen meistens verstehen. Zweitens fand ich es auch super, dass du von allem einen Privatvorrat hast im Labor und dass du mir erzählt hast, was ich wo finden kann. Das hat meinen Experimenten sicherlich geholfen! Für die stetige Betreuung von den SF9-Zellen möchte ich Barbara danken. Hoffentlich werden die Viecher sich irgendwann mal besser benehmen... Viel

Erfolg mit den nächsten ARTD10 Experimenten! Tim und Tanja - durch die Betreuung von eurem Praktikum beziehungsweise eurer Bachelorarbeit habe ich auch vieles gelernt und es hat sicherlich auch Spaß gemacht. Viel Erfolg mit dem was ihr im Moment macht. Nadine, Kai, Marc und Franzl, ihr werdet demnächst das Labor aufrecht erhalten müssen! Ich wünsche euch viel Erfolg damit... Falls ihr Tipps braucht zum basteln von Trockeneisbomben - ihr habt ja meine Emailadresse! Vielen Dank Franzl für deine Hilfe mit meiner deutschen Zusammenfassung. Jorgo, Andrea und Alex, da ihr auch bald Promovieren werdet/solltet, möchte ich euch viel Erfolg damit wünschen. Christian C. natürlich auch viel Erfolg mit deinem anstehenden "richtigen" Postdoc irgendwo! Juliane, Jörg V., Elena, die stabile Faktoren im Labor, danke für praktische Hilfe, Antworten auf blöde Fragen sowie deutsche Übersetzungen für z.B. acetic acid und urea aber auch für intelligentere Diskussionen. Ferdi und Jörg H., danke für hilfreiche Kommentare. Euch möchte ich noch viel Erfolg wünschen mit dem Aufbau vom eigenen Labor.

An die Mädels und Jungs von der AG Bernhagen geht ein wohlgemeintes Dankeschön für allen Restkuchen. Und vielleicht können wir dann doch noch eine Verknüpfung zwischen euren Arbeiten – Wachstumsfaktoren – und ARTD10 herstellen!

Voor het af en toe zorgen voor de hoognodige ontsnappingen aan het lab: Pauline, de weekendjes Zeeland en Rotterdam waren perfect om even niet aan onderzoek te denken, heerlijk! Sandy en Björn, de restaurantjes die we samen geprobeerd hebben, waren eigenlijk allemaal goed. Of misschien lag dat ook aan jullie gezelschap! Maud, super dat ik jouw kamer als hotel mocht gebruiken tijdens de EMBO Meeting in Amsterdam en later voor je updates vanuit Sierra Leone, die hebben me af en toe wel aan het denken gezet... Guus, misschien heb je me dan niet helemaal afgeleid van m'n onderzoek, maar bedankt voor de frisse kijk op dit project, de snelle aanlevering van artikelen en ook voor het proofreaden van delen van dit proefschrift!

Rina, Henk en Marjolijn, de schoonfamilie. Bedankt voor support, weekendjes weg, avondjes uit eten, poezenoppassen, Ik had het slechter kunnen treffen! Petra en Chris H., leuk dat jullie tegenwoordig in de grote stad Kerkrade wonen. Af en toe een glühweintje of een biertje is toch wel gezellig. Veel succes en plezier ook met jullie monstertjes!! Mam, pap. Zonder jullie had dit proefschrift er nu natuurlijk niet gelegen, dus danke voor jullie ondersteuning. Bij deze beloof ik later een leuk tehuis voor jullie uit te zoeken!

Chris... Dank je voor de af en toe kritische input die me op de goede weg heeft gehouden en die voor op z'n minst een beetje orde gezorgd heeft de afgelopen jaren. Maar bedankt nog meer voor de support, bijvoorbeeld door een deel van onze vakantie op de EMBO Meeting door te brengen of door me te ondersteunen als ik zeg een jaartje naar "het buitenland" te willen...